Dynamic Risk-based Integrity Management of Subsea Pipelines

By

Ehsan Arzaghi

M.Eng. (Maritime Engineering), B.Sc. (Mechanical Engineering)

Submitted in fulfilment of the requirements for the degree of

Doctor of Philosophy

National Centre for Maritime Engineering and Hydrodynamics

Australian Maritime College

University of Tasmania

August 2018

[Page intentionally left blank]

Dedicated to:

*My father **Gholam-Reza**, who blessed me with his wisdom.*

It is his memory that I try to emulate in all I do.

*My mother **Parvin**, for whom nothing has ever been more important than educating me,*

*and my brother **Aslan,** who has always been the greatest support and my best friend.*

[Page intentionally left blank]

Declarations

Declaration of Originality and Authority of Access

I declare that this thesis is my own work and contains no material which has been submitted in any form for another degree or diploma at any university or other institution of tertiary education. Information derived from the published or unpublished work of others has been duly acknowledged in the text and list of references of the thesis. The thesis does not contain any material that infringes copyright.

This thesis may be made available for loan and limited copying and communication in accordance with the Copyright Act 1968.

Signature: Date: 08/08/2018

Ehsan Arzaghi

[Page intentionally left blank]

Statement of Published Work Contained in Thesis

The following four published journal articles constitute the content of this thesis. The publishers of the papers comprising Chapters 2 to 5 hold the copyright for that content, and access to the material should be sought from the respective journals.

- Chapter 2: Arzaghi E., Abbassi R., Garaniya V., Binns J., Chin C., Khakzad N., Reniers G., Developing a Dynamic Model for Pitting and Corrosion-fatigue Damage of Subsea Pipelines, Journal of Ocean Engineering, 150 (2018), pp. 391-396.

- Chapter 3: Arzaghi, E., Abaei M.M., Abbassi, R., Garaniya, V., Binns, J., Chin, C., Khan F., A Hierarchical Bayesian Approach to Risk Analysis of Oil Spill Accidents in Marine Environment, Journal of Process Safety and Environmental Protection, 118 (2018), pp. 307-315.

- Chapter 4: Arzaghi E., Abbassi R., Garaniya V., Binns J., Khan F., Ecological Risk Assessment Model of Arctic Oil Spills from a Subsea Pipeline, Marine Pollution Bulletin, 135 (2018), pp. 1117-1127.

- Chapter 5: Arzaghi, E., Abaei M.M., Abbassi, R., Garaniya, V., Chin, C., Khan F., Risk-based maintenance planning of subsea pipelines through fatigue crack growth monitoring, Journal of Engineering Failure Analysis, 79 (2017), pp. 928-939.

Statement of Co-Authorship

Prof Genserik Reniers and Dr Nima Khakzad have contributed in conceiving the idea behind the proposed methodology of the journal article presented in chapter two. The co-authorship of remaining journal articles is as follows:

- *Conception of the idea, designing the case studies:*

  Arzaghi, Abaei, Abbassi, Garaniya, Khan

- *Performing the case studies and data analysis:*

  Arzaghi

- *Manuscript writing:*

  Arzaghi

- *Manuscript evaluation and submission:*

  Abbassi, Garaniya, Binns, Chin

The name and details of all the people contributing to the publications out of this PhD research are listed below:

Mr Ehsan Arzaghi

National Centre for Maritime Engineering and Hydrodynamics,
Australian Maritime College, University of Tasmania,
Launceston, Tasmania, Australia

Associate Professor Jonathan Binns

Director, ARC Research Training Centre for Naval Design and Manufacturing
Deputy Associate Dean Research
Infrastructure and Collaborations
College of Science and Engineering, University of Tasmania
Launceston, Tasmania, Australia

Dr. Rouzbeh Abbassi

Senior Lecturer
School of Engineering, Faculty of Science and Engineering
Macquarie University
Sydney, NSW, Australia

Dr. Vikram Garaniya

Senior Lecturer
National Centre for Maritime Engineering and Hydrodynamics,
Australian Maritime College, University of Tasmania
Launceston, Tasmania, Australia

Dr. Christopher Chin

Senior Lecturer
National Centre for Maritime Engineering and Hydrodynamics,
Australian Maritime College, University of Tasmania
Launceston, Tasmania, Australia

Professor Faisal Khan

Director, Centre for Risk, Integrity and Safety Engineering (C-RISE),
Canada Research Chair (Tier I) in Safety and Risk Engineering,
Head, Department of Process Engineering,
Faculty of Engineering and Applied Science, Memorial University of Newfoundland,
St. John's, NL, Canada

Dr Nima Khakzad

Assistant Professor
Safety and Security Science Group, Department of Values, Technology and Innovation
Delft University of Technology
Delft, Netherlands

Professor Genserik Reniers

Safety and Security Science Group, Department of Values, Technology and Innovation
Delft University of Technology
Delft, Netherlands

Mr Mohammad Mahdi Abaei

National Centre for Maritime Engineering and Hydrodynamics,
Australian Maritime College, University of Tasmania,
Launceston, Tasmania, Australia

Associate Professor Jonathan Binns

Director, ARC Research Training Centre for Naval Design and Manufacturing
Deputy Associate Dean Research
Infrastructure and Collaborations
College of Science and Engineering
University of Tasmania

Signature: Date: 28/10/18

Associate Professor Shuhong Chai

Principal
National Centre for Maritime Engineering and Hydrodynamics
Australian Maritime College
University of Tasmania

Signature: Date:28/10/18

[Page intentionally left blank]

Acknowledgements

It will be difficult for me to accept that the journey I have always wanted to make is coming to an end. The completion of this PhD, however, will open a door to new opportunities and adventures. Thus, I am pleased to thank those who aided me throughout this journey.

First and foremost I wish to express my sincere gratitude and respect to my supervisors Associate Professor Jonathan R. Binns, Dr Roubzeh Abbassi, Dr Vikram Garaniya and Dr Christopher Chin for their support and guidance throughout my research and studies at the Australian Maritime College. It is needless to say that without their encouragement and help this research may have not been completed.

I would like to thank Dr Rouzbeh Abbassi for being not only a wonderful supervisor, but also an excellent mentor and a kind friend. Throughout this way, I have been learning a lot from his unique dedication, optimism and resolute. I am also thankful to Professor Faisal Khan for his wisdom, and generosity in sharing his invaluable knowledge and experience. I truly hope that I can make an opportunity to pass on the learnt lessons and research/education virtues generously and with utmost responsibility.

I am thankful to AMC/UTAS for providing a grant that supported this Ph.D. and all the staff in this institution for their support during my education and research. I am also thankful to Dr Nima Khakzad and Professor Genserik Reniers for providing an opportunity to visit the Safety and Security Science Group at Delft University of Technology in 2017. I would like to also thank the staff and management of the Centre of Risk, Integrity and Safety Engineering Group at Memorial University (MUN), Canada for their support during my research visit to MUN in 2017.

I would like to acknowledge Mr. Mohammad Mahdi Abaei for his help during my research. Special thanks must go to Samantha Wei Ning Lau, for her precious friendship and support during my life in Tasmania.

Lastly, I am thankful to my family, my father Gholam-Reza, my mother Parvin and my brother Aslan for the spiritual support and continuous encouragement throughout my years of study and research. This accomplishment would have not been possible without them. Thank you.

[Page intentionally left blank]

Abstract

Subsea pipelines are widely used across the globe for transportation of large quantities of hydrocarbons from offshore wells to onshore locations, playing an important role in procurement of fuel for power generation and transport. Although the recorded failure rates in oil and gas subsea pipelines are relatively lower than pipelines in other facilities such as water distribution or wastewater collection systems, a damaged subsea pipeline has significant environmental risk due to the hazardous properties of hydrocarbons and inaccessibility of the facilities. The loss of asset integrity may also delay production resulting in significant financial consequences for the industry operators. To prevent this, frequent inspections and maintenances are essential. Companies however may incur substantial costs to perform regular maintenance activities in such environment with limited accessibility.

This Ph.D. thesis aims at providing a risk-based integrity management framework for maintenance scheduling of subsea pipelines. This method, unlike previous approaches that were mostly concerned with accidents resulting from component failures, focuses on structural deterioration due to fatigue and corrosion phenomena. In this research, advanced probabilistic techniques such as Bayesian Network (BN) are adopted to account for the uncertainty of parameters that are influential in the problem. By estimating the life of a structure and evaluating the consequences of failure, the proposed framework provides a cost-effective maintenance planning solution that ensures a safer and more reliable operation.

In the first stage, this study develops a probabilistic methodology for modelling the useful life of a subsea pipeline degraded by corrosion-fatigue damage. Deterioration of the pipeline, in the presence of corrosive agents and cyclic loads, starts with nucleation of corrosion pits which continue to grow in size. These defects can provide the required condition for initiation of fatigue damage and the growth of cracks which may lead to fracture. The entire process is influenced by many factors such as material and process conditions, each incorporating a high level of uncertainty. This methodology presents an integrated Dynamic Bayesian Network (DBN) model, incorporating the temporal nature of the damage process and its varying growth rates. It is observed that the established model is an efficient tool for predicting the fatigue life of subsea pipelines.

This is mainly due to the computational efficiency of BN in considering a large number of parameters and its updating capacity that enables the inclusion of monitoring results in the analysis.

A fracture in a subsea pipeline may result in an underwater release of hydrocarbons with detrimental impacts on the species in the sea environment. United States Environmental Protection Agency (USEPA) provides an Ecological Risk Assessment (ERA) framework for analyzing risks involved in such accidents. The present study attempts to develop a novel methodology, based on this framework, to predict the exposure concentration of contaminants in a marine environment. For this purpose, the stochastic fate and transport of spilled oil is estimated using a level IV fugacity model. A hierarchical Bayesian approach (HBA) is adopted to estimate the probability distribution of time to reach a concentration, based on the observational data. The estimated times can be utilized for the preparation of contingency and remediation plans by operation and safety managers. Probability distributions are also developed for the exposure concentration in different media in contact with oil (e.g. water column, sediment), using the results of fugacity model. To establish a Bayesian-based ERA methodology for accidental release of oil in marine environment, the 95^{th} percentile of Predicted Exposure Concentration ($PEC_{95\%}$) is used, along with 5^{th} percentile Predicted No Exposure Concentration ($PNEC_{5\%}$). The model incorporates causal effects from the likelihood of each event (e.g. exposure to contaminant) into the risk assessment methodology. Additionally, the presented method uses a DBN model for including the seasonal effects on the ecological risk profile. Upon obtaining the likelihood of fatigue failure and estimating the associated risk with these accidents, a dynamic risk-based methodology is developed for maintenance planning of deteriorating subsea pipelines. The established DBN model of the deterioration process is extended to an Influence Diagram (ID) for identifying the optimum decision alternative, being possible maintenance actions (e.g. continuing operation, repairing the structure). The presented model is able to consider the consequences of failure as well as the cost of each decision alternative, while estimating the expected utilities. Observation of damage state is added into the model to improve the reliability of predictions and efficiency of the decision making process. This methodology can assist asset managers to select the optimum approach for mitigating the consequences of failure while minimizing the maintenance costs.

This thesis overall attempts to provide a comprehensive source of knowledge and technique to form a better understanding of the failure of subsea pipelines and associated consequences due to deterioration processes. It will assist in ensuring a safer and more reliable operation of these structures through a more efficient maintenance planning approach.

[Page intentionally left blank]

Table of Contents

List of Tables

Abbreviations

AMC	Australian Maritime College
ARC	Australian Research Council
BN	Bayesian Network
BT	Bow Tie
CPT	Conditional Probability Table
DBN	Dynamic Bayesian Network
ERA	Ecological Risk Assessment
ET	Event Tree
EU	Expected Utility
FT	Fault Tree
FORM	First-Order Reliability Method
HBA	Hierarchical Bayesian Approach
HBM	Hierarchical Bayesian Modelling
ID	Influence Diagram
IMO	International Maritime Organisation
LC	Lethal Concentration
LB	Lower Bound
MCMC	Markov Chain Monte Carlo
MCS	Monte-Carlo Simulation
NCMEH	National Centre for Maritime Engineering and Hydrodynamics
PEC	Predicted Exposure Concentration
PNEC	Predicted No Effect Concentration
PRA	Probabilistic Risk Assessment
RV	Random Variable
RQ	Risk Quotient
RBM	Risk-based Maintenance
TRC	Time to Reach a Concentration
US EPA	United States Environmental Protection Agency
UB	Upper Bound

Chapter 1: Introduction

1.1 Background

Over the past decades, the offshore oil and gas industry has expanded significantly worldwide, mainly due to the continuous increase in energy demand. Global crude oil production was about 92 million barrels per day in 2016, of which about one-third was produced offshore. This ratio is about a fifth of the 3.5 trillion cubic-metres of natural gas produced per day [1, 2]. Subsea pipelines play an integral role in the oil and gas industry for transporting large quantities of hydrocarbons from extraction wells to offshore platforms or process facilities located onshore. For instance, across the North Sea alone, more than 45,000 km of subsea pipelines, umbilical and cables were installed by 2013 for delivering hydrocarbons to the facilities and end-users [3]. According to previous research [4], recorded failure rates of subsea pipelines are relatively lower than those utilized in water or wastewater distribution networks. The United Kingdom Offshore Operators Association reports that in pipelines operating in the North Sea, with an exposure of 328,858 km-yrs, only 542 historical failures occurred before 2001, representing an average failure rate of 0.0016 events per km/yr [5].

According to Mansor et al. [6], the design of subsea pipelines is based on a strength capacity of approximately 1.5 times higher than the specified minimum yield stress. Across the world, the oil and gas pipelines comply with the American Petroleum Institute (API) specifications which has become an international standard since 1948. The recommended practices has been updated based on a limit state design concept for the sake of achieving a uniform safety level [26]. API documents identify the steel grade by its yield strength such as X42, X60 and X70 where the number refers to the yield strength in thousands of pounds per square inch. According to Bai et al. [26], several factors including cost, resistance to corrosion, weight requirement and walkability are taken into account when selecting material grades. In recent years, developments in high-strength steels such as X80 and X100 has enabled pipeline operators to significantly reduce the construction cost while not compromising pipeline operating pressure limits [7]. According to Wang et al. [8], these types of high-strength steel have been more frequently used in the oil and gas industry wherein 2012 there were more than 4000 km of X80 pipelines operating in China.

In spite of its economic and reliable nature, a damaged pipeline poses major potential risk from the hazardous properties of hydrocarbons as well as the critical elements associated with their operational environment. A few of these elements include inaccessibility of the facilities, possible extreme environmental conditions and sensitivity of the surrounding ecosystem. Subsea pipeline failure has caused many catastrophic accidents resulting in fatal damages or substantial capital costs. In 2006, more than 42,000 gallons of crude oil were released into the Gulf of Mexico due to a rupture in a pipeline [9]. Similarly, a cracked pipeline resulted in 16,000 barrels of oil spilled below the Gulf of Mexico southeast of Venice in 2017. With concerning environmental impacts, this accident was reported as the largest since the Deepwater Horizon Accident in 2010 [10]. It is then essential to improve the integrity management techniques currently used by the oil and gas industry. This can be achieved by developing a better understanding of pipeline failure, predicting and continuously updating the likelihood of such accidents, and mitigating the catastrophic consequences using dynamic risk-based approaches.

Degradation of structural properties is recorded as the major cause of failure in subsea pipelines [11]. A review of the literature summarizing historical subsea pipeline accident data indicates that corrosion and external interference (including fatigue damage) contribute to more than 70% of pipeline failures [12-14]. Fatigue phenomena caused by the cyclic wave loads continuously acting on the pipeline leads to cracking of the tubular sections and decreasing the resistance capacity of the structure [15]. Natarajan et al. [16] assert that a major contributor to fatigue of subsea infrastructure (flowlines and risers) is from interactions with fluid flow and interactions between infrastructure and the seabed. Pipeline wall thickness may also be reduced due to the presence of corrosive agents in an aqueous environment. Formation of corrosion pits can therefore decrease the strength of material and, at times, result in ultimate failure and loss of containment [17-19]. Moreover, generated pits may provide the required conditions for initiation of fatigue cracks. It is explained that when pits are present, under circumstances which can be met in the marine environment, cracks can be initiated faster than those generated in non-aggressive media [20]. Many researches have investigated corrosion-fatigue damage and attempted to predict its effect on the service life of structures [21-24]. However, the main focus of these methods has been on structures constructed from aluminum or buried steel pipelines that more often experience a third-party damage rather than continuous cyclic loads. There have been other attempts to prognostic health assessment of subsea pipelines [20, 25] which are mostly deterministic or require conducting complex experimental tests for acquiring necessary data. This highlights a need for a

probabilistic framework that models the entire pitting and corrosion-fatigue deterioration process of subsea pipelines.

Loss of pipeline integrity may pose substantial financial risk to the companies and significantly affect their future in the oil and gas industry. The incurred costs in such incidents are made up of the notional cost of fatalities, cost of repair activities, and cost of delayed production [26]. In the case of containment loss where the pipeline is ruptured or has a leakage due to deterioration, released hydrocarbons are wasted and likely to be dispersed across the offshore environment exposing the ecosystem to toxic chemicals [27]. The effect of such accidents on different species (lethal or sub-lethal) can be acute or often extend to long-term consequences. The operators and integrity managers should therefore incorporate the risk of environmental damage caused by loss of containment into their risk management plans. A comprehensive framework is then required for the probabilistic risk assessment of oil spill accidents affecting the lives of marine ecological habitants. Ecological Risk Assessment (ERA) involves estimating the concentration of chemicals in different media representing the level of exposure as well as evaluating the ecological effects on various organisms.

Mackay [28] developed a methodology for estimating the fate of chemicals in multimedia based on various transport and transformation processes. For this purpose, four levels of fugacity models have been introduced with different applications such as investigating the distribution of chemical detergents in rivers and lakes [29]. Fugacity models are also used by Nazir et al. [30] and Afenyo et al. [31] for modelling the multimedia fate of oil in marine environment. Sadiq [32] suggests that fugacity concept can be adopted for any applications where the body of water is completely mixed and flow characteristics are well-defined. To analyze the ecological risk, many researchers have adopted Risk Quotient (RQ) concept which is the ratio of predicted exposure concentration of pollutants to the predicted no effect concentration (PEC/PNEC) [33-35]. Nazir et al. [36] also adopted RQ for estimating the level of risk. The extent of ecological impact is dependent on many parameters such as the amount and type of released hydrocarbon, environmental conditions (e.g. wind and current speed) and the species present around the contaminated area [37]. Each of these parameters may involve a degree of uncertainty. The probabilistic dependency of contamination level and the overall risk on these parameters must be incorporated into the risk assessment model. This has not been fully addressed by most of the previous research mentioned above.

In order to mitigate the severe financial and environmental risks of subsea pipeline accidents, frequent inspections and repairs are essential. However, companies can incur substantial costs for performing regular maintenance activities in inaccessible areas [38]. The main challenge of maintenance engineers and integrity managers is therefore to adopt maintenance strategies that control the rate of equipment deterioration, maximize availability of the facility and minimize the total cost of operation, while not compromising safety nor environmental issues [39]. Maintenance techniques have experienced major development over the recent decades. Arunraj and Maiti [40] provide an overview of the changes in these techniques categorizing them into first, second, third and recent generation. The review suggests that the recent generation, which includes efficient methods such as condition monitoring and risk-based maintenance (RBM), is the result of an integrated approach towards maintenance and safety initiated in 2000. Inspection and maintenance scheduling based on risk assessment minimizes the probability of failure and its consequences. By incorporating the estimated risk and required costs for repair activities, RBM assists management in making optimum decisions with respect to maintenance actions. This approach is used by several researchers for inspection and maintenance planning of process and offshore facilities [11, 39, 41, 42].

Many methods have been used by researchers for conducting dynamic risk assessment and risk-based maintenance planning, among which fault tree (FT), event tree (ET), bow tie (BT), and Bayesian network (BN) are the most commonly used. Conventional methods (FT, ET and BT) have been able to provide a capacity for improving operational and system safety in the oil and gas and process industry, however, their application is becoming limited. The restrictions of these techniques include inability of modelling common cause failures and the assumption that different events occur independently. Khakzad Rostami [43] provides an extensive review on the limitations of conventional methods in risk assessment. It is frequently reported that these methods are significantly inefficient in dealing with large engineering applications, mainly because of the number of parameters that make performing a risk assessment an intractable task. The static nature of FT and ET also fails to account for the dynamics of a system which are usually caused by changes in operational parameters. Bayesian techniques, on the other hand, can be utilized as an efficient solution to risk analysis and decision-making problems. An overview of Bayesian network (BN) applications in risk analysis and decision making is provided by Weber et al. [44]. This review suggests that Bayesian techniques are effective approaches to dealing with scarce data and a wide range of information including subjective probabilities.

1.1.1 Application of Bayesian Approaches in Integrity Management

BNs are advanced probabilistic techniques used for reasoning under uncertainty. These graphical models are established based on the causal dependencies amongst a number of random variables (RVs). BN efficiently performs inference using the joint probability distribution of RVs and Bayes' theorem. More details about the fundamentals of BN and its application will be provided in the following chapters of this thesis. Major factors that resulted in the selection of this method for developing a dynamic risk-based integrity management framework are listed below:

- Significant improvement in the computational efficiency of BN, compared to conventional methods, assists in modelling a large problem such as structural deterioration that is influenced by a wide range of parameters;
- BN is able to incorporate dependency of events, multiple states for each variable and various sources of uncertainty affecting the RVs or the entire process. This makes BN a strong tool for modelling the physical/mathematical relationships within the process of interest;
- Providing a platform for failure assessment, risk analysis and more importantly, including a probabilistic decision-making model into the same structure is remarkably flexible, user-friendly and straightforward;
- BN's feature of probability updating based on Bayes's theorem provides the capacity to improve the estimation of risk and decision-making outcome when new observations are available.

1.2 Research Overview

The primary aim within this Ph.D. research is "*improving the availability and safety of subsea oil and gas pipelines subjected to deterioration processes by using advanced probabilistic and risk-based approaches*".

1.2.1 Research Questions

In order to realize this aim, the following research questions were established:

- How to develop a predictive model for estimating the remaining useful life of deteriorating subsea pipelines.
- How to develop a probabilistic model of the environmental damage caused by the loss of containment of an oil and gas pipeline.

- How to more precisely assess the ecological consequences of subsea pipeline accidents posed to the marine environment.
- How to mitigate these consequences with optimal maintenance planning that also considers the overall operational cost in decision making process.

1.2.2 Research Objectives

The main objective of this thesis is to develop a dynamic risk-based framework for integrity management of deteriorating subsea pipelines. At first, the purpose of this research is to develop a probabilistic model that simulates the deterioration process of the structures. This process consists of several stages, such as pitting corrosion and fatigue crack growth, each influenced by a number of factors such as material properties and environmental conditions. The dynamic model is therefore able to evaluate the likelihood of pipeline accidents caused by structural degradation. A fracture in a subsea pipeline may result in the underwater release of hydrocarbons with adverse impacts on the marine ecosystem. To evaluate these consequences, this study aims at predicting the exposure concentration of chemicals in a marine environment, in case an oil spill occurs. The exposure distribution is later required for estimating the level of ecological risk posed to various aquatic organisms. This can be achieved by comparing predicted exposure concentrations with the degree of tolerance to chemicals that the organisms of concern have. Upon the assessment of failure likelihood and analyzing its financial and environmental consequences, this study attempts to propose a risk-based maintenance framework for optimizing the maintenance plans of subsea pipelines. In order to accomplish these objectives, the research framework completed the following tasks:

- developing a dynamic methodology for prognostic health assessment of subsea pipelines degraded by pitting and corrosion-fatigue damage.
- developing a fate and transport model of spilled oil from a ruptured subsea pipeline.
- conducting an ecological risk assessment of marine oil spill accidents.
- developing a risk-based model for maintenance planning of subsea pipelines subjected to progressive structural deterioration.

1.3 Organization of Thesis

This Ph.D. thesis is presented in manuscript format on a publication basis. Chapters 2-5 are standalone and can be read independently. An outline of each chapter including the novel components, are provided below.

Chapter 2: Developing a Dynamic Model for Pitting and Corrosion-fatigue Damage of Subsea Pipelines

This chapter presents a novel probabilistic methodology for integrated modelling of pitting and corrosion-fatigue degradation processes of subsea pipelines. The entire deterioration process is modelled using a Monte-Carlo Simulation (MCS) and Dynamic Bayesian Network (DBN), representing its temporal nature and varying growth rates. This process starts with pitting nucleation, continued by the growth of pit and transition to fatigue damage, in the form of short and long cracks. The model incorporates various factors influencing each stage of the process. The developed methodology is applied to estimate the remaining useful life of high strength steel pipelines and can be used as a tool by asset managers for optimal inspection and maintenance scheduling. The chapter has been published in the *Journal of Ocean Engineering, 150 (2018), pp. 391-396.*

Chapter 3: A Hierarchical Bayesian Approach to Modelling Fate and Transport of Oil Released from Subsea Pipelines

This paper presents a methodology for predicting the stochastic fate and transport of spilled oil from a subsea pipeline into ice-infested regions. A level IV fugacity model is used to estimate the time-variable concentration of oil in multimedia. A hierarchical Bayesian approach (HBA) is adopted to estimate the probability of time to reach a concentration (TRC) based on the observations made from the fugacity model. By evaluating the distribution of time to different concentrations, this method can be used as a tool to implement more effective risk contingency and remediation plans which improve the safety of offshore oil and gas facilities. This chapter has been published in the *Journal of Process Safety and Environmental Protection, 118 (2018), pp. 3-7-315.*

Chapter 4: An Ecological Risk Assessment Model for Arctic Oil Spills from a Subsea Pipeline

This paper presents a probabilistic methodology for Ecological Risk Assessment (ERA) of accidental oil spills in the Arctic ecosystem. A fugacity approach is adopted to model the fate and transport of released oil, taking into account the uncertainty of input variables. Based on the Risk Quotient (RQ) concept that uses the ratio between extent of pollutant exposure to ecological effects, a Dynamic Bayesian Network (DBN) model is established to assess the ecological risk posed to the aquatic community. The model enables accounting for the occurrence likelihood of input parameters as well as analyzing the time-variable risk profile caused by seasonal changes. This chapter has been published in *Marine Pollution Bulletin, 135 (2018), pp. 1117-2227.*

Chapter 5: Risk-based Maintenance Planning of Subsea Pipelines through Fatigue Crack Growth Monitoring

This paper presents a dynamic risk-based methodology for maintenance scheduling of subsea pipelines subjected to corrosion and fatigue damage. A Bayesian network (BN) is developed to model the probabilistic deterioration process and then it is extended to an influence diagram for decision making with regard to maintenance activities. Observation of damage state is included in the model to improve the predictions of damage state and to enhance the decision-making capacity. The economic risk associated with investment on maintenance is minimized by suggesting the optimum maintenance technique among multiple possible methods of repair. The proposed method can assist asset managers to select the optimum approach for mitigating the risk of subsea pipeline failure while minimizing maintenance costs. This chapter has been published in the *Journal of Engineering Failure Analysis, 79 (2017), pp. 928-939.*

Chapter 6: Summary and Conclusion

This chapter provides a summary of the Ph.D. thesis as well as the conclusions made throughout this research.

Chapter 2: Developing a Dynamic Model for Pitting and Corrosion-Fatigue Damage of Subsea Pipeline

Abstract

Degradation of subsea pipelines in the presence of corrosive agents and cyclic loads may lead to the failure of these structures. In order to improve their reliability, the deterioration process through pitting and corrosion-fatigue phenomena should be considered simultaneously for prognosis. This process that starts with pitting nucleation, transits to fatigue damage and leads to fracture, is influenced by many factors such as material and process conditions, each incorporating a high level of uncertainty. This study proposes a novel probabilistic methodology for integrated modelling of pitting and corrosion-fatigue degradation processes of subsea pipelines. The entire process is modelled using a Dynamic Bayesian Network (DBN) methodology, representing its temporal nature and varying growth rates. The model also takes into account the factors influencing each stage of the processes. To demonstrate its application, the methodology is applied to estimate the remaining useful life of high strength steel pipelines. This information along with Bayesian updating based on monitoring results can be adopted for the development of effective maintenance strategies.

2.1 Introduction

One of the major causes of failure in offshore structures such as oil and gas pipelines is degradation of structural properties during their lifespan [12, 13, 45]. Corrosion is the most well-known form of steel deterioration resulting in generation of pits or more extended damage [17, 46, 47]. Fatigue, on the other hand, is the disintegration of material due to cyclic loads applied on the structure. Coupled corrosion-fatigue results from applied cyclic stresses in tandem with presence of corrosive agents, where localized corrosion in the form of pits may provide the required conditions for initiation of fatigue crack initiation. Many parameters including material properties and environmental conditions influence this process. These factors, each incorporating a level of uncertainty, may be adopted to estimate the remaining useful life of the structure. While these predictions will provide reliable measures for improving maintenance strategies, a dynamic framework is also required for updating the estimations based on new observations during the service life.

A great deal of research has been conducted to predict the state of damage and fatigue life in steel and aluminum alloy structures subjected to pitting and corrosion-fatigue. Kondo [48] developed a model for the prediction of fatigue crack initiation time based on pit growth, however, the damage process was not entirely simulated. Goswami and Hoeppner [49] proposed a seven-stage model that considers the effect of electrochemical processes on pit formation as well as the role of pitting in fatigue crack initiation; however, this model was conceptual and failed to provide a computational framework. A probabilistic model is developed by Harlow and Wei [23] for prediction of corrosion-fatigue life comprising the time for crack initiation, surface crack growth and the growth of damage to the critical size. This model, however, does not consider the time of pit nucleation as well as the effect of short cracks in service life modelling. Kaynak and Baker [50] assessed the effect of short cracks on fatigue life of steel structures concluding that the growth rates of short cracks are different (usually smaller) from those of long cracks. Shi and Mahadevan [24] proposed a mechanics-based probabilistic model of the entire pitting and corrosion-fatigue process suggested by Goswami and Hoeppner [49]. They adopted Monte Carlo simulations and the First-Order Reliability Method (FORM) approach to conduct the probabilistic analysis. Although their framework provides a guideline for estimating fatigue life, the application of FORM may result in computational complications.

Alternatively, Bayesian network (BN) as an advanced probabilistic model has widely been applied to reliability analysis of complex systems. Application of BN significantly reduces the method complexity and computational time of inference, by factorizing the joint probability distribution of the parameters of interest based on local dependencies.

Various applications of BN in risk and reliability engineering can be found in previous research [44, 51-54]. However, only a few studies adopted BNs for modelling deterioration processes in structures. Friis-Hansen [55] studied the application of Dynamic Bayesian Network (DBN) in modelling fatigue crack growth of offshore jacket structures. The developed probabilistic network was also used to identify optimum inspection plans. Straub [56] developed a generic computational framework using DBN for modelling deterioration processes with potential applications in inspection, maintenance, and repair planning. Arzaghi et al. [57] developed a methodology for probabilistic modelling of fatigue crack growth using BN. The model was extended to an Influence Diagram for finding the optimum maintenance plan among multiple repair alternatives with different economic impacts.

In the present study, a probabilistic methodology is developed for modelling corrosion-fatigue deterioration in offshore structures. This methodology consolidates the entire damage process including pit nucleation, pit growth transited to short and long fatigue cracks, and the fracture of structure. To improve the accuracy of corrosion-fatigue life estimations, the model incorporates the randomness in the parameters influencing the process. For this purpose, DBN is adopted as an efficient probabilistic tool. The advantages of this methodology are illustrated through the remaining useful life assessment of an offshore pipeline subjected to pitting and corrosion-fatigue.

2.1.1 Bayesian Networks

BNs are directed acyclic graphs used for reasoning under uncertainty by considering the causal relationships (represented by directed edges) among a number of random variables, represented by chance nodes [58]. BN estimates the joint probability distribution of a set of random variables based on the conditional independencies and the chain rule, as in Eq. (2-1):

$$P(U) = P\left(X_1, X_2, \ldots, X_n\right) = \prod_{i=1}^{n} P\left(X_i \mid pa\left(X_i\right)\right) \tag{2-1}$$

where $P(U)$ is the joint probability distribution, and $pa(X_i)$ is the parent set of random variables X_i. **Figure 2-1** depicts a conventional BN comprising random variables X_1-X_4. As the main advantage of Bayesian networks, when new information about any of the chance nodes becomes available, the model can update the probabilities for a more efficient knowledge elicitation. For instance, if variable X_2 is observed to be in state e, the joint probability distribution is updated based on Bayes' theorem:

$$P(X_1, X_3, X_4 \mid e) = \frac{P(X_1, X_3, X_4, e)}{\sum_{X_1, X_3, X_4} P(X_1, X_3, X_4, e)} \tag{2-2}$$

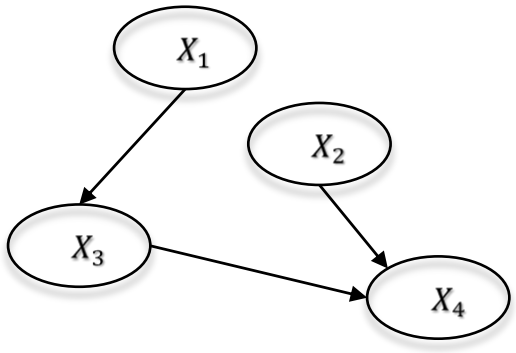

Figure 2-1. A conventional BN.

Dynamic Bayesian networks (DBNs) particularly represent stochastic processes and enable explicit modelling of the evolution process of a set of random variables [59]. A DBN divides the time line into a discrete number of time slices $t \in [0, T]$ and allows a node in time slice $i+1$ to be conditionally dependent on a node in time slice i as well as its parents in time slice $i+1$. **Figure 2-2** illustrates a DBN in which the evolving process of the variable Y_t is modelled. This variable in time slice t is dependent on Y_{t-1} as well as X_t. In order to establish a DBN, the conditional probability tables for evolving nodes should be completed, for instance $P(Y_t \mid Y_{t-1}, X_t)$ for variable Y_t in the DBN presented in **Figure 2-2**.

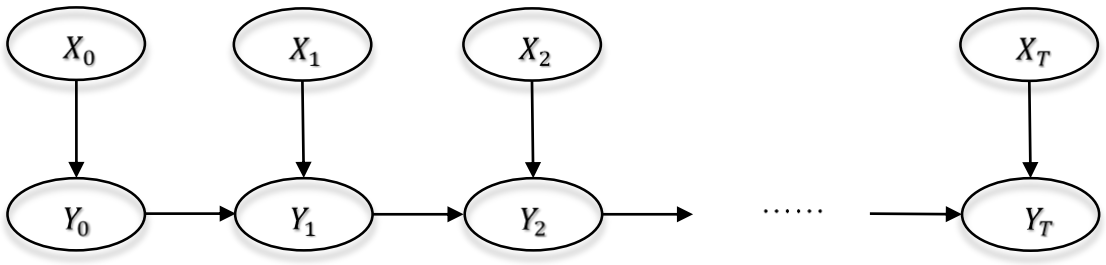

Figure 2-2. A Dynamic BN.

The transition between two consecutive time slices may be for instance dependent upon the physical features of the stochastic process being modelled. A detailed explanation of inference algorithms developed specifically for DBN structures can be found in Ref. [60].

2.2 Pitting and Corrosion-Fatigue Modelling Methodology

To develop the probabilistic model, it is first required to assess the entire damage process identifying the physics behind pitting and the corrosion-fatigue phenomena. This will also facilitate developing the computational framework for predicting damage states and establishing the DBN. The seven-stage model proposed by Goswami and Hoeppner [49] is adopted as the basis for analyzing the service life in the present study. **Figure 2-3** illustrates the total corrosion fatigue life (t_{fl}) initiated with pit nucleation time (t_{pn}) and eventually resulting in fracture. This process also includes three damage growth times for pit (t_{pg}), short crack (t_{sc}) and long crack (t_{lc}) as well as two transition stages, i.e., "pit-to-crack transition" and "short-crack to long–crack transition".

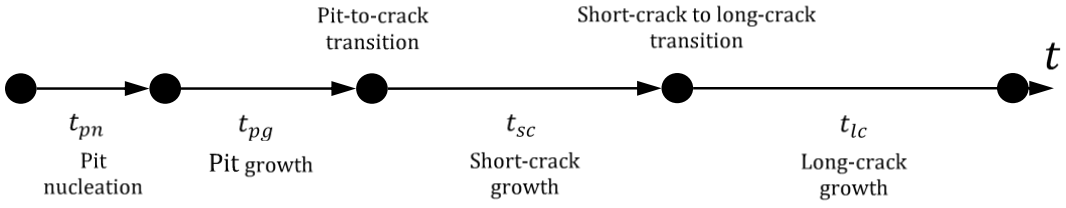

Figure 2-3. Different stages of pitting corrosion-fatigue life.

$$t_{fl} = t_{pn} + t_{pg} + t_{sc} + t_{lc} \tag{2-3}$$

The proposed methodology models the entire deterioration process including pitting corrosion and fatigue damage growth. **Figure 2-4** presents an overview of the entire methodology and its key elements.

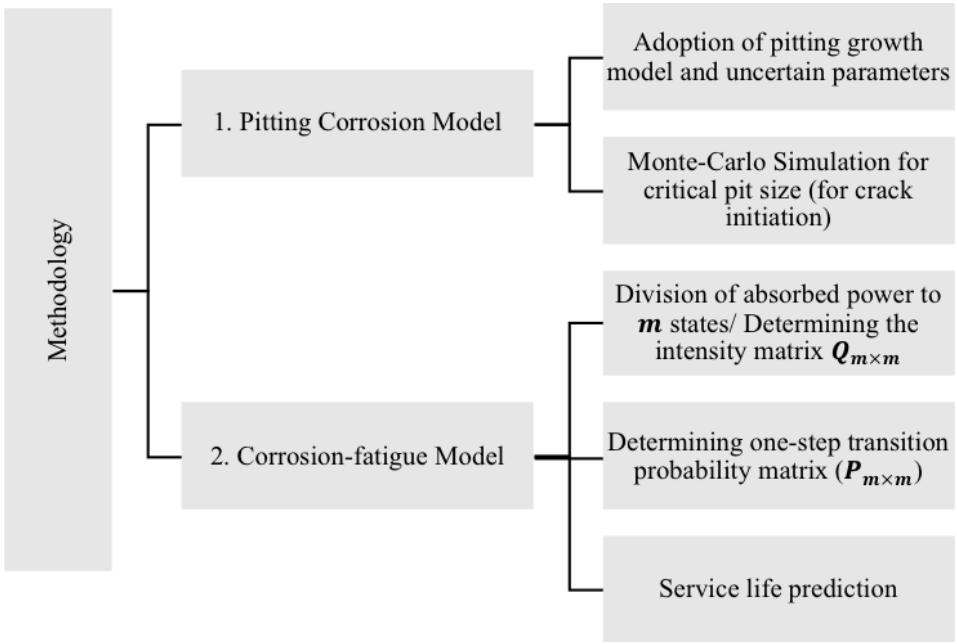

Figure 2-4. Developed methodology for service-life prediction of deteriorating subsea pipelines.

The computational methods for each component of the total failure time represented in Eq. (2-3) will be discussed in the following subsections:

2.2.1 Pit Nucleation

The time for pit initiation has attracted a great deal of research, yet the dependence on many influencing factors such as materials and electrochemical has not been fully investigated. Hence, the developed model considers this stage of damage life as a random variable modelled by a lognormal distribution. The adopted distribution parameters, suggested by Shi and Mahadevan [24] are later provided.

2.2.2 Pit Growth

According to Kondo [48] and Harlow and Wei [23], pits are assumed to remain in a hemispherical shape while growing at a constant volumetric rate. This yields a pit growth rate, given by:

$$\frac{dc}{dt} = \frac{C_p}{2\pi c^2} \tag{2-4}$$

$$C_p = \frac{MI_{P0}}{nF\rho}\exp\left(-\frac{\Delta H}{RT}\right) \tag{2-5}$$

where c is the pit radius, M is the molecular weight of the material, I_{P0} is the pitting current constant, n is the valence number, $F = 96,514$ (c/mol) is Faraday's constant, ρ is density, ΔH is the activation energy, $R = 8.314$ (J/molK) is the universal gas constant, and T is the temperature.

The transition from pit growth to crack initiation is dependent on mechanical characteristics such as stress intensity factor, ΔK. Two criteria is considered as the boundary conditions for crack initiation: (1) the stress intensity factor for the equivalent surface crack growth of the pit reaches the threshold stress intensity factor of the fatigue crack growth (Eq. (2-6)), and (2) the fatigue crack growth rate exceeds the pit growth rate.

$$\Delta K_{pit} = \Delta K_{crack} \tag{2-6}$$

Kondo [48] suggests that the critical crack length (c_{cr}) that satisfies the conditions for transition from pit growth and crack initiation can be calculated as:

$$c_{cr} = \left(\frac{1}{2}\right)\left(\frac{2Q}{\pi\alpha}\right)\left[\frac{\Delta K_{cr}}{2.24\Delta\sigma}\right]^2 \tag{2-7}$$

where $Q = 1.464\alpha^{1.65}$ is the shape factor, $\alpha = \frac{a}{c} = 0.7$ is the aspect ratio of pit (c and a are half length of the major and minor axes of pit shape), $\Delta K_{cr} = 2.4\,Mpa\sqrt{m}$ is the threshold stress intensity factor, and $\Delta\sigma$ is the stress range experienced by the structure.

2.2.3 Short and Long Crack Growth

Long cracks are usually considered when using fracture mechanics for fatigue analysis, and Paris law is widely used for estimating damage sizes. The effect of short cracks on fatigue life has attracted researchers' attention, however, there is no explicit formula derived for short crack growth. According to Kaynak and Baker [50] and Shi and Mahadevan [24], a probabilistic model based on Paris law that accounts for the uncertainty of parameters such as stress intensity factor may be applied. Eq. (2-8) represents the empirical formula for damage growth:

$$\frac{da}{dN} = C(\Delta K)^m \tag{2-8}$$

where N is the number of applied load cycles, C and m are material parameters specifically obtained for short and long cracks resulting in two identical growth rates from the equation. ΔK is the stress intensity factor, which can empirically be expressed as:

$$\Delta K = Y(c)\Delta\sigma\sqrt{\pi c} \tag{2-9}$$

where $Y(c)$ is the geometry function dependent on the crack depth, and $\Delta\sigma$ is the stress range. While the explicit solution of Eq. (2-8) is not possible, by assuming that the geometry function is independent of crack depth c and the stress range $\Delta\sigma$ follows a Weibull distribution, an analytical solution can be achieved [61]:

$$a_{t+1} = \left(a_t^{\frac{2-m}{m}} + SA^m \right)^{\frac{2}{2-m}}, m \neq 2 \tag{2-10}$$

$$S = C\ N\Gamma\left(1+\frac{m}{B}\right)Y^m\ \pi^{\frac{m}{2}}\left(1-\frac{m}{2}\right) \tag{2-11}$$

where A and B are the scale and shape parameters of the Weibull distribution, respectively, and Γ is the gamma function. Eq. (2-10) enables the computation of crack size in current time step as a function of crack size in the previous time step and the material constants m and C, where these parameters are obtained from empirical models for short and long cracks. Different methods are developed to identify the transition size c_{th} from short crack growth to long crack growth. Kaynak and Baker [50] suggested this value is about 1 to 2 mm for En7A steel. Similarly, in this study the critical size is regarded as a random variable with a mean value of 2 mm.

2.2.4 Probabilistic Analysis and BN Model

The probability analysis was performed using MCS in tandem with implementation of a DBN. To estimate the time for the initial part of damage life where pitting corrosion is dominant, 104 samples where generated from random variables involved in Eq. (2-4), (2-5) and (2-7). The distributions of these variables are listed in Table 2-1. It should be noted that initial pit size (C_0) was considered as the initial condition when solving Eq. (2-4). The remainder of service life, where fatigue damage progresses, is estimated using a DBN. For this purpose, the generic DBN developed by Straub [56] was adopted to model each of the two growth processes indicated in **Figure 2-5**. The developed network qualitatively represents a deterioration process describing the state of damage over the life time divided into a discrete number of slices. That is, the damage size is a function of the initial condition (node C_{cr}) that is followed by the process of short crack growth (nodes C_1^{sc} to C_n^{sc}), transition to long crack at a critical crack size (node C_{th}) and eventually the long crack growth process (nodes C_1^{lc} to C_m^{lc}). The occurrence of failure event is assessed by defining a limit state G, as:

$$G = C_f - C_i \tag{2-12}$$

where C_i and C_f are the actual and critical crack size, respectively.

2.3 Application: Corrosion Fatigue Damage of a Subsea Pipeline

To demonstrate the applicability of the developed method in predicating corrosion-fatigue service life, a numerical study is carried out on the failure of an offshore pipeline. The mechanical properties of the structure are listed in **Table 2-2**. It is assumed that $N = 10^6$ load cycles are experienced by the pipeline every year and critical size of damage for failure is $Cf = 10 \times 10^{-3}$ m.

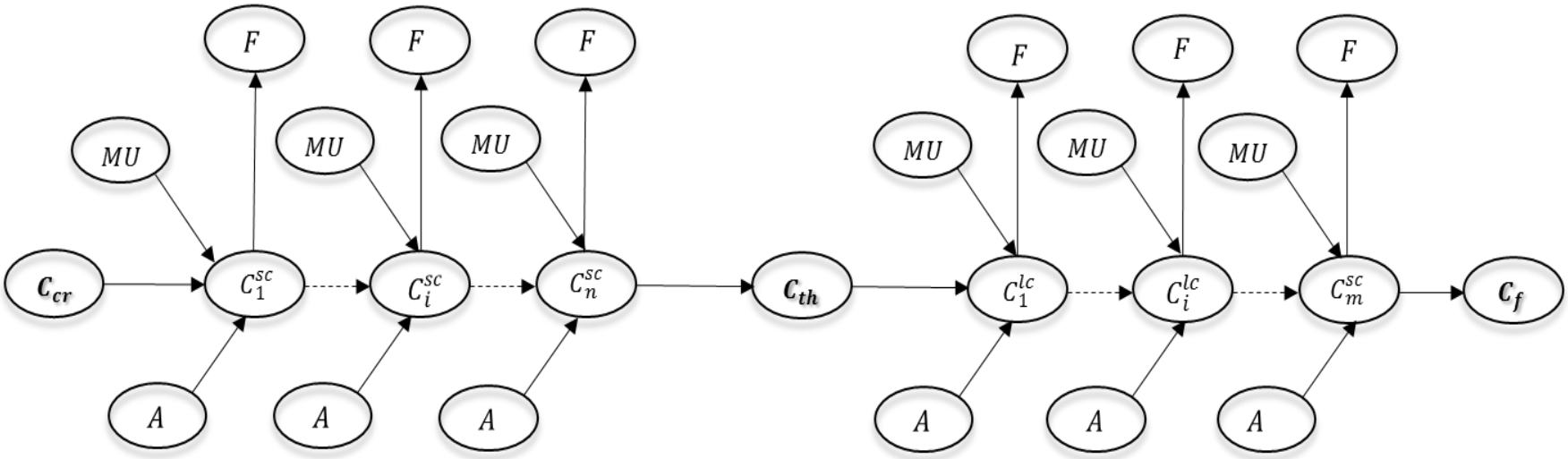

Figure 2-5. Developed Bayesian network for modelling corrosion-fatigue life.

Table 2-1. Random values used in pitting corrosion-fatigue model

Variable	Description	Distribution	Mean	Standard Deviation
$\Delta\sigma$	Stress range (MPa)	Normal	60	10
T	Temperature (K)	Normal	293	1
A	Weibull scale parameter (MPa)	Normal	5.35	0.963
MU	Model uncertainty	Normal	1	0.18
C_0	Initial pit size (m)	Exponential	1.98×10^{-6}	0.99×10^{-7}
C_{cr}	Initial crack size (m) [from Monte Carlo sim]	Exponential	0.8×10^{-3}	-
C_{th}	Fatigue crack threshold (short to long) (m)	Normal	2.0×10^{-3}	

Table 2-2. Deterministic values used in pitting corrosion-fatigue model

Variable	Description	Mean
ρ	Density (gm/m^3)	7.8×10^6
n	Valence	2
M	Molecular weight (gm)	55.75
ΔH	Activation energy (KJ/mol)	5.0×10^4
m_{sc}, m_{lc}	Short/long crack growth exponent	3.0
C_{sc} / C_{lc}	Material parameter for short/long crack	2.17×10^{-13} 1.45×10^{-14}
Y	Geometry function	1
B	Weibull shape parameter	0.66
N	Load cycles	10^6 / year

The results of Monte Carlo simulation showed that the critical pit size for transition to short crack has a mean of $E[C_{cr}] = 8\times10^{-4}$ m. The cumulative probability distribution of this variable is presented in **Figure 2-6**. This distribution was discretized into 20 exponentially growing intervals which form the upper bounds of states of damage size nodes in the DBN. This was performed to avoid rounding errors caused by uniform interval lengths in the last intervals where the probabilities are significantly low. As illustrated in **Figure 2-5**, the DBN model contained two consecutive periods corresponding to corrosion fatigue cracks with different growth rates. An adequate number of time slices were included in the short crack growth process so that the mean size of predicted damage equals the critical transition size, C_{th}, before long crack growth is initiated. Then the long crack process was extended for a number of time slices (each representing a year) until fracture occurs, $P(F=1)=1$.

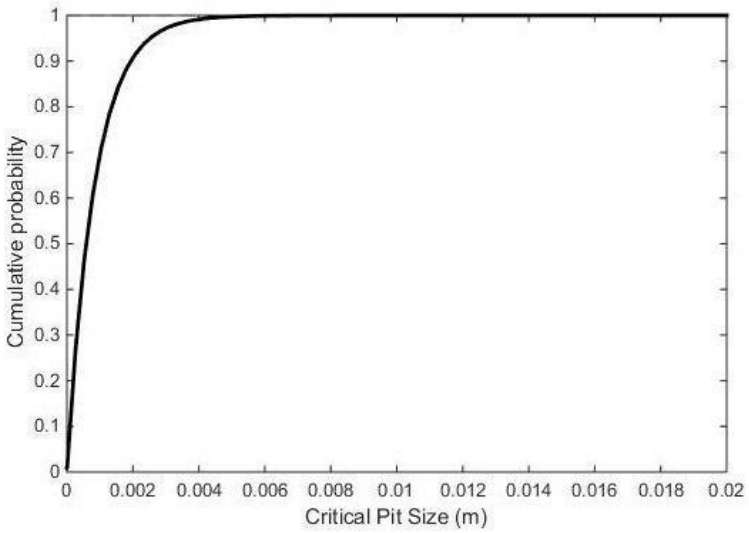

Figure 2-6. Cumulative probability distribution of critical pit size leading to the transition to short crack.

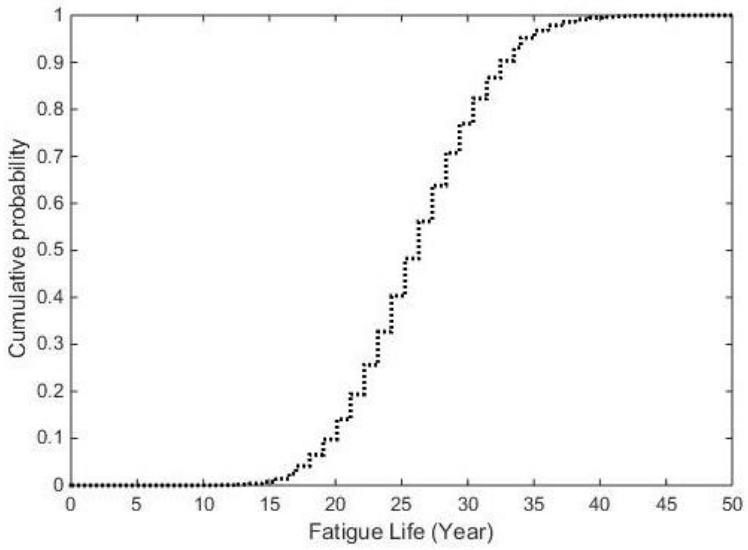

Figure 2-7. Cumulative probability distribution of corrosion-fatigue life for an offshore pipeline.

The results of the case study, presented in **Figure 2-7**, suggest that within the third year of operation the grown pits will satisfy the conditions required for initiation of fatigue cracks and damage will be growing in the form of short cracks. The prediction of pipeline corrosion fatigue life indicates that the transition from short crack to long cracks takes place in year 12 from which the damage develops with a significantly faster rate. After 15 years from the start of the operation the extent of damage will be significantly increasing where the probability of failure is about 0.1 in the 20th year, given no repairs were performed. This probability will reach to almost 0.5 in the 25th year of operation and approximately 10 years later the structure is extremely close to failure event, $P(F=1) \approx 0.95$.

These results highlight the strength of the methodology for predicting the service life of a corroded subsea pipeline subjected to cyclic loads. The proposed methodology can be readily used to update the predictions based on new damage size inspection results and also provides a great potential for optimization of maintenance plans. Moreover, by enhancing the DBN model with a monitoring capacity, the predictions can be updated along the operation period with observation of influencing parameters.

2.4 Conclusion

This paper presents a probabilistic methodology for prediction of pitting and corrosion fatigue service life in offshore pipelines. For this purpose, MCS are used to analyze the time of pit growth as well as estimating the size of pit in which transition to short crack growth occurs. It was observed that pits with mean size of about 0.8 mm have the required condition for crack initiation in steel pipelines. A DBN model was implemented for simulating short and long crack growth which may lead to fracture. The predictions suggest that in the 20^{th} year of operation, probability of failure is about 0.1 where due to faster growth of long crack this value reaches to about 0.95 after 15 years, given that no maintenance is performed on the pipeline. The results of this study highlight the capability of the method in prediction of corrosion fatigue life considering the randomness of the parameters involved in the problem. These capabilities can also be enhanced for efficient monitoring, inspection and maintenance planning strategies.

Acknowledgements

The authors affiliated with University of Tasmania gratefully acknowledge the financial support provided by National Centre for Maritime Engineering and Hydrodynamic (NCMEH) at the Australian Maritime College (AMC) of the University of Tasmania. The authors also acknowledge the support of the ARC Research Training Centre for Naval Design and Manufacturing (RTCNDM) in this investigation. The RTCNDM is a University-Industry partnership established under the Australian Research Council Industry Transformation grant scheme (ARC IC140100003)

Chapter 3: A Hierarchical Bayesian Approach to Modelling Fate and Transport of Oil Released from Subsea Pipelines

Abstract

The significant increase in global energy demand has drawn the attention of oil and gas industries to exploration of less-exploited resources. Arctic offshore region is reported to hold a great proportion of un-discovered oil reserves. While this can be a promising opportunity for the industry, more exploration activities will also increase the possibility of oil spill during the entire process including production and transport. A comprehensive risk assessment based on Ecological Risk Assessment (ERA) method is then required during the planning and operation stages of future Arctic oil production facilities. In the exposure analysis stage, ERA needs an evaluation of the oil concentration profile in all media. This paper presents a methodology for predicting the stochastic fate and transport of spilled oil in ice-infested regions. For this purpose, level IV fugacity models are used to estimate the time-variable concentration of oil. A hierarchical Bayesian approach (HBA) is adopted to estimate the probability of time to reach a concentration (TRC) based on the observations made from a fugacity model. To illustrate the application of the proposed method, a subsea pipeline accident resulting in the release of 100 tonnes of Statfjord oil into the Labrador Sea is considered as the case study.

3.1 Introduction

There has been increasing attention on the possibility of oil exploration in the Arctic Ocean which is mainly attributed to some parts of this region becoming ice-free due to climate change. According to Khon et al. [62], the thickness and extent of Arctic ice cover has been declining, with a 40% reduction observed from 1979 to 2007. As a consequence, the Northwest Passage which connects Europe and Asia became ice free for the first time in the summer of 2007 [63]. These changes, in addition to the rising global energy demand, may facilitate the exploration of the substantial hydrocarbon reserves in the Arctic Ocean becoming the next frontier of oil and gas explorations. Gautier et al. [64] suggest that about 30% of the world's undiscovered gas and 13% of undiscovered oil reserves can be found in the Arctic region, of which more than 80% is expected to be in offshore locations [65]. This exploration can bring many opportunities to the energy industry and in turn the world economy, however, the existing risk factors in the region can significantly increase the threat of oil spill during the exploration process and transport. DNV [66] highlights the major risk factors as the extremely low temperatures that influence the properties of the structure material as well as loads caused by the impact from drifting icebergs. In addition to the higher likelihood of accidents in the ice-infested waters, the consequences of an oil spill, such as distortion of the reproduction cycles of species and ecological changes, will be exacerbated in such regions [67]. This is mainly due to the slower decomposition of hydrocarbons in low temperatures making them more available to affect the marine life and greater sensitivity of the Arctic ecosystems which have slower reproduction rates and more simple trophic structures [66, 68, 69]. Moreover, an oil spilled in the Arctic is likely to remain in the environment for a long time, as the logistics challenges diminish the effectiveness of strategies for containing and cleaning up oil spills [37]. Parameters such as the type and quantity of the spilled oil as well as the seasonal variations in the environment can influence the extent of damage to the Arctic which can often be extended to long-term consequences. Camus and Smit [70] investigated the environmental impacts arising from a potential Arctic oil spill based on a joint review program conducted in 2012 [71]. Camus and Smit [70] suggest that the results of their study provide a better understanding of the effects from such accidents assisting in the development of more effective management strategies. However, this research does not provide any method for quantification of the extent of impact or an approach to estimating the overall risk level. A comprehensive Ecological Risk Assessment (ERA) method is then required for the entire well delivery process, from feasibility studies to asset management and operations. This assessment is performed to evaluate whether the activities are

acceptable with respect to the industry's criteria as well as for developing effective contingency plans [72].

The three main steps of ERA are problem formulation, exposure analysis and risk characterisation. Exposure analysis is the key component of risk assessment of an accidental oil release in marine environment [73]. This phase of the analysis assists in estimating the extent of contamination in the environment, identifying the organisms exposed, pathways to exposure and the possible responses of the organisms to the stressor (i.e. hydrocarbons) [31, 36]. In order to determine the level of contamination, the concentration of the stressors must be estimated. To achieve this objective, many researchers have used fugacity concept (mostly level IV fugacity) as an approach to partition modelling [32, 36, 74]. A fugacity approach is capable of generating time-series of contaminant concentration in every medium in the environment, by simplifying the analysis due to continuity between the interfaces of the phases. Afenyo et al. [31] developed a dynamic fugacity model for estimating the exposure of four media, including air, sea water, sediments and ice, to the oil released during Arctic shipping. The proposed model provides a profile for oil concentration in these media, however, it fails to consider the uncertainty of many parameters involved in the model which is essential for accurately estimating the ecological risk associated with the spill accident.

Nazir et al. [36] developed a methodology for ERA of oil spill from a riser. The developed model is based on level IV fugacity for estimating the oil concentration in water and sediment medium, and utilizes Monte Carlo Simulations (MCS) to incorporate the uncertainty of multimedia input parameters. Similarly, Afenyo et al. [33] proposed a probabilistic ERA model for Arctic marine oil spills. Their model provides probability distributions of the exposure concentration in different media as well as 95% percentile risk. However, due to the adoption of conventional methods that only propagate the uncertainty in input variables to model outputs, the probabilistic dependency of concentration on those inputs is neglected.

Unlike classical statistical methods, Bayesian techniques are useful for probabilistic risk assessment (PRA) applications because they are able to deal with a wide range of information types and provide useful estimation of model parameters when the data is sparse or the correlation between them is hard to perceive [75]. Bayesian inference is adopted by several researchers for the conduct of probabilistic analyses [76, 77], probabilistic risk assessment [53, 54] and maintenance scheduling of offshore structures [42, 57, 78]. Advances in Bayesian statistics such as developments of hierarchical Bayesian modelling (HBM) have brought them to a wider

audience for solving complex engineering problems [79]. This method can be carried out using open source Markov Chain Monte Carlo (MCMC) software packages such as OpenBUGS.

The main objective of this study is to develop a probabilistic methodology for the fate and transport modelling of oil released from subsea pipelines in a marine environment. The results of this research provide the necessary information for conducting a comprehensive ERA and the development of oil spill contingency plans. A fugacity-based model is utilized to predict the multimedia fate of oil upon the generation of an oil slick on the surface. An HBA is then adopted to incorporate the uncertainty of the parameters involved in fugacity model, and estimate the level of oil concentration dependent on these parameters. A case study is carried out to demonstrate the application of the proposed methodology through predicting the time taken to reach specific oil concentrations in the Arctic region in ice-infested waters.

3.1.1 Fugacity Model

Fugacity (f) is known as the tendency of a chemical to escape from a phase and has the unit of pressure. The concept of fugacity is used as a substitute for chemical potential which is a criterion for thermodynamic equilibrium describing the fate of chemicals in a multiple media system. The relationship between concentration and fugacity is given in Eq. (3-1), proposed by Mackay et al. (1981):

$$C = Z \times f \tag{3-1}$$

where C is the concentration of chemical (mol/m^3), f is the fugacity (Pa) and Z is the fugacity capacity (mol/m^{3}Pa). Fugacity capacity, Z, represents the tendency of a medium to absorb a chemical. Therefore a medium with a larger Z will have a higher concentration of chemicals due to more tendency to absorb [74]. Mackay [28] proposes four levels of fugacity-based models with different applications. Although level III models are used most, because of less complexity and requiring less data, the present study adopts level IV model as it is more realistic and can estimate the time-dependent behavior of the chemicals. The model proposed by Yang et al. [76] is used as the basis for the developed probabilistic framework. More detailed discussions on fugacity models can be found in [28, 36, 74].

3.1.2 Hierarchical Bayesian Modelling (HBM)

Observations of physical processes are regarded as *data* and may be subjected to different sources of uncertainty. *Information* can be achieved through the process of evaluation, manipulation and organizing data which eventually adds to *knowledge*. Statistical inference is defined as obtaining a conclusion based on the gained knowledge [79]. HBM is an advanced probabilistic approach to performing inference based on real-world observations. Bayes' theorem is considered for carrying out Bayesian inference, given in Eq. (3-2):

$$\pi_1(\theta \mid x) = \frac{f(x \mid \theta)\pi_0(\theta)}{\int_{\theta} f(x \mid \theta)\pi_0(\theta)\, d\theta}, \tag{3-2}$$

where θ is the unknown parameter of interest, $f(x \mid \theta)$ is the likelihood function, $\pi_0(\theta)$ is the prior distribution of θ and $\pi_1(\theta \mid x)$ is the posterior distribution of θ. The term hierarchical in HBA represents the use of multistage prior distributions. As suggested by Kelly and Smith [79], the prior distribution for a parameter of interest is given in Eq. (3-3):

$$\pi(\theta) = \int_{\Phi} \pi_1(\theta \mid \varphi)\pi_2(\varphi) d\varphi, \tag{3-3}$$

where $\pi_1(\theta \mid \varphi)$ is the first-stage prior representing the population variability in θ, given the value of φ; $\pi_2(\varphi)$ is the hyper-prior distribution representing the uncertainty of φ as a vector of hyper-parameters. HBM can assist in probabilistic analysis and risk modelling by propagating the uncertainties through complex models. Recently, a number of studies have been conducted to bring the application of HBM to PRA [76, 77, 80]. In the present paper, HBM is utilized to develop a methodology for predicting the likelihood of the oil concentration profile in the Arctic environment.

3.2 Methodology: Multimedia Fate Modelling

The proposed methodology aims at providing a model for predicting the concentration of oil spilled from a subsea pipeline while accounting for the uncertainty of input parameters. The results of the methodology are required for conducting an ERA assisting the designers and operators during well delivery processes as well as carrying out effective asset management in such

environment. The proposed model can also help in preparation of remediation plans for oil release accidents. **Figure 3-1** illustrates different stages of the proposed methodology and the key elements covered in each stage.

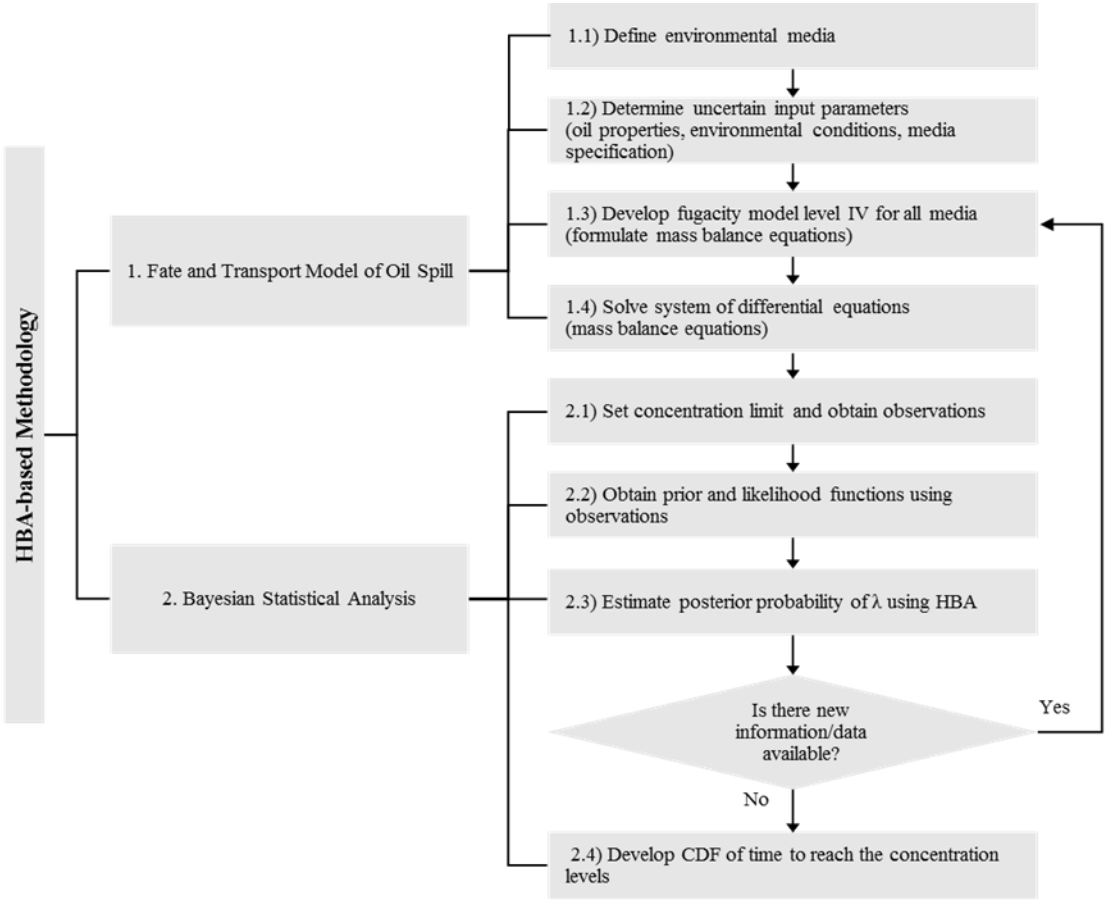

Figure 3-1. Developed methodology for probabilistic fate and transport modelling of oil spills in marine environment.

3.2.1 Fate and Transport Model

In order to model the fate and transport of oil in open sea, level IV fugacity model is adopted as the basis of the developed methodology. As highlighted in **Figure 3-1**, the first step is to define the media involved in the oil spill scenario. Based on the objective of risk assessment of release accidents in the Arctic, four media, or bulk compartments, are considered in the present study including air, water, ice and sediments. In fact, each of these media includes several sub-compartments. That is, air consists of pure air and aerosols; ice cover consists of pure ice, liquid water, air and organic matters; water compartment consists of pure water, suspended solids and

biota and sediment medium consists of sediments solids and pore water. The properties of the media and sub compartments are listed in **Table 3-1**, as suggested by Yang et al. [74].

Table 3-1. Properties of all media involved in the problem (VF: Volume Fraction, OCF: Organic Carbon Fraction).

Bulk Compartment (i)	Sub-compartment (j)				OCF Solids	Medium Density (kg/m^3)	Depth (m)
	VF Air (φ_{i1})	VF Water (φ_{i2})	VF Solids (φ_{i3})	VF Biota (φ_{i4})			
Air (1)	1.00	0.00	2×10-11	0.00	N/A	1.19	100.00
Ice Cover (2)	0	0	5×10-6	0	0.2	916	2.5
Water (3)	0	1	5×10-6	1×10-6	0.2	1000	100
Sediment (4)	0	0.63	0.37	0	0.04	2500	0.05

The next step in the methodology is to determine the information in relation to input parameters (i.e. oil properties and environmental conditions and specifications of the media). This also includes quantifying the uncertainty of variables such as oil viscosity and density, ambient temperature, and wind speed. This information, including the type and specifications of probability distributions, will be provided later in the case study. In the third step, the level IV fugacity model must be developed based on formulating the mass balance equations. The general form of unsteady-state mass balance functions for bulk phase i and sub-compartments j is given in Eq. (3-4):

$$V_i Z_i \frac{df_i}{dt} = I_i + \sum D_{ij} f_j - f_i \left(\sum D_{ij} + D_{ai} + D_{Ri} \right), \tag{3-4}$$

where I_i is the input rate of a chemical compound in ith bulk phase and its unit is (mol/s). Z_i is the fugacity capacity of each bulk compartment and D_{ij}, D_{ai} and D_{Ri} are the transport parameters, referred to as D-values. The fugacity capacity of each bulk phase can be estimated using Eq. (3-5):

$$Z_i = \sum_j \varphi_{ij} Z_{ij}, \tag{3-5}$$

where φ_{ij} is the volume fraction and Z_{ij} is the fugacity capacity of the sub-compartment. Details of fugacity capacity calculations are provided in **Table 3-2**.

Table 3-2. Calculation of fugacity capacity for all media, Z -values in (mol/m^3.Pa), for sub-compartments and bulk compartments.

Sub-compartment (j)	Z_{ij}	**Comment**	**Reference**
Air (Z_{i1})	$1/RT$	$R = 8.314$ (Pa.m^3/mol.K), T is absolute temperature (K).	
Water (Z_{i2})	$1/H$ or C^s/P^s	H is Henry's law const. (Pa.m^3/mol), C^s is aqueous solubility (mol/m^3), P^s is vapour pressure (Pa).	[33]
Solids (Z_{i3})	$x_{ij}K_{oc}\rho_{ij}H$	x_{ij} is organic carbon fraction, $K_{oc} = 0.41K_{ow}$ is organic carbon partition coefficient, $\rho_{ij} = 2.4$ is density of solids (kg/L).	[33]
Aerosols (Z_{13})	$6\times10^6/P_L^S\ RT$	P_L^S is liquid vapour pressure (Pa).	[71]
Biota (fish) (Z_{34})	$0.048\rho_{24}K_{ow}/H$	$\rho_{24} = 1000$ is density of biota (kg/m^3), K_{ow} is octanol-water partition coefficient.	[33]
Ice-air interface (Z_{ia})	K_{ia}/RT	K_{ia} is ice surface-air partition coefficient, $\ln K_{ia}(12.5^\circ C) = 0.68\ln K_{ow} - 19.63 + \ln K_{wa}$ K_{wa} is water-air partition coefficient.	[28]
Organic carbon in ice cover (Z_{23})	$0.41K_{ow}Z_l$	$Z_l = K_{wa}/RT = 1/H$	[71]
Bulk compartment (i)	Z_i	**Comment**	
Air (1)	$Z_1 = Z_{11} + \varphi_{13}Z_{13}$		
Ice cover (2)	$Z_2 = \varphi_{21}Z_{21} + \varphi_{22}Z_{22} + \varphi_{23}Z_{23} + (A_{2a}/V_2)Z_{2a}$	A_{2a} ice-air interface area, V_2 is ice cover volume.	
Water (3)	$Z_3 = Z_{32} + \varphi_{33}Z_{33} + \varphi_{34}Z_{34}$		
Sediment (4)	$Z_4 = \varphi_{42}Z_{42} + \varphi_{43}Z_{43}$		

Transport parameters must also be determined before generating the mass balance equations. According to Yang et al. [74], in addition to loss processes of advection and degrading reactions, three inter-media processes can be considered including diffusion, deposition and re-suspension and D-values can be calculated as detailed in **Table 3-3**.

Table 3-3. Calculation of transport parameters considering two loss processes (advection and reaction) and three transport processes (diffusion, deposition and re-suspension)

Interface	Comment	Details	Total D -value
Air (1)-Ice cove (2)	Diffusion	$D_v = 1/(1/K_{va}A_{12}Z_{11} + 1/K_{vi}A_{12}Z_{22})$	$D_{12} = D_v + D_{di}$
	Deposition	$D_{di} = A_{12}U_{di}\varphi_{13}Z_{13}$	$D_{21} = D_v$
Ice cover (2)- Water (3)	Melting	$D_{iw} = A_{23}U_{iw}Z_{22}$	$D_{32} = D_{iw}$
	Icing	$D_{ii} = A_{23}U_{ii}Z_{33}$	$D_{23} = D_{ii}$
Water (3)-Sediment (4)	Diffusion	$D_y = 1/(1/K_{pw}A_{34}Z_{33} + Y_4/B_{w4}A_{34}Z_{33})$	$D_{34} = D_y + D_{ds}$
	Deposition	$D_{ds} = A_{34}U_{ds}Z_{34}$	
	Re-suspension	$D_{rs} = A_{34}U_{rs}Z_{43}$	$D_{43} = D_y + D_{rs}$
	Reaction	$D_{Ri} = K_{Ri}V_iZ_i$	
	Advection	$D_{ai} = G_iZ_i$	

Upon calculating the fugacity capacities and transport parameters, the fugacity model can be generated considering all of the four bulk phases. The mass balance equations for air, ice cover, water and sediment are given in Eqs. (3-6)-(3-9):

$$V_1Z_1\frac{df_1}{dt} = I_1 + D_{21}f_2 - f_1(D_{12} + D_{a1} + D_{R1}), \tag{3-6}$$

$$V_2Z_2\frac{df_2}{dt} = I_2 + (D_{12}f_1 + D_{32}f_3) - f_2(D_{21} + D_{23} + D_{a2} + D_{R2}), \tag{3-7}$$

$$V_3Z_3\frac{df_3}{dt} = I_3 + (D_{23}f_2 + D_{43}f_4) - f_3(D_{32} + D_{34} + D_{a3} + D_{R3}), \tag{3-8}$$

$$V_4Z_4\frac{df_4}{dt} = I_4 + D_{34}f_3 - f_4(D_{43} + D_{a4} + D_{R4}), \tag{3-9}$$

where the direct input into the air, ice-cover and sediment phases are considered negligible (i.e. $I_1 = I_2 = I_3 = 0$). However, the input rate into water can be estimated by $I_3 = Q_3 \times C_i$, where Q_3 is the volumetric flow rate of oil in (m^3/s) and C_i is the molar concentration of oil in (mol/m^3). A detailed discussion on input rate values can be found in [74]. In the next methodology step, the set of differential equations are solved simultaneously using the fourth-order Runge-Kutta method, to obtain the fugacity of all compartments. Each time-dependent fugacity is then multiplied by the

corresponding fugacity capacity to obtain the concentration profile of the phase. The concentration profiles are used in the next steps for statistical analysis.

3.2.2 Bayesian Inference of Random Durations

Upon obtaining the time varying concentration of oil in each phase, a statistical model is developed to predict the stochastic fate and transport in a marine environment. An HBA is applied to establish the model and in order to obtain the observations required for the Bayesian modelling, a critical level is defined for the concentration of oil in a medium. That is, the time of j^{th} observation, denoted by T_i^j, is the time when the actual concentration of phase i, C_{actual}^j, reaches a specific limit of C_{Cr}.The defined limits of concentration can be the value of interest of operators and risk managers developing contingency plans or dealing with remediation planning of spill accidents. An upper bound (UB) and a lower bound (LB) are considered slightly higher and lower than the concentration limit, to ensure one observation is made among a discrete number of actual concentration levels. Eq. (3-10) provides the details of observation recording.

$$\begin{cases} T_i^j \neq T_{actual} & \text{if } C_{actual}^j > C_{Cr}^{UB} \text{ or } C_{actual}^j < C_{Cr}^{LB}, \\ T_i^j = T_{actual} & \text{if } C_{Cr}^{LB} < C_{actual}^j < C_{Cr}^{UB}. \end{cases} \tag{3-10}$$

The observations highlight the randomness of time to reach a concentration (TRC). A stochastic model is then needed to model these random durations. The most basic approach to model random durations is to use exponential distribution, as performed by US Nuclear Regulatory Commission [81] for evaluating the fire suspension time in nuclear applications. However, Kelly and Smith [79] suggest that the assumption of time-independent rate (of concentration, in the present study) is not realistic and exponential distribution is not an appropriate model. This leads to the need for models that allow HBAs to problems with time-dependent rates. These approaches can be implemented in WinBUGS. As a candidate for modelling the duration time, Weibull distribution with shape parameter α and scale parameter β is selected [82], given by Eq (3-11).

$$f(t) = \frac{\alpha}{\beta}\left(\frac{t}{\beta}\right)^{\alpha-1} \exp\left[-\left(t/\beta\right)^{\alpha}\right]. \tag{3-11}$$

This ensures that a time-dependent rate is modelled in the analysis, specifically if the results confirms that $\alpha \neq 1$. For $\alpha = 1$, the rate will be a constant value. In order to estimate parameters α and β, HBM is employed by developing a script in OpenBUGS software. According to Rodionov et al. [83], a number of likelihood function can be formulated for modelling random durations. In the present study, a Weibull function is used for writing the script, given in Eq. (3-12).

$$f\left(T_i^j \mid \alpha, \beta\right) = \frac{\alpha}{\beta}\left(\frac{T_i^j}{\beta}\right)^{\alpha-1} \exp\left[-\left(T_i^j / \beta\right)^{\alpha}\right], \tag{3-12}$$

where α and β are the hyper parameters of the model. **Figure 3-2** illustrates the directed acyclic graph (DAG) model for Weibull-distributed random durations of TRC limits.

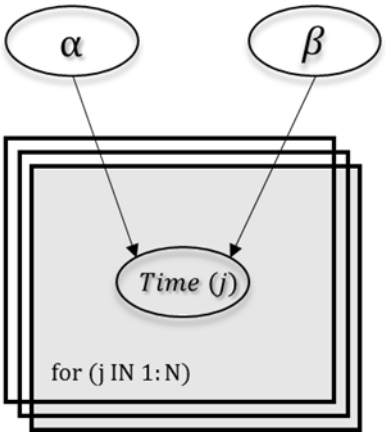

Figure 3-2. DAG model for Weibull-distributed random duration of TRC limit

The independent diffusive Gamma distribution in Eq. (3-13) is used for the prior distribution of hyper-parameters, as suggested by Kelly and Smith [79].

$$\begin{aligned} \alpha &\sim Gamma(0.0001, 0.0001) \\ \beta &\sim Gamma(0.0001, 0.0001) \end{aligned} \tag{3-13}$$

Bayesian inference is now carried out by Markov Chain Monte Carlo MCMC sampling from the likelihood function and prior distribution for obtaining the posterior distribution of the hyper parameters. The MCMC sampling process must be performed for $j = 1, 2, ..., N$ to estimate the posterior distribution for each bulk compartment. These distributions are then adopted to predict the probability of TRC level based on a Weibull distribution function. This process is repeated for the concentration profile in each medium to investigate the fate and transport of oil in the environment. The resulting probability distributions can be utilized for conducting exposure analysis in the environmental risk assessment, development of contingency plans or remediation planning of actual release accidents. At this stage, the posterior distributions can be updated if new information or data becomes available. The estimated posteriors of α and β will be used to obtain the probability distributions of TRC.

3.3 Case Study

To illustrate the application of the proposed methodology, an oil release scenario in offshore Labrador is simulated, since this region is reported to be an advent in Arctic oil and gas exploration. The possible increase in exploration activities and establishment of production facilities will cause the industry to face the threat of oil spills in this region. This case study, with its settings taken from [74], is adopted to demonstrate the application of proposed methodology in predicting fate and transport of oil in ice-infested areas. A rupture in a subsea pipeline operating in the region resulted in release of 100×10^3 kg of Statfjord oil in the Labrador Sea. The physical characteristics of spilled oil and environmental conditions are listed in **Table 3-4**.

Table 3-4. Characteristics of spilled oil and environmental conditions in the Labrador accident case study.

Oil Characteristics	**Notation**	**Value**	**Units**
Density	ρ_{oil}	832.0	Kg/m^3
Viscosity at 40ºC	μ	3.03	cP
Initial boiling point (zero evaporation)	T_0	301	K
Gradient of boiling point	T_G	500	KJ
Oil-water interfacial tension	S_t	2000	Dyne/m
Parameter	**Notation**	**Value**	**Units**
Wind speed	V	15.0	Km/h
Water temperature	T_w	273	K
Ambient air temperature	T_a	253	K
Initial oil slick thickness	t	0.02	m
Initial area of spill	A_{oil}	6000	m^2
Ice-cover area (entirely covered by ice)	A_{ice}	5400	m^2

Naphthalene is used as a surrogate stressor, representing various compounds of oil. The physiochemical characteristics of naphthalene is detailed in **Table 3-5**. The use of a surrogate for crude oil is a simplification of the scenario, as suggested by Nazir et al. [36]. It is also assumed the release is instantaneous and after the spill the oil is partitioned into the air, ice and sediment phases. The weathering processes such as emulsification and natural dispersion are not accounted for, however, the fate and transport of a low-concentration spill is analyzed. Other parameters for transport process modelling are given in **Table 3-6**.

Table 3-5. Physiochemical characteristics of naphthalene as a surrogate for Statfjord oil.

Parameter	Notation	Value	Units
Molecular weight	MW	128.2	g/mol
Solubility at 25ºC	C^s	31.7	g/m^3
Vapour pressure at 25ºC	P^s	10.4	Pa
Concentration	C_i	8	mol/m^3
$\text{Log}\, K_{ow}$	N/A	3.35	N/A

Table 3-6. Transport parameters and their uncertainty level used in level IV fugacity model.

Parameter	Notation	Distribution	Mean	Standard Deviation	Units
Air-side MTC over ice cover	K_{va}	Normal	2.0	0.01	m/h
Ice-side MTC	K_{vi}	Normal	0.01	0.001	m/h
Aerosols deposition velocity	U_{di}	Point Estimate	10.8	N/A	m/h
Melting rate	U_{iw}	Lognormal	3.9×10^{-5}	8.0×10^{-6}	m/h
Icing rate	U_{ii}	Normal	2.3×10^{-5}	5.0×10^{-6}	m/h
Water-side MTC over sediment	K_{pw}	Lognormal	0.01	0.001	m/h
Diffusion path length in sediment	Y_4	Point Estimate	5.0×10^{-3}	N/A	M
Molecular diffusivity in water	B_{w4}	Normal	4.0×10^{-6}	3.5×10^{-7}	m^2/h
Sediment deposition rate	U_{ds}	Normal	4.6×10^{-8}	4.0×10^{-9}	m/h
Sediment re-suspension rate	U_{rs}	Normal	1.1×10^{-8}	5.0×10^{-9}	m/h

The parameters listed in **Table 3-4, 3-5 and 3-6** are incorporated into the mass balance equations and solved simultaneously to estimate the fugacity of all four phases under consideration. Probability distributions are sampled in order to account for the uncertainty of input parameters.

As discussed earlier, fourth-order Runge-Kutta method is used to solve the differential equations. The calculated time-variant fugacity values are multiplied by the fugacity capacity of each compartment to obtain the corresponding concentrations according to Eq. (3-1). **Figure 3-3** illustrates the results of numerical simulations carried out for estimating the time-variant concentration profile of oil in all media including air, ice cover, water and sediment. In a general comparison, **Figure 3-3**(a) and (b) suggest that the concentration of oil in air and ice cover decreases quickly within the first few hours and remains constant at an extremely low value thereafter. However, as depicted in **Figure 3-3**(c) and (d), the concentration in water and sediment column continues to decrease for about 10 hours and remains at a higher value in comparison to air and ice cover. This is mainly due to the higher fugacity capacity of water and sediment enabling them to absorb more quantity of chemicals. The approximately constant concentrations in water and sediment are 3×10^{-6} and 9.5×10^{-5} respectively. These results are in good agreement with a previous study by Yang et al. (2015). However, the main exclusivity of the present research is the estimation of oil concentration while accounting for the uncertainty of input parameters. This has resulted in a number of configurations (curves) for the concentration time-series in each phase, as shown in different plots in **Figure 3-3**. To better illustrate this, a number of the concentration profiles predicted for the ice cover are presented in a magnified form in **Figure 3-4**.

.

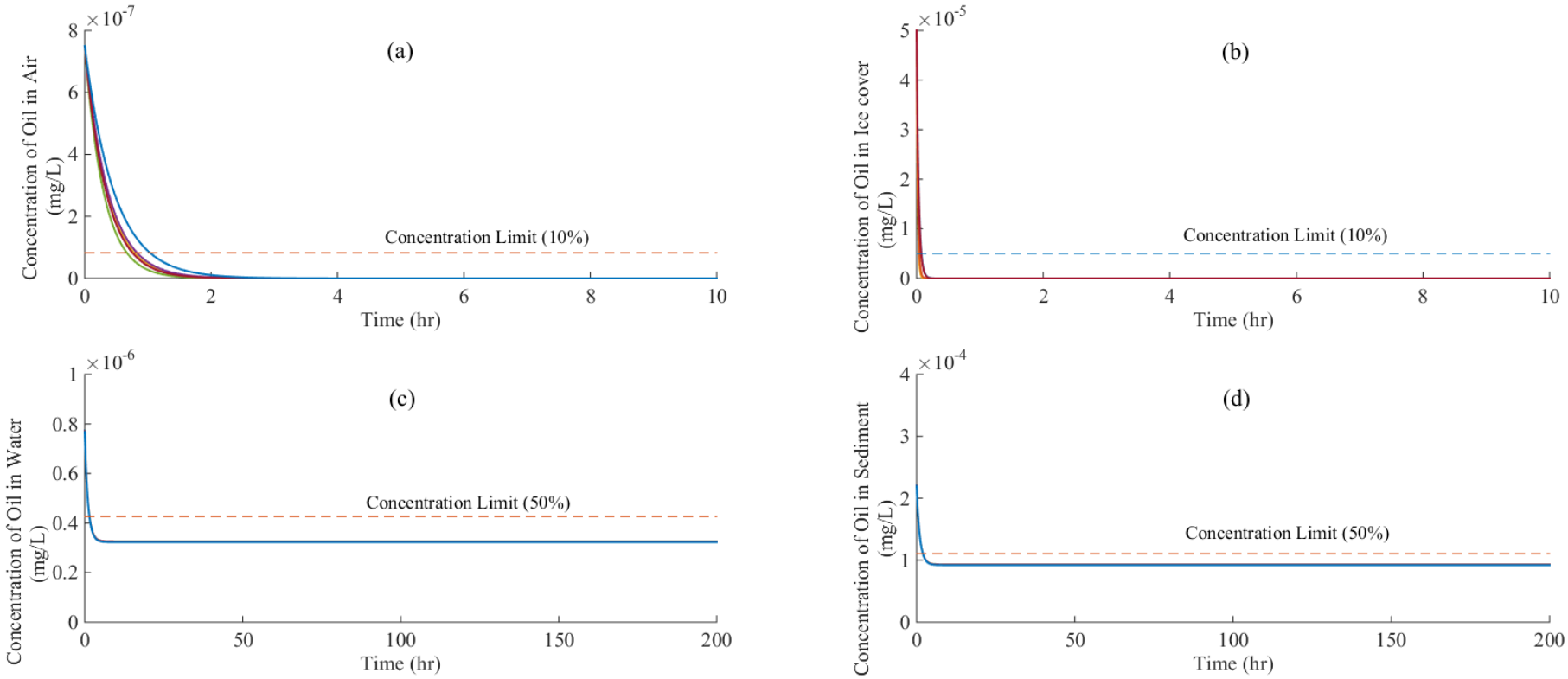

Figure 3-3. Numerical results of level IV fugacity model for concentration of oil in different media, multiple curves in each plot depict the influence of uncertainty of input parameters on concentration profile.

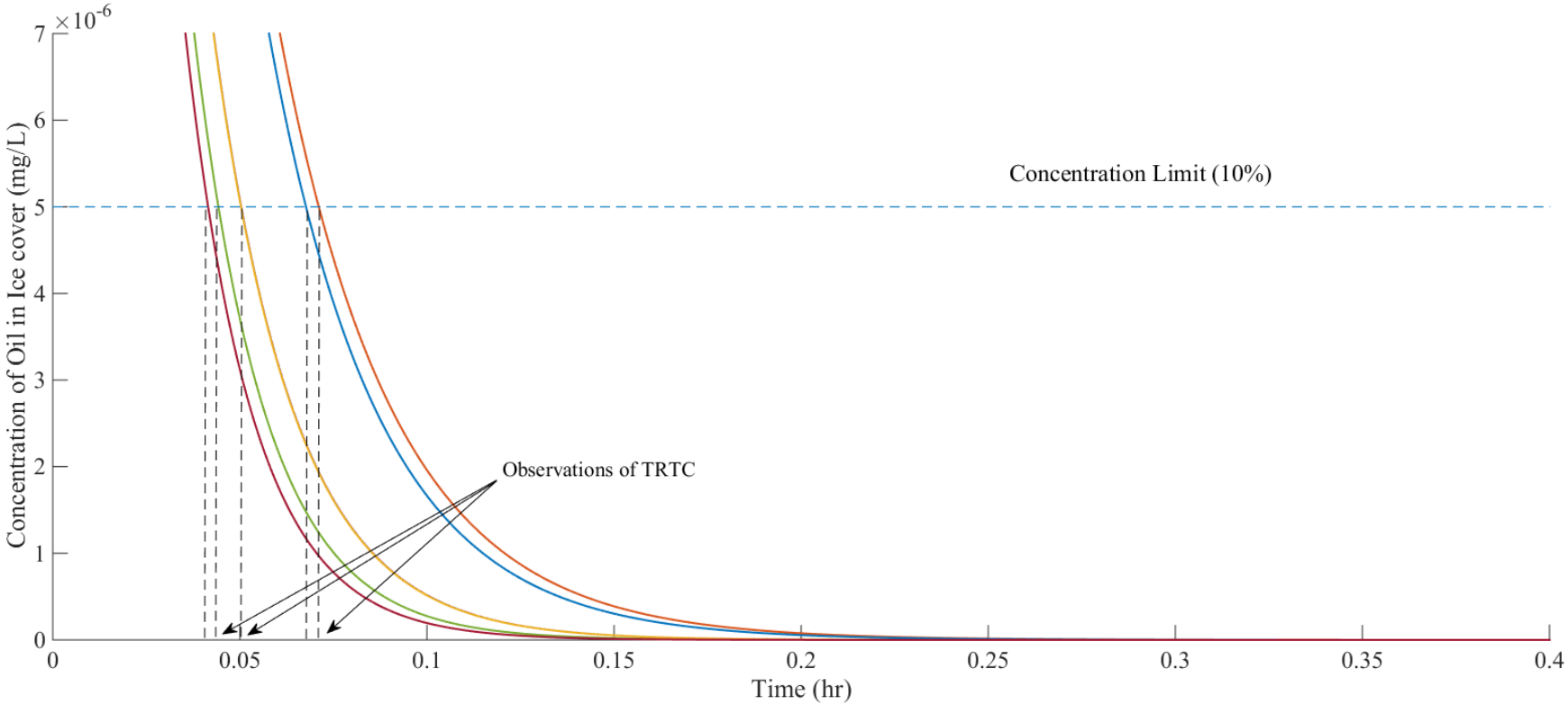

Figure 3-4. Illustration of observations of TRC made from the numerical results of ice cover mass balance function.

A concentration limit is considered for obtaining the observations of TRC. These limits are an example of those that can be defined by the operators or safety managers. As explained in the methodology section, an observation is the time in which the concentration of oil in the medium becomes equal to the specified limit. Some of these observations made within the ice cover simulation results are presented in **Figure 3-4**. The times recorded for these phases confirm the faster fate and transport of oil in this medium compared to that of others. The observations are then used for developing the likelihood functions and estimating the posterior distribution of Weibull parameters, α and β, as discussed in 3.2.2. For the Bayesian inference in OpenBUGS, the model is initiated for three chains, each simulating 10^5 iterations. **Figure 3-5** presents the estimated posterior distribution of shape parameter α for two of the media, air and ice cover. In this figure, the complete trace plots of predicted parameter α for air phase is also depicted confirming the convergence of sampling process.

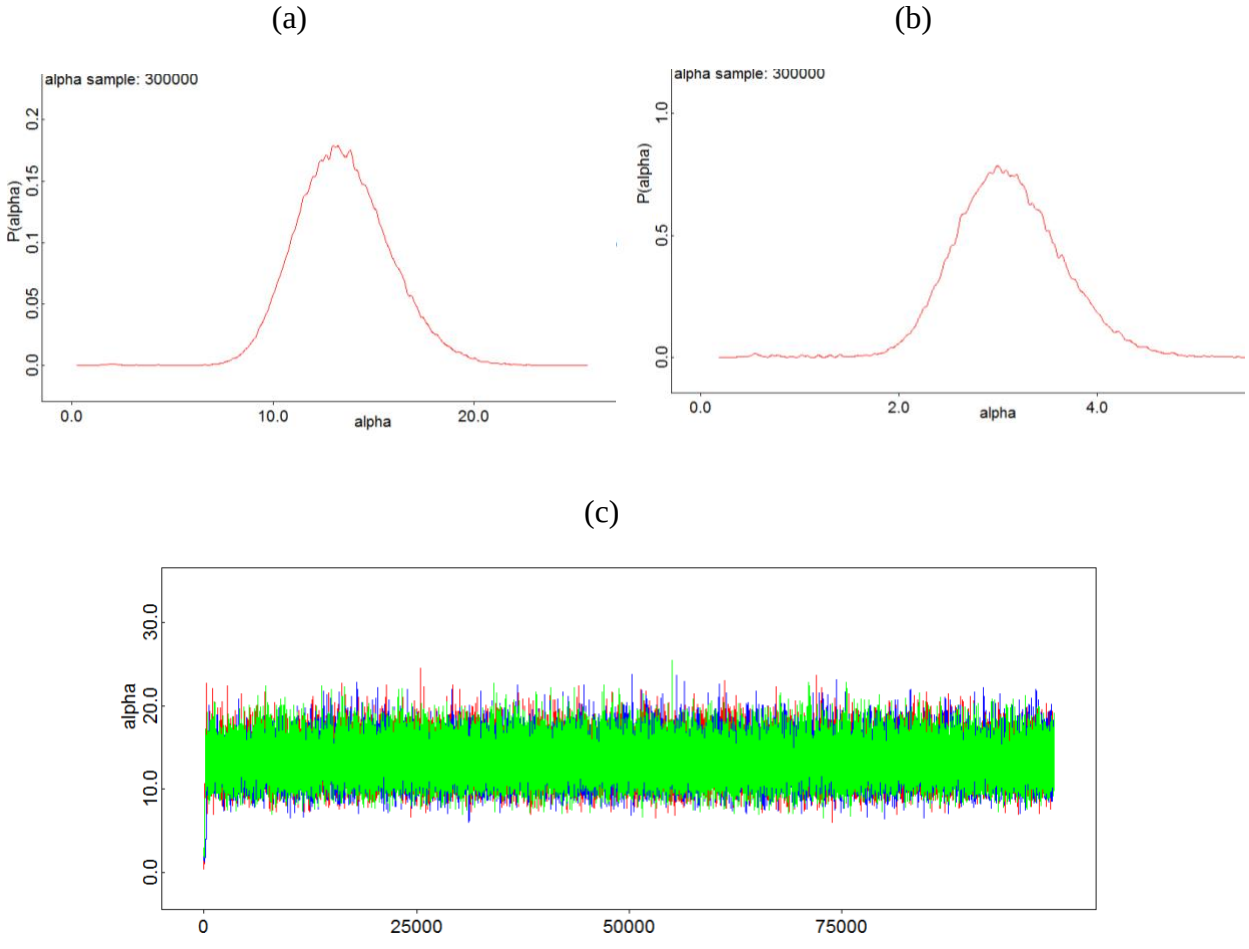

Figure 3-5. Posterior distribution of Weibull shape parameter α for a) TRC in air and b) TRC in ice cover, c) is the trace of Weibull parameters in MCMC sampling.

As shown in **Figure 3-5** , the value of α for 2.5 and 97.5 percentile is $\alpha_1 = [9.383, 18.34]$ for air and $\alpha_2 = [2.14, 4.23]$ for ice cover, respectively. The expected values of alpha are calculated as $E[\alpha_1] = 13.5$ and $E[\alpha_2] = 3.1$, highlighting the importance of time-dependent assumption for the occurrence rate of TRC, as discussed in the methodology section.

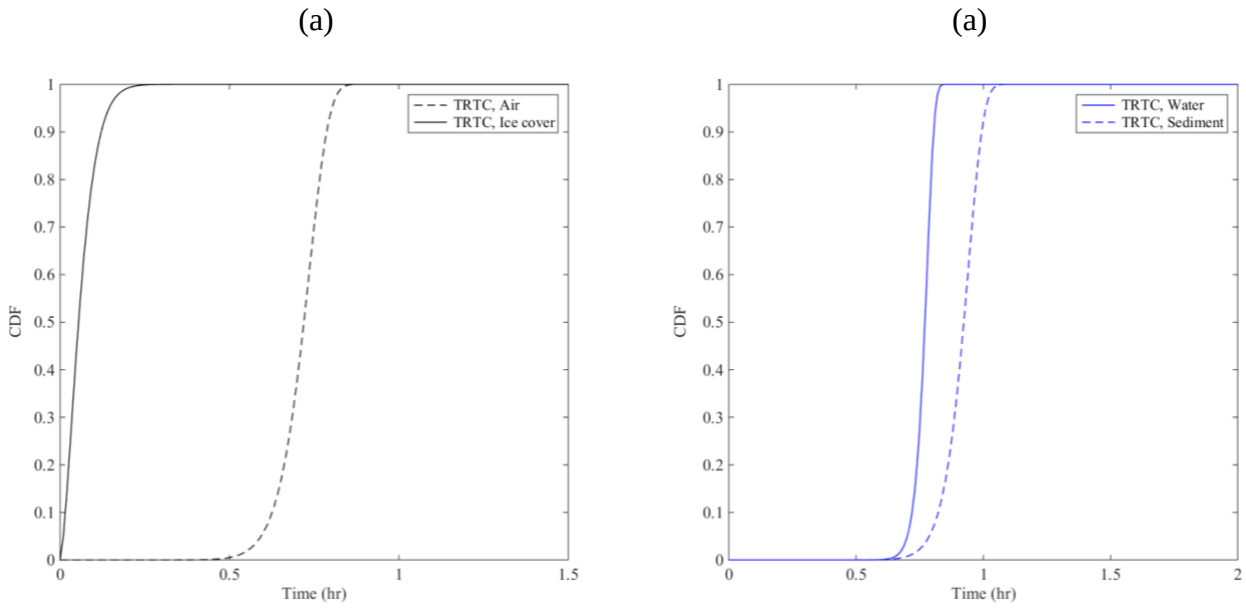

Figure 3-6. Estimated cumulative distribution function of TRC in all media.

The obtained shape and scale parameters of Weibull distribution are used to develop the cumulative distribution functions of TRC, which is the time that the concentration of oil in each phase will reach the specified limits. The estimated probabilities are illustrated in **Figure 3-6** for all media. It is observed in **Figure 3-6**(a) that with 0.95 probability the concentration of oil in air will reach 10% of its maximum level within the first 50 minutes. However, this period is predicted to be less than 15 minutes for the ice cover medium. As shown in **Figure 3-6**(b), it is predicted that, with 0.95 probability, the concentration of stressor in water column will be reduced to 50% of the maximum within 50 minutes. After that, the concentration will be reduced at a slower pace and become approximately constant at 35% of its maximum level. The TRC for sediment column is estimated at approximately one hour with a similar level of confidence. It is observed from the results that the fate and transport of oil in all media is substantially rapid, despite the relative

difference between different phases. This highlights the importance of establishing sound, efficient remediation plans in the case of an oil release accident in such a vulnerable environment. The present methodology is a useful tool for improving the reliability of such risk management strategies.

3.4 Conclusion

The present paper proposes a methodology for predicting the stochastic fate and transport of spilled oil in ice-infested regions, as an essential component of risk assessment in the planning and operation stages of future Arctic oil production facilities. The developed method integrates the conventional fate and transport models of chemicals with an HBA to achieve its objective. This allows incorporating the uncertainty associated with the influencing parameters. A fugacity-based model is developed and numerically solved to obtain the time-variant concentration of oil in the media. As a case study, a hypothetical scenario is simulated in which a significant amount of Statfjord oil is released from a subsea pipeline into the Labrador Sea. The results indicate that the concentration of oil in air and ice cover decreases quickly within the first few hours, however this process takes up to 10 hours for the concentration in water and sediment column. It is predicted, with 0.95 confidence, that the concentration of oil in air and ice cover phases reaches 10% of its maximum level within the first hour. However, this time is enough to only reduce the concentration of stressor in water column and sediment to 50% of the maximum level. The proposed framework can predict the concentration profile of oil released in an offshore accident more accurately by considering the dependency on input parameters using the observation data. The methodology can be readily applied by operation and safety managers to improve the safety of offshore oil and gas facilities by increasing the effectiveness of contingency plans. It can also be used for developing more efficient remediation plans.

Acknowledgements

Authors thankfully acknowledge the financial support provided by National Centre for Maritime Engineering and Hydrodynamic (NCMEH) at the Australian Maritime College (AMC).

Chapter 4: An Ecological Risk Assessment Model for Arctic Oil Spills from a Subsea Pipeline

Abstract

There is significant risk associated with increased oil and gas exploration activities in the Arctic Ocean. This paper presents a probabilistic methodology for Ecological Risk Assessment (ERA) of accidental oil spills in this region. A fugacity approach is adopted to model the fate and transport of released oil, taking into account the uncertainty of input variables. This assists in predicting the 95^{th} percentile Predicted Exposure Concentration ($PEC_{95\%}$) of pollutants in different media. The 5^{th} percentile Predicted No Effect Concentration ($PNEC_{5\%}$) is obtained from toxicity data for 19 species. A model based on Dynamic Bayesian Network (DBN) is developed to assess the ecological risk posed to the aquatic community. The model enables accounting for the occurrence likelihood of input parameters, as well as analyzing the time-variable risk profile caused by seasonal changes. It is observed through the results that previous probabilistic methods developed for ERA can be overestimating the risk level.

4.1 Introduction

The significant rise in global energy demand has increased the attention of oil and gas industry to exploiting the hydrocarbon reserves in less explored areas. This includes the Arctic Ocean, containing about 13% of the world's undiscovered oil reserves [63, 65]. Despite the unique opportunity, the socio-environmental impact of exploration activities is an important aspect to be taken into account in decision making. Over the past few years, the concerns around oil spill accidents in the Artic region has prompted the stakeholders including the governments of countries in those regions and the International Maritime Organisation (IMO), to review and amend existing regulations with respect to marine pollution [84, 85]. This is due to the major risk factors associated with the region which will definitely influence the likelihood (e.g. exerted loads from drifting icebergs) and consequences (e.g. slower decomposition of hydrocarbons in lower temperatures) of possible oil release accidents [66, 68, 69]. These are the two components of risk that must be analysed for the amendment of in place policies as well as for the development of contingency plans.

There can be a significant risk posed by underwater release of oil [86]. The toxicity of chemicals can also adversely affect marine organisms with possible long-term consequences. There has been a great deal of research conducted on the ecological risk assessment (ERA) of waste from offshore oil production platforms [27, 32, 87]. However, this aspect of subsea oil spill has recently achieved even more attention. Nazir et al. [36] developed a methodology for ERA of oil spill from a riser. The proposed model is based on US EPA framework and adopts a fugacity-based approach to estimate the exposure to contaminants in the marine environment. A Monte-Carlo Simulation (MCS) was applied to incorporate the uncertainty of multimedia input parameters, and the analysis of stressor effect on the organisms was achieved by using toxicity data adopted from literature. Their method characterizes the ecological risk by transforming risk quotient (RQ) into probability distributions. French-McCay [88] presents a biological effects model coupled to an oil trajectory and fate model for supplying the required spatial and temporal estimation of oil component concentrations. In this method, the long-term effects are quantified using food web modelling and MCS is performed for evaluating the risk of a spill scenario.

In the Arctic oil spill context, there have been several attempts towards ERA based on both qualitative and quantitative approaches. Afenyo et al. [33] proposed a probabilistic ERA model specifically for Arctic marine oil spills. In their model, a combination of dispersion fugacity-based

fate modelling and MCS is used to develop probability distributions for the exposure concentration and to predict the 95th percentile risk. The presented probabilistic approach propagates the uncertainty of input variables through the model. However, the probabilistic dependency of risk on those inputs is neglected. Moreover, the proposed methods do not provide a platform for the assessment of environmental risk with respect to important influencing parameters such as seasonal conditions.

Unlike classical probabilistic methods, Bayesian techniques are promising for probabilistic risk assessment (PRA) applications. This is mainly because they are able to deal with a wide range of information types and provide useful estimation of model parameters when the data is sparse or the correlation between them is hard to perceive [75]. Bayesian network has been adopted by several researchers for conducting PRA [53, 54, 89]. Nevalainen et al. [37] have used BN for analysing the ecological impacts of oil spills on the Arctic environment and for providing a holistic view of such accidents. The authors assert that a food web approach be used as a more appropriate choice for ERA. In their model the influence of input parameters such as oil spill size and season on the acute and long-term ecological impacts are incorporated into the BN. However, it is suggested that the model must be enhanced with the quantification of problem variables. This is essential from a quantitative risk assessment viewpoint as well as for utilising the optimum capacity of BN.

The main objective of this study is to develop a probabilistic methodology for conducting ERA of an oil spill accident in the Arctic. A fugacity model is utilized to simulate the fate and transport of released oil and to predict the exposure concentration in different media. A BN is established, based on the US EPA framework, to estimate the risk posed by release of oil from a subsea pipeline, on the environment containing a wide range of organisms. To demonstrate the application of the proposed methodology, a case study of the Kara Sea is selected.

4.1.1 Ecological Risk Assessment (ERA)

A framework is suggested by the United States' EPA for conducting ERA. The main steps of this framework are i) problem formulation, ii) exposure analysis, iii) risk characterisation and iv) risk management and communication [27]. The problem formulation phase focuses on aggregating information, involving the assessment of endpoints, and planning for the risk analysis. The endpoints are selected based on the criteria provided by guidelines. In the case of underwater oil spills, marine organisms will be influenced by toxic chemicals with a concentration above an

acceptable threshold. It is recommended by previous researchers that selecting a food web is more realistic than assessment with single species or groups as an endpoint [37, 90]. However, this is a challenging task since the toxicity data of an entire food web is hard to obtain, particularly from the Arctic ecosystem. The present study therefore chooses the endpoints based on the availability of toxicity data in the literature. In the analysis step, the aim is at assessing the exposure and corresponding effects on the endpoints. The risk characterization phase uses the obtained results from the previous steps for mapping the risk profile posed by the presence of contaminant(s) in the studied environment. This assists in developing risk mitigation strategies or contingency plans to be shared with the stakeholders [36]. The present paper focuses on developing a quantitative ERA model using US EPA framework. In the next section a brief discussion on fundamentals of BN is presented. In Section 4.2, the proposed methodology is explained in detail followed by a numerical example in Section 4.3. Lastly, the concluding remarks of this paper are provided in Section 4.4.

4.1.2 Bayesian Network (BN)

BN is a directed acyclic graph used for reasoning under uncertainty by considering the causal relationships. These relationships are represented by directed arcs, among a number of random variables that are represented by chance nodes. BN estimates the joint probability distribution of a set of random variables using the conditional independencies and the chain rule, given in Eq. (4-1).

$$P(X_1, X_2, ..., X_n) = \prod_{i=1}^{n} P(X_i \mid pa(X_i)) \qquad (4\text{-}1)$$

where $pa(X_i)$ is the parent set of variable X_i. As an example, the joint probability distribution of the random variables X_1 - X_4 illustrated in **Figure 4-1** is estimated by $P(X_1, X_2, X_3, X_4) = P(X_1)P(X_2)P(X_3 \mid X_1)P(X_4 \mid X_2, X_3)$.

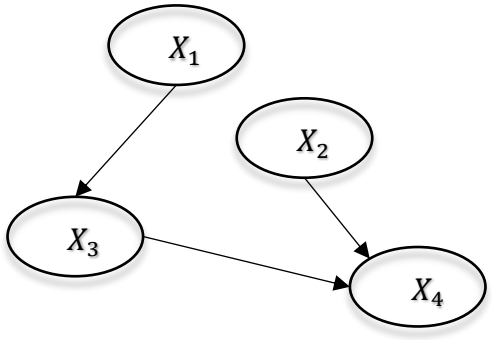

Figure 4-1. Schematic of a BN.

BN is capable of updating the estimated probabilities when new information becomes available about any of the random variables (i.e. evidence to chance nodes). For instance, if the variable X_2 in **Figure 4-1.** Schematic of a BN. is known to be in state *e*, the joint probability distribution is updated based on the Bayes' theorem, given by Eq. (4-2):

$$P(X_1, X_3, X_4 \mid e) = \frac{P(X_1, X_3, X_4, e)}{\sum_{X_1, X_3, X_4} P(X_1, X_3, X_4, e)} \tag{4-2}$$

Dynamic Bayesian Networks (DBNs) represent stochastic processes and can be used for modelling the temporal behaviour of a set of random variables [57]. They divide the time line into a series of time slices each of which are connected from nodes in time slice $t - \Delta t$ to the node in time slice t , as shown in **Figure 4-2**. This figure illustrates a schematic of DBN for which the joint probability distribution of its variables can also be estimated using Eq. (4-1).

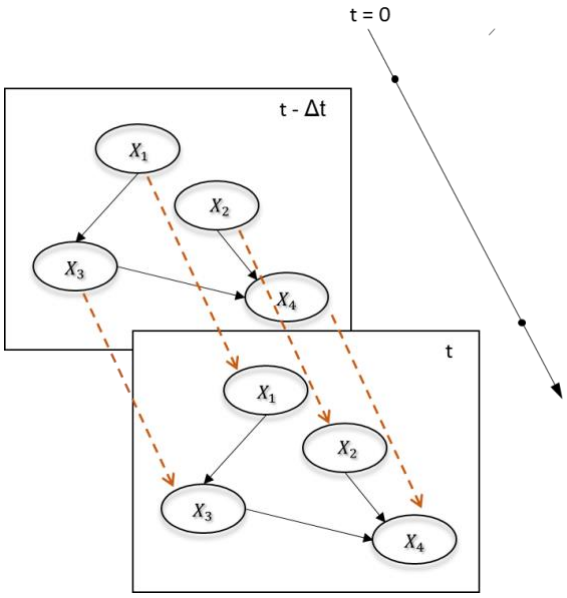

Figure 4-2. Schematic representation of a DBN.

An extensive outline of BN and probabilistic knowledge elicitation is provided by Barber [91] and Pearl [58]. BN has a wide range of applications in risk and reliability assessment of engineering problems. Further details on using BN in different engineering applications can be found in previous research [42, 51, 52, 92-94].

4.2 Methodology: Ecological Risk Assessment using BN

The proposed methodology provides a model based on US EPA framework of probabilistic analysis of ecological risk posed by release of oil from a subsea pipeline in the Artic region. This method can be adopted to improve the preparedness for more oil and gas industrial activities in the Arctic region and for amending the safety policies and regulations currently in place. The model can also help in preparing risk mitigation plans for oil release accidents. An overview of the proposed methodology is illustrated in **Figure 4-3**, incorporating the key elements covered in each stage.

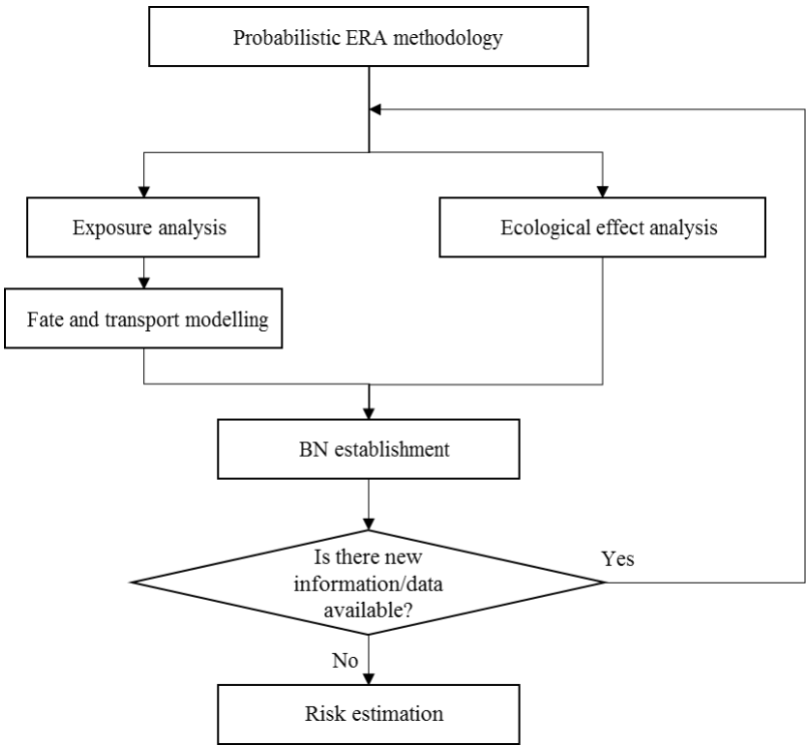

Figure 4-3. Developed methodology for probabilistic ERA of oil spills in the Arctic environment.

4.2.1 Exposure Analysis

Exposure analysis is the key component of ERA of an accidental oil release in marine environment, which estimates the extent of contamination, identifies the exposed organisms, the exposure pathways and the possible responses to stressors [31, 36, 95]. The level of contamination can be assessed by a fate and transport model. This results in obtaining the spatio-temporal concentration profile of pollutants in the environment.

4.2.1.1 Dispersion Model

An accidental release from a subsea pipeline or riser will result in a plume of oil on the surface of the sea. This release can be instantaneous or continuous, however, the present study focuses on a sudden spill [96]. The released oil may be subjected to several processes including evaporation, dispersion and advection. Among these, dispersion models can be used for evaluating the transport of oil from a generated plume to further locations. Concentrations can therefore be estimated as a function of location and time. The model presented by Logan [97] is used for the analysis. Assumptions made for this model are that the pollutant is uniformly distributed in the water column

and no degradation occurs during the movement. This results in Eq. (4-3) for transport along the x axis.

$$C(r,t,x) = K \frac{\exp\left[\frac{-(x-wt)^2}{4D_x t}\right]}{\sqrt{4\pi D_x t}}, \tag{4-3}$$

where K is the released amount of oil per area and w is the wind speed. Eq. (4-3) confirms the reduction of oil concentration in further locations from the point of release. Although this equation can be used for computing the time-series concentration in specific locations, a model is also required to account for the transport processes in the bulk phases (e.g. water and sediment) and their sub-compartments. For more details of the dispersion model and consideration of trajectories refer to previous studies by Afenyo et al. [93], Afenyo et al. [30].

4.2.1.2 Fate and Transport

For modelling the fate and transport of spilled oil in the Arctic region, a fugacity approach is followed, as suggested by Yang et al. [74] and Afenyo et al. [31]. Fugacity (f), having a unit of pressure, is known as the tendency of a chemical to escape from a phase and it is used as a substitute for chemical potential. The relationship between fugacity and concentration is given by Eq. (4-4):

$$C = f \times Z \tag{4-4}$$

where C is the concentration of chemical (mol/m^3), f is the fugacity (Pa) and Z is the fugacity capacity (mol/m^{3}Pa). Fugacity capacity represents the tendency of a medium to absorb a chemical and a medium with a larger Z will have a higher concentration of chemicals. Mackay [28] proposes four levels of fugacity models providing the advantages of each level and its different applications. The present study adopts the level IV model as it is more realistic and can estimate the time-dependent behavior of the chemicals. The method proposed by Yang et al. [74] is used as the basis for the developed probabilistic framework. More detailed discussions on fugacity models can be found in [28, 36, 74].

The initial step to develop the fugacity model is to define the media involved in the oil spill scenario. Since risk assessment of an accident in the Arctic is the interest of this study, four bulk

compartment including air, water, ice and sediments are considered. Each of these media may carry few sub-compartments. For instance, ice cover may consist pure ice, liquid water, air and organic matter. The properties of the media and their sub compartments must be determined prior to the modelling process. In addition to these properties, the input variables of the model including the contaminant properties and environmental conditions must be known. This also involves quantifying the associated uncertainty with influencing parameters. Uncertainties are often classified into aleatory, accounting for the variability of environment, and epistemic uncertainty that represents the lack of knowledge about the process. The present paper only addresses the uncertainty associated with data while the analysis of model uncertainty is not in the scope of this paper. The information regarding the type and specifications of probability distributions will be later provided in the case study section. The level IV fugacity model can now be developed by formulating the unsteady-state mass balance equations, with a general form given in Eq. (4-5):

$$V_i Z_i \frac{df_i}{dt} = I_i + \sum D_{ij} f_j - f_i \left(\sum D_{ij} + D_{ai} + D_{Ri} \right), \tag{4-5}$$

where i and j denote the bulk phase and sub-compartment, respectively. I_i is the input rate of a chemical compound in i^{th} bulk phase and its unit is (mol/s). Z_i is the fugacity capacity of each bulk compartment and D_{ij}, D_{ai} and D_{Ri} are the transport parameters, referred to as D-values. The fugacity capacity of each bulk phase is estimated using Eq. (4-6).

$$Z_i = \sum_j \varphi_{ij} Z_{ij}, \tag{4-6}$$

where φ_{ij} is the volume fraction and Z_{ij} is the fugacity capacity of the sub-compartment. More details on calculation of fugacity capacity are provided in **Table 4-1**. Transport parameters (D-values) must also be determined to formulate the fugacity equations. The calculation methods for these considered values are detailed in **Table 4-2**.

Table 4-1. Calculation of fugacity capacity for all media, Z -values in (mol/m3.Pa), for sub-compartments and bulk compartments.

Bulk compartment (i)	Z_i	**Comment**	
Air (1)	$Z_1 = Z_{11} + \varphi_{13} Z_{13}$		
Ice cover (2)	$Z_2 = \varphi_{21} Z_{21} + \varphi_{22} Z_{22} + \varphi_{23} Z_{23} + (A_{2a} / V_2) Z_{2a}$	A_{2a} ice-air interface area, V_2 is ice cover volume.	
Water (3)	$Z_3 = Z_{32} + \varphi_{33} Z_{33} + \varphi_{34} Z_{34}$		
Sediment (4)	$Z_4 = \varphi_{42} Z_{42} + \varphi_{43} Z_{43}$		
Sub-compartment (j)	Z_{ij}	**Comment**	**Reference**
Air (Z_{i1})	$1/RT$	$R = 8.314$ (Pa.m^3/mol.K), T is absolute temperature (K).	
Water (Z_{i2})	$1/H$ or C^s/P^s	H is Henry's law const. (Pa.m^3/mol), C^s is aqueous solubility (mol/m^3), P^s is vapour pressure (Pa).	[33]
Solids (Z_{i3})	$x_{ij} K_{oc} \rho_{ij} H$	x_{ij} is organic carbon fraction, $K_{oc} = 0.41 K_{ow}$ is organic carbon partition coefficient, $\rho_{ij} = 2.4$ is density of solids (kg/L).	[33]
Aerosols (Z_{13})	$6 \times 10^6 / P_L^S \, RT$	P_L^S is liquid vapour pressure (Pa).	[71]
Biota (fish) (Z_{34})	$0.048 \rho_{24} K_{ow} / H$	$\rho_{24} = 1000$ is density of biota (kg/m^3), K_{ow} is octanol-water partition coefficient.	[33]
Ice-air interface (Z_{ia})	K_{ia} / RT	K_{ia} is ice surface-air partition coefficient, $\ln K_{ia}(12.5^\circ C) = 0.68 \ln K_{ow} - 19.63 + \ln K_{wa}$ K_{wa} is water-air partition coefficient.	[28]
Organic carbon in ice cover (Z_{23})	$0.41 K_{ow} Z_l$	$Z_l = K_{wa} / RT = 1/H$	[71]

Table 4-2. Calculation of transport parameters considering two loss processes (advection and reaction) and three transport processes (diffusion, deposition and re-suspension).

Interface	**Comment**	**Details**	**Total D -value**
Air (1)-Ice cove (2)	Diffusion	$D_v = 1/(1/K_{va} A_{12} Z_{11} + 1/K_{vi} A_{12} Z_{22})$	$D_{12} = D_v + D_{di}$ $D_{21} = D_v$
	Deposition	$D_{di} = A_{12} U_{di} \varphi_{13} Z_{13}$	
Ice cover (2)- Water (3)	Melting	$D_{iw} = A_{23} U_{iw} Z_{22}$	$D_{32} = D_{iw}$ $D_{23} = D_{ii}$
	Icing	$D_{ii} = A_{23} U_{ii} Z_{33}$	
Water (3)-Sediment (4)	Diffusion	$D_y = 1/(1/K_{pw} A_{34} Z_{33} + Y_4 / B_{w4} A_{34} Z_{33})$	$D_{34} = D_y + D_{ds}$ $D_{43} = D_y + D_{rs}$
	Deposition	$D_{ds} = A_{34} U_{ds} Z_{34}$	
	Re-suspension	$D_{rs} = A_{34} U_{rs} Z_{43}$	
	Reaction	$D_{Ri} = K_{Ri} V_i Z_i$	
	Advection	$D_{ai} = G_i Z_i$	

The mass balance equations for air, ice cover, water and sediment are given by Eqs. (4-7) to (4-10).

$$V_1 Z_1 \frac{df_1}{dt} = I_1 + D_{21} f_2 - f_1(D_{12} + D_{a1} + D_{R1}), \tag{4-7}$$

$$V_2 Z_2 \frac{df_2}{dt} = I_2 + (D_{12} f_1 + D_{32} f_3) - f_2(D_{21} + D_{23} + D_{a2} + D_{R2}), \tag{4-8}$$

$$V_3 Z_3 \frac{df_3}{dt} = I_3 + (D_{23} f_2 + D_{43} f_4) - f_3(D_{32} + D_{34} + D_{a3} + D_{R3}), \tag{4-9}$$

$$V_4 Z_4 \frac{df_4}{dt} = I_4 + D_{34} f_3 - f_4(D_{43} + D_{a4} + D_{R4}), \tag{4-10}$$

where the direct input into the air, ice-cover and sediment phases are considered as negligible (i.e. $I_1 = I_2 = I_3 = 0$). However, the input rate into water can be estimated by $I_3 = Q_3 \times C_i$, where Q_3 is the volumetric flow rate of oil in (m^3/s) and C_i is the molar concentration of oil in (mol/m^3). The fourth-order Runge-Kutta method is adopted to solve the set of above differential equations simultaneously. The fugacity of all compartments is then multiplied by the corresponding fugacity capacity to obtain the concentration profile of each bulk compartment (see Eq. (4-4)). To obtain the predicted exposure concentration (PEC), Eq. (4-11) is used.

$$PEC = P(xp) \times C \times BaF, \tag{4-11}$$

where $P(xp)$ is the exposure probability, given by the ratio of spill impact area to the total area, C is the concentration, and BaF represents the bioavailable fraction. The concentration of oil in different media, C, can be estimated using the fugacity-based method suggested by Arzaghi et al. [98], also explained earlier in Section 3.2. The PEC will represent the extent of present pollutants that will reach the ecosystem and affect them adversely.

The uncertainty is propagated through the model using a MCS. For this purpose, 500 samples are obtained from the input variables of the model and probability distributions are generated for each variable including PEC. As recommended by Sadiq et al. [27], the 95th percentile of the PEC ($PEC_{95\%}$) can be used for calculating the ecological risk. A bootstrapping approach is then adopted to compute the probability distribution of 95th percentile. This involves resampling 10,000 times, with replacement, from the available PEC values. Once the distributions are developed, it is

possible to quantify the mean and standard deviation of $PEC_{95\%}$ needed for further computations in the method.

4.2.2 Analysis of Ecological effects

The adverse ecological effects on the ecosystem is dependent upon the extent of pollution (i.e. released chemicals) as well as the level of tolerance that the ecosystem has to the present toxicants, which can be up to thousands of compounds in the case of an oil spill. The process of analysis will be intractable if all compounds are to be considered. Because its acute toxicity is significantly more than moderate in comparison with other chemicals, this paper employs naphthalene as a surrogate to oil. That is the level of risk posed to the environment by oil can be represented by naphthalene due its high level of toxicity. This makes naphthalene of great concern from a risk assessment viewpoint. Moreover, the proposed method can be readily used for other hydrocarbons as well. Based on the availability of data, marine aquatic life is selected as the assessment endpoint.

A number of measures are usually used for assessing the effect of pollutants on different organisms among which Lethal Concentration at 50% mortality (LC_{50}) and No Effect Concentration (NEC) data are less scarce. These parameters describe the extent of chemical accumulation in the organisms as well as being a representative of the concentration threshold above which chronic effects can be experienced [99, 100] . Predicted No Effect Concentration (PNEC) data is estimated by dividing the acute toxicity data (LC_{50} for 96-hours period) by 100, as suggested by Sadiq et al. [24]. Based on the recommended framework, the data for shorter durations are converted to LC_{50} 96-hours exposure times.

In order to obtain the PNEC values, temperate species are a good substitute for those living in the Arctic environment [101]. PNEC data were gathered for 19 species of 5 groups adopted from previous research. To account for the associated uncertainty, probability distributions are developed for the lowest 5^{th} percentile of toxicity data. This also assists in ensuring a higher level of safety through representing the entire community by the most susceptible ecological habitants. A unique component of the proposed methodology is that it divides the species into two categories for conducting ERA. This is because some of the species are exposed to the contamination in sediment compartment, in addition to the water phase. This may potentially make them more susceptible to lethal effects from the pollution. Bootstrapping is therefore carried out to generate the $PNEC_{5\%}$ for both ecological groups. Using 10,000 samples, with replacement, from each group, the mean and standard deviation of PNEC5% are calculated.

4.2.3 Risk Assessment

Risk quotient concept is used in this study as the basis of PRA method. The mathematical relationship for RQ is given by Eq. (4-12):

$$RQ = \frac{PEC_{95\%}}{PNEC_{5\%}} \tag{4-12}$$

By considering $PNEC_{5\%}$ and $PEC_{95\%}$, it is ensured that for an RQ values of 1, the 95% of the aquatic ecological habitants are protected 95% of the time. The uncertainty of these variables is modelled using lognormal probability distributions. Lognormal distributions are multiplicative reproductive, hence the sum of two lognormally distributed parameters will follow a lognormal distribution. This property is used to develop the probability distributions of RQ parameter, with properties given by Eqs. (4-13) and (4-14). That is, based on the relationship in Eq. (12) a lognormal distribution can be established for RQ using the properties of PNEC5% and PEC95% distributions.

$$\mu_{\ln RQ} = \mu_{\ln PEC_{95\%}} - \mu_{\ln PNEC_{5\%}} \tag{4-13}$$

$$\sigma^2_{\ln RQ} = \sigma^2_{\ln PEC_{95\%}} - \sigma^2_{\ln PNEC_{5\%}} \tag{4-14}$$

Therefore, the mean and variance of RQ is obtained for both groups of the species, one exposed to contaminants in water column and the other from both water and sediment phases. 10,000 samples are generated from each lognormal distribution for evaluating the risk, given by Eq. (4-15).

$$R(i) = \varphi\left(\frac{1}{S_m}(\ln(RQ(i)) - X_m)\right), \tag{4-15}$$

where $\varphi(x)$ is the normal distribution function with a mean of 0 and standard deviation of 1. X_m and S_m are the mean and standard deviation of logarithmically transformed data. These values are calibrated to 2.85 and 1.736, respectively, as recommended by [102]. The calibration is done based on the lognormal distribution function (see Eq. (4-15)) to ensure that an acceptable risk of 5% is achieved with an RQ value of 1. That is, through the risk assessment only 5% of species may be at risk while 95% of the population are protected. The total risk can also be estimated by combining the effect from contaminant in different bulk phases and proposed method can also incorporate the risk estimate of multiple stressors.

4.2.4 BN Model Establishment

A BN model has previously been developed before by Nevalainen et al. [37] for conducting risk assessment of Arctic oil spills and evaluating acute and long-term impacts on marine species. However, the model uses expert judgment for constructing the network and compiling its Conditional Probability Tables (CPTs), overall presenting a tool for qualitative risk assessment. The present paper, however, proposes a BN model that is developed for a quantitative approach to PRA and uses mathematical relationships in conjunction with the knowledge of oil and gas and environmental engineering experts to build the model. The DBN is established based on the causal dependencies of each variable on its parent nodes, as discussed in Section 4.1.2. These dependencies are obtained from the physical interpretations of the methods provided in previous sections of the methodology. **Figure 4-4** depicts a single time slice of the developed DBN. For instance, the dependency of node *PEC in sediment* on the *Exposure probability* and *Concentration in water* nodes shown in **Figure 4-4** is defined based on their relationship in Eq. (4-11). Based on the literature, it is considered that the seasonal condition greatly influences the likelihood of an accidental release in the environment resulting in a concentration of contaminant in the media; hence the relationship between *Season*, *Accident* and *Concentration* nodes.

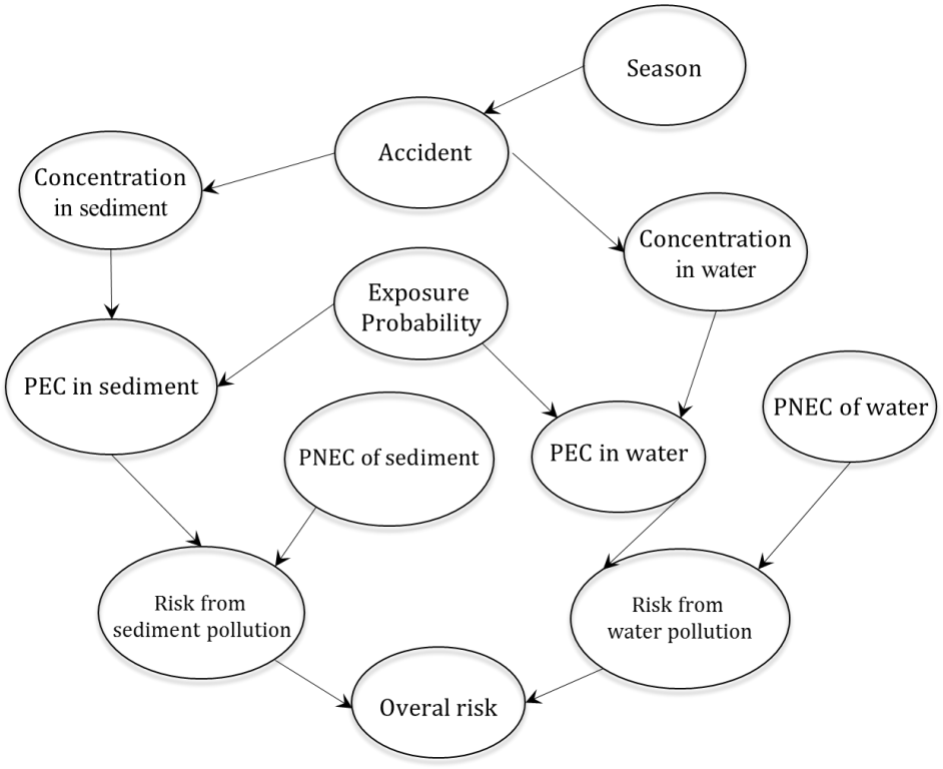

Figure 4-4. A single time slice of the developed DBN for ecological risk assessment of oil spill in the Arctic region (Note that this network is replicated for a number of time slices to simulate the time frame of interest).

In the next step, numerical simulations are developed in MATLAB to solve the level IV fugacity equations, dispersion model and other mathematical equations from the previous sections. By incorporating the uncertainty of input variables, probability distributions are obtained for output parameters such as the concentration in water or $PNEC_{5\%}$ of sediment phase. The data is then fit to appropriate probability density functions for each parameter. In order to quantify the relationships among the variables in the DBN model, the conditional probability distributions of random variables are specified (e.g. $P(PEC \mid pr, C)$). Since the variables are in a continuous space, discretization is performed providing the probability values for a number of mutually exclusive states. The probability mass functions are included in the CPTs of the network nodes. As recommended by Friis-Hansen [103], the discretization is performed by individually discretizing the variables of the domain considering the hierarchy of the nodes (i.e. discretization of the parent nodes before child nodes). This ensures that the properties of the variable distributions are preserved. It should be noted that the model shown in **Figure 4-4** only presents a time slice of the DBN. This network is reproduced for a number of time slices to simulate a timeline which can be an entire year. This included four time slices each representing a season of the year. Conditional probability tables of the nodes influenced by seasonal changes were altered in each time slice according to the corresponding season. The transition between time slices is through the connection of the node *Season* from one time slice to the similar node in another time slice.

4.3 Application of Methodology: Case Study

This section is devoted to a case study that illustrates the application of proposed methodology. For comparison of the developed model and the previous studies, the case study is designed using the available data adopted from previous research [33, 104]. The adopted values within this numerical example are mainly selected to highlight the applicability of the method. A subsea riser operating in the Kara Sea is impacted by a drifting iceberg causing a rupture in the structure and release of 11,500 kg of oil. The spill area is 1,500 m^2 and the average water depth is 200 m. This part of the Arctic region has a large amount of ice-cover with an average water temperature of -1.5 ºC in winter. More information on the physical characteristics of spilled oil and existing environmental condition in the region are listed in **Table 4-3**. As discussed before, naphthalene is the surrogate stressor having the physiochemical characteristics provided in **Table 4-4**. The

released pollutant will be partitioned into the air, ice and sediment phases. The properties of all four media involved in the scenario and their sub-components are detailed in **Table 4-5**.

.

Table 4-3. Characteristics of spilled oil and environmental conditions in the Labrador accident case study.

Oil Characteristics	**Notation**	**Value**	**Units**	**Reference**
Density	ρ_{oil}	832.0	Kg/m^3	
Viscosity at 40ºC	μ	3.03	cP	
Initial boiling point (zero evaporation)	T_0	301	K	[73]
Gradient of boiling point	T_G	500	KJ	
Oil-water interfacial tension	S_t	2000	Dyne/m	
Parameter	**Notation**	**Value**	**Units**	
Wind speed	V	10.0	Km/h	
Ambient air temperature	T_a	253	K	
Initial oil slick thickness	t	0.02	m	[73]
Initial area of spill	A_{oil}	6000	m^2	
Ice-cover area (entirely covered by ice)	A_{ice}	5400	m^2	

Table 4-4. Physiochemical characteristics of naphthalene as a surrogate for spilled oil.

Parameter	**Notation**	**Value**	**Units**
Molecular weight	MW	128.2	g/mol
Solubility at 25ºC	C^s	31.7	g/m^3
Vapour pressure at 25ºC	P^s	10.4	Pa
$\text{Log}\,K_{ow}$	N/A	3.35	N/A

Table 4-5. Properties of all media involved in the problem (VF: Volume Fraction, OCF: Organic Carbon Fraction).

Bulk Compartment (i)	Sub-compartment (j)				OCF Solids	Medium Density (kg/m^3)	Depth (m)
	VF Air (φ_{i1})	VF Water (φ_{i2})	VF Solids (φ_{i3})	VF Biota (φ_{i4})			
Air (1)	1.00	0.00	2×10-11	0.00	N/A	1.19	100.00
Ice Cover (2)	0	0	5×10-6	0	0.2	916	2.5
Water (3)	0	1	5×10-6	1×10-6	0.2	1000	100
Sediment (4)	0	0.63	0.37	0	0.04	2500	0.05

The present study does not include the weathering processes such as emulsification and natural dispersion in the modelling analysis only focusing on dispersion and fate and transport of a low-concentration spill. The input variables of model that carry a level of uncertainty are given in.**Table 4-6**.

Table 4-6. Transport parameters and their uncertainty level used in level IV fugacity model.

Parameter	Notation	Distribution	Mean	Standard Deviation	Units
Air-side MTC over ice cover	K_{va}	Normal	2.0	0.01	m/h
Ice-side MTC	K_{vi}	Normal	0.01	0.001	m/h
Aerosols deposition velocity	U_{di}	Point Estimate	10.8	N/A	m/h
Winter water temperature	T_{ww}	Uniform	(-5, 0)	N/A	ºC
Water temperature (other seasons)	T_{ws}	Uniform	(0, 8)	N/A	ºC
Melting rate	U_{iw}	Lognormal	3.9×10^{-5}	8.0×10^{-6}	m/h
Icing rate	U_{ii}	Normal	2.3×10^{-5}	5.0×10^{-6}	m/h
Water-side MTC over sediment	K_{pw}	Lognormal	0.01	0.001	m/h
Diffusion path length in sediment	Y_4	Point Estimate	5.0×10^{-3}	N/A	M
Molecular diffusivity in water	B_{w4}	Normal	4.0×10^{-6}	3.5×10^{-7}	m^2/h
Sediment deposition rate	U_{ds}	Normal	4.6×10^{-8}	4.0×10^{-9}	m/h
Sediment re-suspension rate	U_{rs}	Normal	1.1×10^{-8}	5.0×10^{-9}	m/h

The mass balance equations and dispersion model are solved using the input parameters in **Table 4-3 to 4-6** . The concentration of pollutant is estimated between 0.025 ppm and 0.04 ppm within a metre distance from the release point. The difference in this range with the estimations in the model by Afenyo et al. [33] is due to a higher wind velocity considered here. The fugacity distribution of all four phases under consideration is computed by sampling the probability distributions of input variables. The long term fugacity values which correspond to zero rate of change in this parameter (i.e. $\frac{df_i}{dt}=0$) are multiplied by the fugacity capacities, resulting in the concentration of each bulk compartment. Only concentration in water and sediment columns are presented here, since the long term concentration in other phases (ice and air), and consequently the ecological risk posed by pollution in these phases, are insignificant. This is in agreement with observations in previous studies [31, 74]. PEC in water and sediment are obtained with Eq. (4-11), assuming an exposure probability of $P(xp)=1$. According to Clark et al. [105], bioavailable fraction can be considered as $BaF=1$, since the pollutant has a log of octanol-water partition less than 5 ($\mathrm{Log}\,K_{ow}<5$).

The properties of lognormal distributions for $PEC_{95\%}$ is computed through a bootstrap simulation for 10,000 samples from the PEC distribution. The results of simulations for both water and sediment phase are presented in **Figure 4-5** in the form of Cumulative Distribution Function (CDF). The mean $PEC_{95\%}$ is 5.2×10^{-4} ppm and 5.9×10^{-3} ppm in water and sediment, respectively. To validate the obtained data, they are compared with a study by Brussaard et al. [106]. In their study, the exposure concentration of spilled oil in water was predicted between 3.0×10^{-4} ppm to 7.2×10^{-4} ppm. The median concentration in sediment column was reported as 4.2×10^{-3} ppm in a research by Afenyo et al. [33]. Despite the difference in this parameter, which stems from some changes made to the case study, the predictions confirm are consistent with the exposure concentration from field data indicating that concentration in sediment is considerably higher than that in water. This observation highlights the accumulation of chemicals into the sediment column during the transport processes among different media. The higher concentration of contaminants in sediment in comparison to the water phase was reported previously [107].

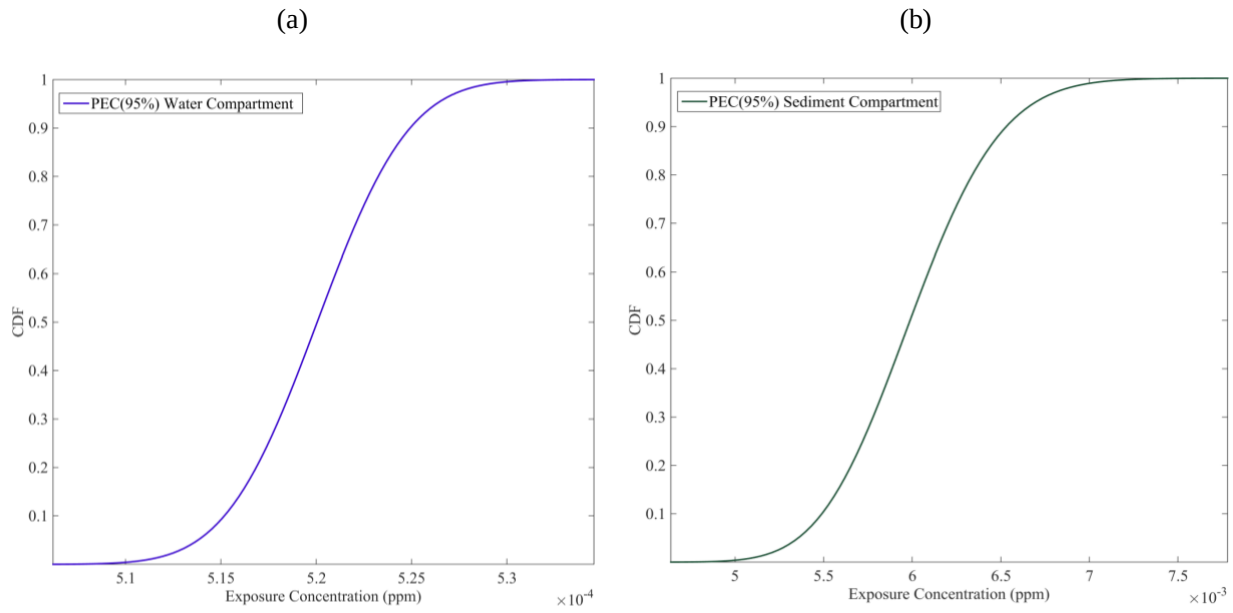

Figure 4-5. Estimated CDF for $PEC_{95\%}$ of pollutant in (a) water and (b) sediment compartment.

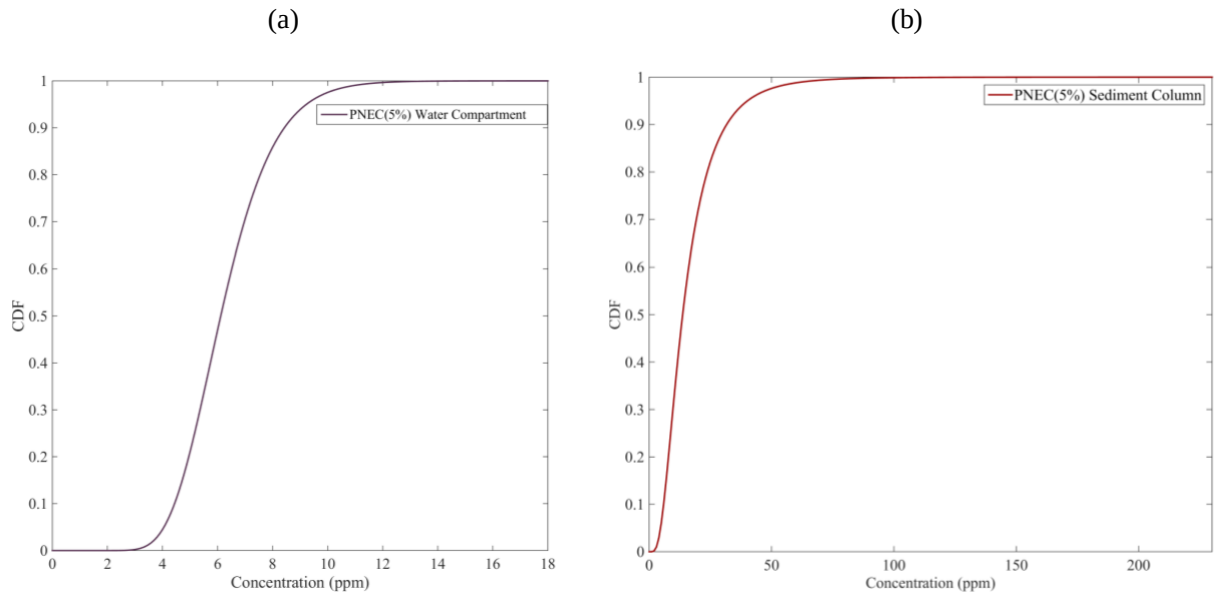

Figure 4-6. Estimated CDF for PNEC5% of species influenced by contamination in (a) water and (b) sediment compartment.

In order to aggregate the toxicity data, LC_{50} values of 19 aquatic species are adopted from the literature. PNEC data is obtained by extrapolating the 96-hours LC_{50} values. While the aquatic organisms are exposed to the pollutant in the water column, some may also be in contact with contamination in the sediment. The total ecological risk of these species is then a combination of both elements. The lowest 5^{th} percentile of PNEC ($PNEC_{5\%}$) is generated by bootstrapping from both categories (i.e. 19 species exposed to water and 7 species exposed to both water and sediment). The resultant probability distributions of $PNEC_{5\%}$ in both compartments are presented in **Figure 4-6**. The mean value of predicted $PNEC_{5\%}$ is $5.75\,\text{ppm}$ and $15.05\,\text{ppm}$ for species exposed to water and sediment phases, respectively. Although the mean value for $PNEC_{5\%}$ has not been provided before by any study with a similar context, the estimated value for water column is comparable with that reported in [36] which is 5.22 ppm. Afenyo et al. [33] has previously adopted the deterministic figure $PNEC_{5\%} = 2.0$ ppm for marine water, from a report [108]; however, this does not include the uncertainty involved with the parameter not providing the requirements for a probabilistic risk assessment. Probability distributions shown in **Figure 4-5** and **Figure 4-6** are used to establish the DBN for the assessment of ecological risk. Lognormal distributions were considered for $PEC_{95\%}$, $PNEC_{5\%}$ and the consequent estimated risk.

In a single time slice of the DBN model, the generic risk level is dependent on the risk posed from pollution in the water and sediment column. The estimated risk results are presented in **Figure 4-7**, where risk states A,B, …,E are the ranges used for the discretization process. These ranges are provided in **Table 4-7**. The figures selected for discretization are for illustration and comparison purposes. The results suggest that with more than 0.83 probability the risk is less than 8×10^{-12} and the probability of having a risk more than 5×10^{-11} is less than 0.01. A comparison is carried out between the risk distribution obtained from the BN model and those resulting from previous research. Those studies that adopt a Monte-Carlo approach for the probabilistic assessment suggest a lower probability for the minimum risk level. For instance, using the generic framework provided by Nazir et al. [36] and later improved by Afenyo et al. [33], the median risk will be estimated at 7.8×10^{-12}. However, the proposed BN model in the present paper suggests a median risk of 4.2×10^{-12}. This highlights that by not including the dependency of output parameters on input variables, this risk parameter can be overestimated. A Bayesian approach, however, incorporates the likelihood of input variables as well as the causal dependency of the random variables on each other providing a more accurate and efficient risk assessment framework.

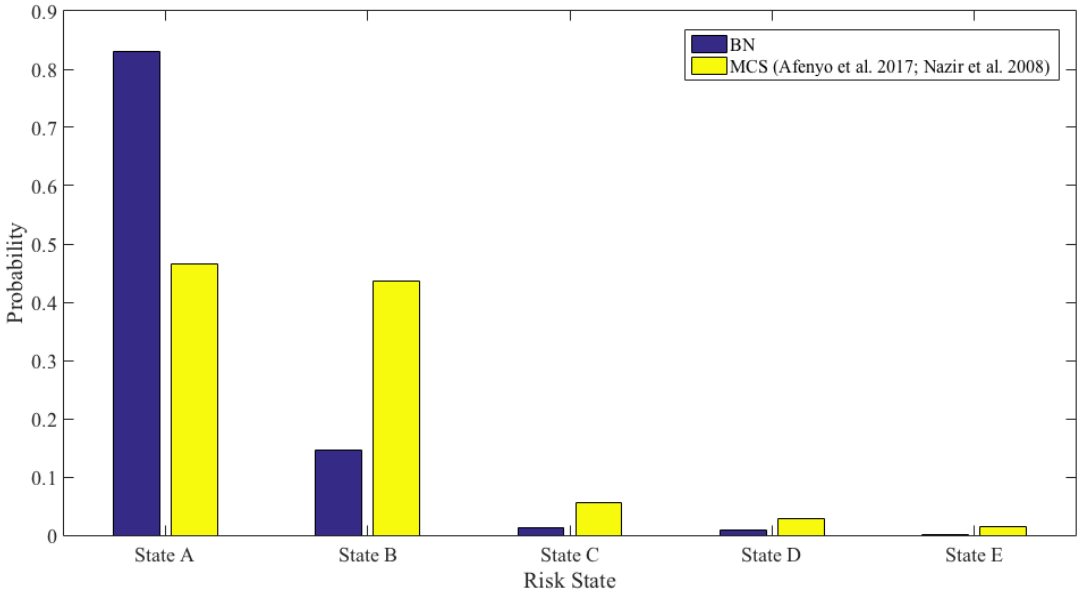

Figure 4-7. Estimated Probabilities of ecological risk posed to the entire community of aquatic organisms. A comparison is provided between the results of present study (ERA using BN) and previous methods (based on MCS) (for details on definition of each risk state refer to **Table 4-7**).

Table 4-7. Definition of ranges used to discretize the risk posed by oil spill on aquatic species community

Risk State	State A	State B	State C	State D	State E
Range	$R(t) < 8E-12$	$8E-12 < R(t) < 3E-11$	$3E-11 < R(t) < 5E-11$	$5E-11 < R(t) < 8E-11$	$R(t) > 8E-11$

In order to analyse the effect of seasonal changes on the ecological risk, the DBN included three time slices, each representing a seasonal condition. Khan et al. [109] assert that the Arctic region faces extremely rough weather in winter and relatively harsh weather in autumn whereas the conditions in summer and spring are mild. Therefore the likelihood of an accident in an offshore oil and gas facility will differ depending on the season of operation. This will in turn change the ecological risk profile of any such accident. On each time slice of the DBN, evidence is provided for a seasonal condition (i.e. operation in *Spring/Summer*, *Autumn* and *Winter*) and the probability of exceeding an acceptable risk level (here considered as 4×10^{-11} for illustration) is recorded. **Figure 4-8** illustrates the obtained probabilities of ecological risk posed to the environment with respect to seasonal changes. The No Evidence case is provided as a general estimation of posed risk with no seasonal observations. This figure can be used for further analyses or development of risk mitigation plans. However, it is observed that the provided evidence in terms of operating seasons introduces a significant change in the risk profile. For instance, the transition from spring to winter can increase the probability of exceeding the risk limit from 2.3×10^{-6} to, while the predicted probability is approximately 5.9×10^{-5}. This drastic difference in probability of exceeding the acceptable risk level is ascribed to the increase in likelihood of accidents in harsher environment and must draw the attention of designers, operators and risk managers to the importance of operating conditions and their influence on overall risk profile. The developed model can be expanded to decision making frameworks for developing efficient risk mitigation approaches. Such framework is able to accurately identify an optimum remediation plan or risk mitigation action based on the observations made during the operation and/or at the accident time.

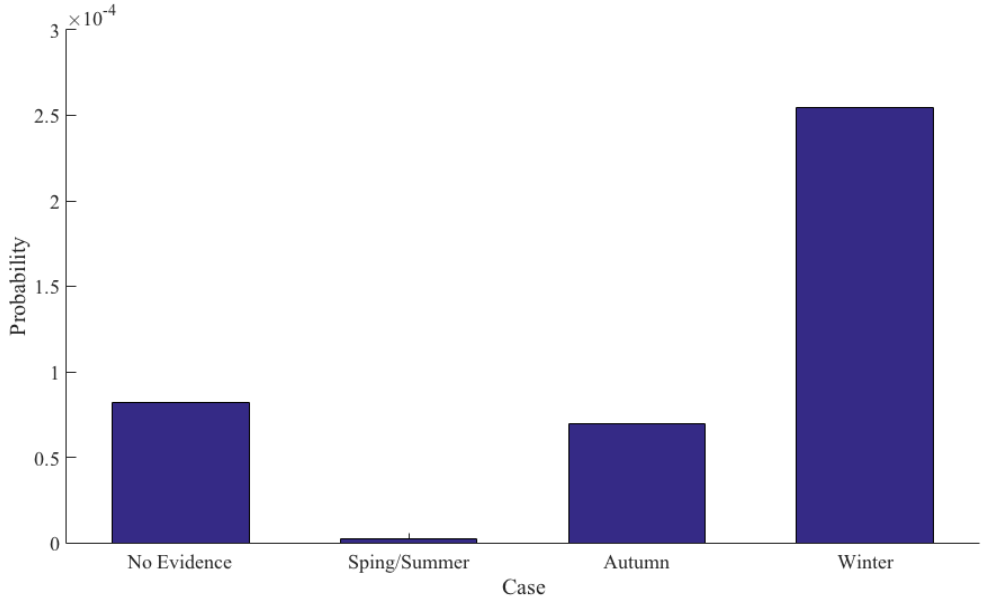

Figure 4-8. Probability of exceeding the acceptable ecological risk level for different seasonal conditions. No Evidence is for a generic BN with no evidence given on the *Season* node.

4.4 Conclusion

This paper proposes a methodology for conducting a probabilistic ERA of an accidental oil spill in the Arctic environment. The proposed method provides a probabilistic tool for estimating the overall risk posed to aquatic species. For this purpose, a fugacity approach in fate and transport modeling of pollutants is adopted. The resultant exposure concentrations, including a level of uncertainty, were used in a BN model along with distribution of ecological effects. As a case study, a scenario is simulated where 11,500 kg of oil is released during the operation of a subsea pipeline in the Kara Sea. The results suggest that the risk posed to aquatic ecological habitants is less than 5×10^{-11}, with approximately 0.99 confidence level. It is observed that the previously developed probabilistic ERA methods are likely to overestimate the risk profile. The BN is extended to a DBN with three time slices, each of which instantiated to a specific seasonal condition. The DBN provides estimates for the likelihood of exceeding an acceptable risk level in each season. Extremer environmental conditions show a significant increase in this probability which highlights the need for more attention from the operators and risk managers to planning appropriate risk mitigation strategies. The proposed framework can be readily applied for improving the safety of Arctic exploration activities. It can also be used for developing more efficient remediation plans during accidental marine oil spills.

Acknowledgement

Author, Ehsan Arzaghi, thankfully acknowledge the financial support provided by National Centre for Maritime Engineering and Hydrodynamic (NCMEH) at the Australian Maritime College (AMC) of the University of Tasmania.

Chapter 5: Risk-based Maintenance Planning of Subsea Pipelines through Fatigue Crack Growth Monitoring

Abstract

Research and development in the field of risk-based maintenance of offshore structures has recently attracted large attention due to the significant level of accident risk and the cost associated with maintenance in such remote facilities. The uncertainties associated with the deterioration of these facilities require a sound decision-making methodology for maintenance planning. This paper presents a dynamic risk-based methodology for maintenance scheduling of subsea pipelines subjected to fatigue cracks. The developed method can assist the asset managers to select the optimum approach for mitigating the consequences of failure while minimizing the maintenance costs. A Bayesian network is developed to model the probabilistic deterioration process and then it is extended to an influence diagram for estimating the expected utility of each decision alternative. Observation of damage state is included in the model to enhance decision making capacity. To demonstrate the applicability of the methodology, three cases with different fatigue crack incidents on a pipeline are considered. Based on the monitoring results, the model is able to determine whether the maintenance should be performed or not. The economic risk associated with maintenance is also minimized by suggesting the optimum maintenance technique among multiple possible methods such as welding or major repair.

5.1 Introduction

Subsea pipelines across the globe are widely used for transportation of large quantities of hydrocarbons from offshore wells to onshore locations, playing an important role in procurement of fuel for power generation and transport. Davis and Brokhurst [4] state that recorded failure rates in oil and gas subsea pipelines are relatively lower than pipelines in other facilities such as water distribution or wastewater collection systems. One of the major causes of failure in offshore pipeline is in degradation of structural properties [12, 13]. Specifically, the mechanical deterioration caused by fatigue phenomena leads to cracking of the tubular joints resulting in reduction of the resistance capacity and depression of service life in long-term [15, 110]. A damaged pipeline has significant environmental risks due to the hazardous properties of hydrocarbons and inaccessibility of the facilities. The loss of asset integrity may also delay production while maintenance is performed.

In order to mitigate severe consequences, frequent inspections and maintenances are essential, however, companies incur substantial costs to perform regular maintenance activities in less accessible areas. Hence, asset managers aim at uninterrupted operation of the system, with minimizing the maintenance cost. Over the last decade, risk-based maintenance methods have attracted a significant attention in the process and offshore industry, since they provide a cost-effective tool to reduce the probability of failure in the structures and associated consequences [39-41]. Dey [11] developed a risk-based model using the Analytic Hierarchy Process (AHP) to identify the risk factors that influence failure of petroleum pipelines. Dey asserted that the developed technique can assist in reducing the cost of maintenance although it does not totally eliminate subjectivity. Similarly, Singh and Markeset [111] proposed an expert system for the establishment of Risk-Based Inspection (RBI) programs for oil and gas pipelines. Their fuzzy-based methodology can also be used for calculating the estimated rate of corrosion; however, it does not provide a physics-based degradation model. Khan and Haddara [41] developed a methodology for optimizing the maintenance intervals in offshore production facilities. In their study, fault tree analysis (FTA) was adopted to determine the probability of failure. However, several researchers reported the negative side of FTA such as its incapability in capturing dependent failures and common cause failures [112, 113]. Moreover, FTA does not consider the dynamic nature of parameters such as temperature and pressure in the structures which are time-dependent [89]. In particular, deterioration processes such as cracks which evolve in time are also

prone to significant changes, hence the risk analysis method should be able to take into account the dynamic behavior of the system.

Alternatively, Bayesian network (BN) is an advanced probabilistic model for reasoning under uncertainty and have been widely used in risk and reliability analysis of complex systems. Application of BN significantly reduces the system complexity and inference computational time by factorizing the joint probability distribution of a set of random variables based on local dependencies. Various applications of BN in risk and reliability engineering is presented by Weber et al. [44], Khakzad et al. [114], Yeo et al. [53] and and Holický et al. [115]. Bhandari et al. [78] employed BN to develop a methodology for maintenance scheduling of an offshore production facility by updating the risk profile and comparing it with an acceptable level of risk. Their tool was found to be reliable for minimizing the consequences of system failure while optimizing the asset and capital utilization. Friis-Hansen [55] studied the application of Dynamic Bayesian Networks (DBN) for the modelling of an offshore jacket structure with respect to fatigue crack growth. The developed probabilistic network was then extended to an Influence Diagram (ID) for the risk analysis of the structure failure that identifies the optimum inspection plans. However, Friis-Hansen asserted that by including all the possible states of crack size in the inspection results, the results of inspection planning can be improved. Moreover, the network can be further extended to a maintenance planning tool by considering a number of applicable repair methods as the decision alternatives.

Straub [56] developed a generic computational framework for modelling deterioration processes. Straub's results showed that the framework can be adopted for applications in monitoring, inspection, maintenance, and repair planning due to its efficiency and robustness in Bayesian updating. Later, Nielsen and Sørensen [116] extended the framework to an ID for maintenance planning of offshore wind turbines. As a decision-making tool, their methodology assists in estimating the Expected Utility (EU) of performing or not performing repair on the structure considering the cost of failure and maintenance activities. However, in that study, a comprehensive cost analysis based on the state of deterioration was not incorporated in the risk assessment and the possibility of performing different maintenance tasks was not investigated.

In the present study, a risk-based decision-making methodology is developed for the maintenance scheduling of subsea pipelines. In order to optimize the maintenance plan, the methodology must incorporate the uncertain deterioration process of the structure along with economic aspects of

failure accidents or maintenance activities. To analyze the deterioration process, DBN is used to construct the probabilistic damage model. Bayesian updating capability is enhanced by including observations of damage state in the model based on the inspection/monitoring results. The developed DBN is then extended to an influence diagram for conducting a decision-making process based on the extent of the damage, failure risk and the costs associated with maintenance activities. Multiple maintenance techniques are included in the decision-making process to enable the decision makers to select the repair tasks with optimum expected outcome. In a selected case study, the advantages of this methodology is discussed through planning maintenance activities on detected fatigue cracks in an offshore pipeline.

5.1.1 Bayesian decision making

5.1.1.1 Dynamic Bayesian Network (DBN)

An extensive outline to BN and probabilistic knowledge elicitation is provided by Barber [91] and Pearl [58]. BNs are directed acyclic graphs used for reasoning under uncertainty by considering the causal relationships (represented by directed edges) among components of a system (represented by chance nodes). BN estimates the joint probability distribution of a set of random variables based on the conditional independencies and the chain rule, as in Eq. (5-1):

$$P(X_1, X_2, \dots, X_n) = \prod_{i=1}^{n} P(X_i \mid pa(X_i)) \tag{5-1}$$

where $pa(X_i)$ is the parent set of variables X_i. As an example, the joint probability distribution of the random variables X_1 - X_4 illustrated in **Figure 5-1** is estimated by $P(X_1, X_2, X_3, X_4) = P(X_1)P(X_2)P(X_3 \mid X_1)P(X_4 \mid X_3, X_2)$

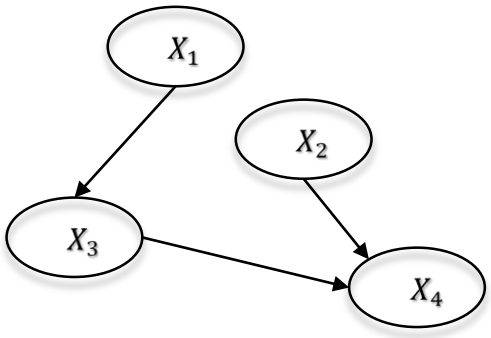

Figure 5-1. Schematic of a BN.

When new information about any of the chance nodes becomes available, BN can update the probabilities. For instance, if the variable X_2 is observed to be in state e, the joint probability distribution is updated based on the Bayes' theorem:

$$P(X_1, X_3, X_4 \mid e) = \frac{P(X_1, X_3, X_4, e)}{\sum_{X_1, X_3, X_4} P(X_1, X_3, X_4, e)} \tag{5-2}$$

DBNs particularly represent stochastic processes and facilitate modelling of temporal behaviour of a set of random variables [117]. They divide the time line into a series of time slices each of which are connected from nodes in slice i to the node in slice $i + 1$. **Figure 5-2** illustrates a schematic of DBN in which joint probability distribution of the variables are estimated by Eq. (5-1).

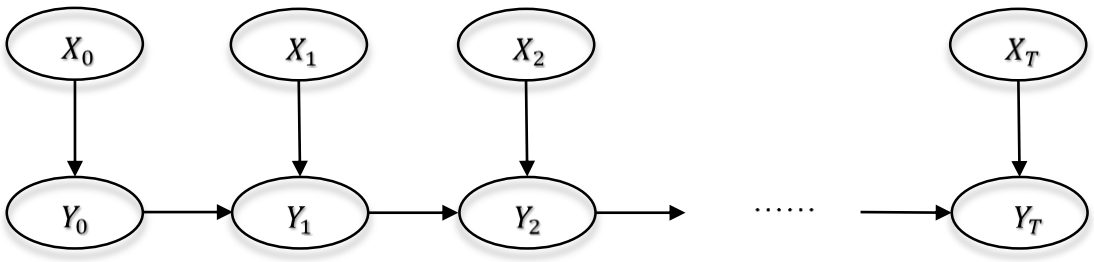

Figure 5-2. Schematic of a DBN.

A detailed explanation of inference algorithms developed specifically for DBN structures can be found in Murphy [60].

5.1.1.2 Influence Diagram (ID)

As an extension to BN, influence diagrams are used as a tool for probabilistic decision-making purposes. The diagram is formed by addition of decision and utility nodes to the network as shown in **Figure 5-3**.

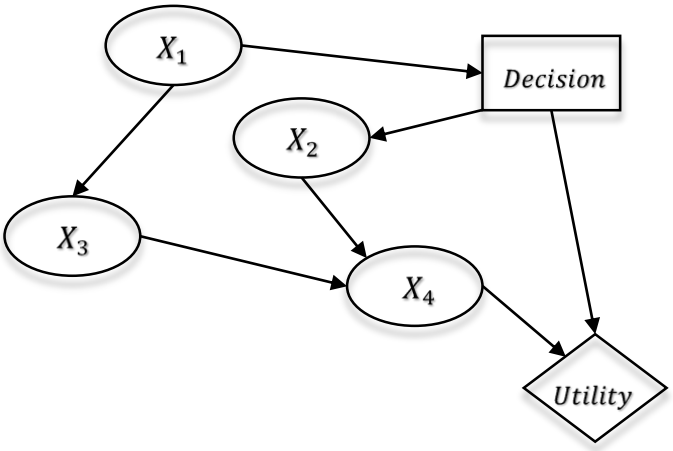

Figure 5-3. Schematic of an ID (Decision and Utility nodes are added to BN).

Decision nodes hold a number of action alternatives and its parent nodes provide the information required for making the decision. The arcs pointing to a decision node is an information arc instead of expressing probabilistic dependence [55]. Utility nodes consist of numeric values rather than probabilities demonstrating the decision makers' preference over each configuration of decision alternative and the utility's parent nodes. For example, for n states of the node X_4 and m alternatives of the decision node, the utility table requires $n \times m$ numeric values which are determined based on experts' knowledge or utility functions. The expected utility of decision alternative d_i is then estimated by Eq. (5-3) and the action with maximum EU will be the optimum decision.

$$EU(d_i) = \sum_{X_4} P(X_4 \mid d_i)\, U(d_i, X_4) \tag{5-3}$$

Jensen and Nielsen [59] provide extensive information about influence diagrams which are widely used in decision making applications. The application of ID to decision making in a marine and process industry is assessed by Eleye-Datubo et al. [93] and Khakzad and Reniers [118].

5.2 Maintenance Planning Methodology

DBNs are a generalization of Markov process models. In a Markov process, the state of a variable at time t_{i+1} is independent of the past given the state at the previous time step, t_i. In general, this assumption does not hold in deterioration modelling, mainly due to the presence of epistemic

uncertainties. However, the damage growth model corresponds to a Markov process if it is conditional on time-invariant random variables [56]. Hence, the deterioration process is modelled using DBN in which the state of damage is evaluated over a sequence of time slices. The model has been adopted from a study byArzaghi et al. [119] reported in Chapter 2 of this thesis and modified to represent the long-term growth of fatigue damage. That is, the transition from short cracks to long cracks (see **Section 2.3**) is here considered as the initial time. This has been done to improve the computational efficiency of maintenance planning model explained in the following sections and concentrate more on the operational time where the extent of damage becomes critical.

5.2.1 Deterioration Model

The generic DBN in **Figure 5-4** developed by Straub [56] qualitatively represents a deterioration model describing the state of damage over a discrete time process. The damage size is a function of the initial condition D_0, a number of time-variant parameters ω_t and a number of time-invariant parameters θ. To facilitate the model construction and for presentation purposes, the variable θ is introduced in the form of $\theta_1, \theta_2, \dots, \theta_T$. Straub [56] suggests that this approach does not affect the computational efficiency of the model.

The Bayesian network modelling also requires the quantification of the relationships between the random variables. This is performed by specifying the conditional probability distribution of random variables which are mostly defined in a continuous space. Although algorithms such as MCMC enable the compiling of continuous variables into the network, the possibility of computational deficiency in particular when the BN is very large makes them impractical. Therefore, the continuous random variables are replaced by discrete random variables (as explained later in a case study) and the corresponding probability mass functions $p(\theta_t|\theta_{t-1})$, $p(\omega_t|\omega_{t-1})$, $p(D_t|D_{t-1}, \omega_t, \theta_t)$ and $p(O_t|D_t)$ are included in each node of the BN in the form of conditional probability table (CPT). It should be noted that the developed DBN is homogenous such that the constructed network and CPTs are identical for all the time slices excluding the first.

As the main motivation of this study, the capability of model for maintenance optimization is enhanced by including observations in the model. The monitoring data can be readily inserted into the network as evidence from different observation of parameters θ and $\omega_1, \dots, \omega_t$ (i.e. direct observations such as stress ranges in the structure or indirect observations such as level of salinity in the pipeline). In the present study, only the state of damage D_t is considered as the results from

inspection and monitoring of the system. In order to increase the model's capacity for decision making about maintenance, the observation node incorporates all the possible sizes of damage as its states rather than a random variable with two states of "detected" and "non-detected" defects. The BN model can be automatically updated when the variables O_t are instantiated with the monitoring results.

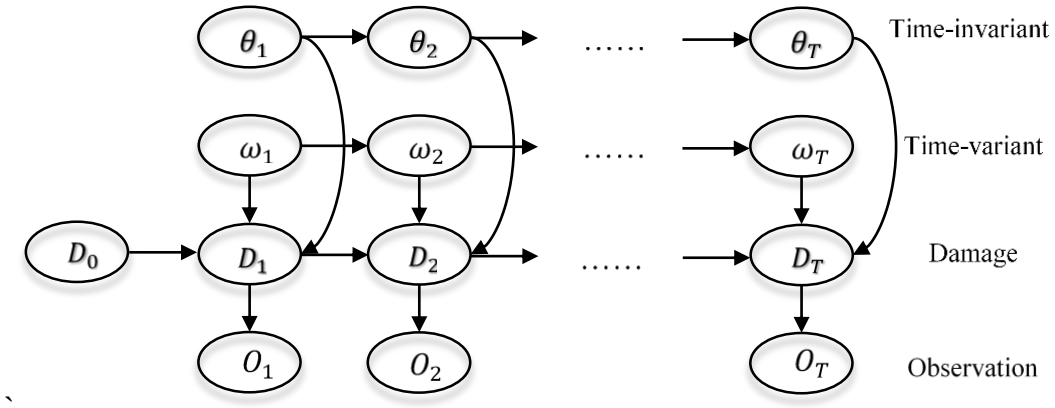

Figure 5-4. A generic DBN for deterioration modelling [53]

5.2.2 Discretization of continuous random variables

All the continuous random variables of the model are replaced by discrete space variables with a number of mutually exclusive states. As recommended by Friis-Hansen [55], univariate discretization is adopted to ensure that the properties of the variables' distributions are preserved. This method is performed by individually discretizing the variables of the domain considering the hierarchy of the nodes (i.e. the parent nodes are discretized before child nodes). Depending on the variables distribution, uniform or non-uniform interval lengths are chosen. In the case of non-uniform intervals (e.g. for exponential distribution), the interval length is considered with inverse proportionality to the gradient of the probability density function. More details about discretization of the variables and how to include the conditional probability tables into the network is later explained in an application to a case study.

5.2.3 Decision model for maintenance planning

The BN is extended to an ID to determine the optimum maintenance plan considering the state of damage. A simplified version of the developed ID is presented in **Figure 5-5**. The decision model

is developed by addition of the decision node "$Main$" consisting of the maintenance alternative. Utility nodes M_C and F_C are also included incorporating the cost of maintenance and failure, respectively. This requires to account for the probability of failure due to the developing damage in the structure. For this purpose, variable F with binary states "Fail" and "Safe" is added to the network. The quantification of failure probability and determining its CPT is explained later in a case study.

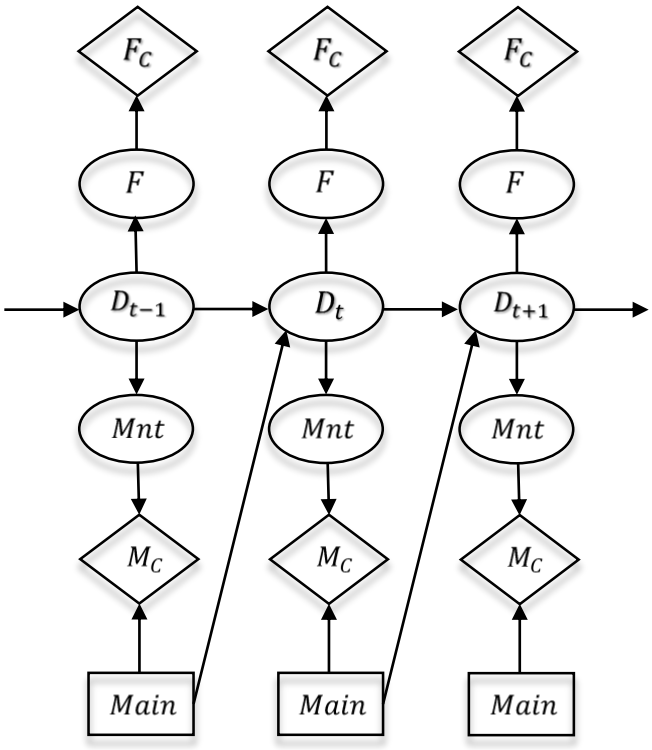

Figure 5-5. Simplified influence diagram used in maintenance planning. Network nodes are FC: failure utility, F: failure of the structure, D: damage size, Mnt: monitoring results, MC: maintenance utility and Main: decision on Maintenance

Utility tables of node M_C are determined based on the preference over each configuration of the states of the utilities' parent nodes and maintenance alternatives. It is considered that the methodology provides a tool for asset managers to evaluate whether the structure should be repaired or not and if yes then which maintenance method minimizes the accident risk and the cost of repair. The expected utility of each decision alternative is then estimated based on the concepts explained in Section 5.1.1.2, enabling the asset maintenance managers to select the action for

optimum outcome. It should be noted that a decision on maintenance influences the state of structures health in future. Therefore node D_t has the decision node of the previous time slice $Main_{t-1}$ as its parent and similarly, node D_{t+1} get input from the decision node $Main_t$.

5.3 Application: Maintenance for Detected Fatigue Cracks

5.3.1 Scenario development

To demonstrate the applicability of the developed influence diagram (ID) in risk-based maintenance of structures under deterioration process, a case study is conducted by modelling growth of fatigue cracks in an offshore pipeline using *GeNie* software. The crack model is extended to an ID for decision making in maintenance schedules for the structure. The fatigue model in this study is based on fracture mechanics and only consist of time–invariant random variable, although the developed methodology is generic and it can include any damage model or monitoring parameter.

5.3.2 Fatigue crack growth model: Paris' Law

Offshore structures such as pipelines are subjected to cyclic loads from wind, current and waves making them susceptible to fatigue phenomena. To predict the development of fatigue cracks, fracture mechanics approach is often adopted taking into account the relationship between load, material properties and the age of the structure. By assuming constant load amplitudes, the growth of crack size a is described by Paris' law:

$$\frac{da}{dN} = C(\Delta K)^m \tag{5-4}$$

where N is the number of applied load cycles, C and m are empirically determined material parameters and ΔK is the stress intensity factor, which empirically can be represented as:

$$\Delta K = Y(a)\Delta\sigma\sqrt{\pi a} \tag{5-5}$$

Here, $Y(a)$ is the geometry function dependent on the crack depth and $\Delta\sigma$ is the stress range. The growth of crack per load cycle on the structure represented in Eq. (5-4) is a function of crack length

and the stress range which is not usually constant due to the environmental nature of the ocean. While the explicit solution of this equation is not possible, by assuming that the geometry function is independent of crack depth a and the stress range $\Delta\sigma$ follows a Weibull distribution, an analytical solution can be achieved [61]:

$$a = \left(a_0^{\frac{2-m}{2}} + CNA^m \Gamma\left(1 + \frac{m}{B}\right) Y^m \pi^{\frac{m}{2}} \left(1 - \frac{m}{2}\right) \right)^{\frac{2}{2-m}} \quad , m \neq 2 \tag{5-6}$$

where A and B are the scale and shape parameters of the Weibull distribution respectively and Γ is the gamma function when the Weibull distribution variable is sampled.

5.3.3 BN Structure and Probability Distributions

The BN assists in accounting for the uncertainties of the parameters in Eq. (5-6). These parameters are considered as random variables and introduced in the network by probability distributions. The load on the structure is described by a Weibull distribution with scale and shape parameters of A and B respectively. It is assumed that parameter B has negligible variation and has a constant value ($B = 0.66$), while parameter A follows a normal distribution with mean value $\mu_A = 5.35$MPa and standard deviation $\sigma_A = 0.963$MPa. A total of five independent nodes are considered for the variable A in each time slice, since at each year the load from the sea is independent of other years. It is considered that $N = 10^6$ load cycles are experienced by the pipeline every year. For the sake of convenience, parameters $C$and m and the geometry function Y are assumed to be deterministic. Therefore, Eq. (5-6) can be written as:

$$a = \left(a_0^{\frac{2-m}{2}} + M_U K A^m \right)^{\frac{2}{2-m}} \quad , m \neq 2 \tag{5-7}$$

where

$$K = CN\Gamma\left(1 + \frac{m}{B}\right) Y^m \pi^{\frac{m}{2}} \left(1 - \frac{m}{2}\right) \tag{5-8}$$

Eq. (5-7) provides a as a function of a_0, however, for the sake of transition from one time slice a_{t-1} to the next one a_t, parameter N was considered as the number of load cycles experienced in one time step (one year). This enables modelling the growth of crack through sequences of constant time steps and calculating the transition probability $p(a_t \mid a_{t-1})$, which is very important for an

accurate inference with the DBN. The parameter M_U accounts for the uncertainty of the model, following a normal distribution. A summary of the parameters used in the crack growth model is presented in **Table 5-1.** Parameters of the crack growth model from Friis Hansen [52].

Table 5-1. Parameters of the crack growth model from Friis Hansen [52].

Variable	Description	Distribution	Mean	Standard Deviation
m	Material parameter	Deterministic	3.0	-
C	Material parameter	Deterministic	2.17×10^{-13}	-
Y	geometry function	Deterministic	1	-
B	Weibull shape parameter	Deterministic	0.66	-
N	Load cycles	Deterministic	10^6 / year	-
A	Weibull scale parameter	Normal	5.35 MPa	0.963 MPa
M_U	Model uncertainty	Normal	1	0.18
a_0	Initial crack depth	Exponential	1 mm	1 mm

The growth of crack is analyzed for a period of 5 years through 5 discrete time slices $(a_0, a_1, \dots, a_5)$, though due to limited space nodes a_0 to a_3 of the decision model are only illustrated in **Figure 5-7**. The initial crack depth, a_0 with exponential distribution was discretized in MATLAB software using 20 exponentially growing interval lengths (see **Figure 5-8**). This was conducted to avoid rounding errors caused by uniform interval lengths in the last intervals where the probabilities are significantly low. It should be noted that crack depth in the following time slices $(a_1, \dots, a_5)$ is discretized using the same intervals as a_0. **Figure 5-6** illustrates the sequence of filling the conditional probability table of crack depth $p(a_t \mid a_{t-1}, M_{U_t}, A_t)$ using Eq. (5-7) in a form of a matrix with binary values. The calculation of crack depth a_t^j is performed in MATLAB for $20 \times 21 \times 11 = 4620$ configurations using 20, 21 and 11 states of a_{t-1}, M_{U_t} and A_t, respectively. Variable $P(i,j)$ represents each array of the CPT for the time-dependent crack size $(a_t \mid a_{t-1})$. The presence event, $\{P(i,j) = 1\}$, occurs if the estimated crack depth of configuration j (a_t^j) is smaller than the upper bound of interval i $(a_{i_{ub}})$ and non-presence event, $\{P(i,j) = 1\}$, occurs if $a_t^j \geq a_{i_{ub}}$. Binary values of $P(i,j)$ are then determined for each of 20 intervals of the crack depth $(1 \leq i \leq 20)$. As suggested by Friis-Hansen [55], in order to allow the probability mass (PM) of the small crack size intervals to grow into the following intervals, the upper bound of intervals are inserted into Eq. 5-(7).

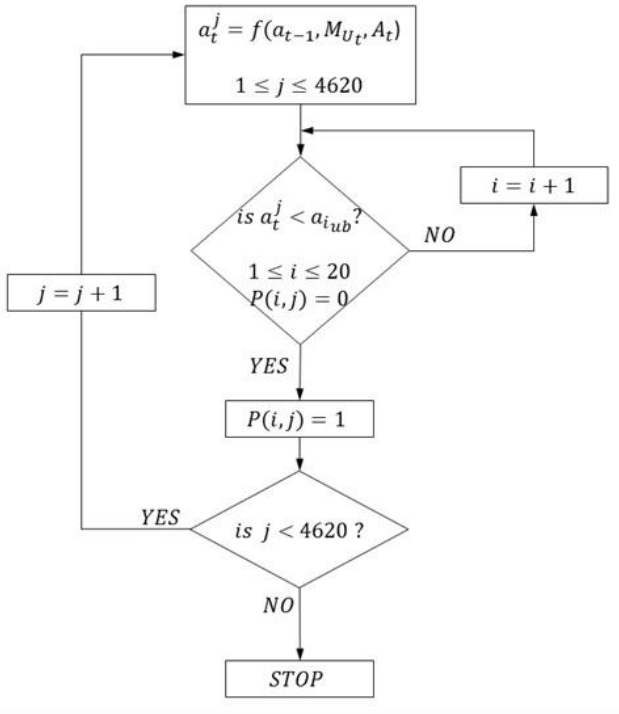

Figure 5-6. Sequence of filling Conditional Probability Tables (CPTs) of node a_t.

Normally distributed variables M_{U_1} and A_1 are discretized into 21 and 11 uniform interval lengths, respectively. To capture the entire distribution, both ends were truncated and the probabilities were lumped into the end intervals. The CPT of other nodes $p(M_{U_t} \mid M_{U_{t-1}})$ and $p(A_t \mid A_{t-1})$ $(t \neq 1)$ are filled using identity matrices. The dependency of parameters A and B on the previous time steps are introduced to enable the use of identical time slices for network establishment. According to Straub [56], this has no effect on the computational efficiency, while it facilitates the modelling process and graphical representation of the network.

The occurrence of failure in the pipeline is assessed by limit state G, described as:

$$G = a_c - a_t \tag{5-9}$$

where a_t is the actual crack depth and a_c the critical crack depth. In the network, binary variables F_t represent failure event, $\{F = 1\}$, if $G \le 0$ and survival event, $\{F = 0\}$, if $G > 0$. The pipeline is assumed to have a wall thickness of 16.5 mm and any damages larger than this is considered in the failure domain, $a_c = 16.5$ mm. Therefore, failure node F_t has two states of *Safe* and *Fail*, the latter with binary value 1 for only the last two states of a_t.

To incorporate the monitoring concept, node Mon was included in the network. For a specific monitoring method, it is more probable to detect cracks with larger depths. Thus the probability of damage detection is modelled with an exponential distribution as:

$$PoD = P_0(1 - \exp(-{}^{a_t}/_{0.4})) \tag{5-10}$$

where $P_0 = 1$ and $a_{i_{ub}}$ is the upper bound of crack depth interval. It should be noted that node Mnt has the states of a_t as well as no detection state.

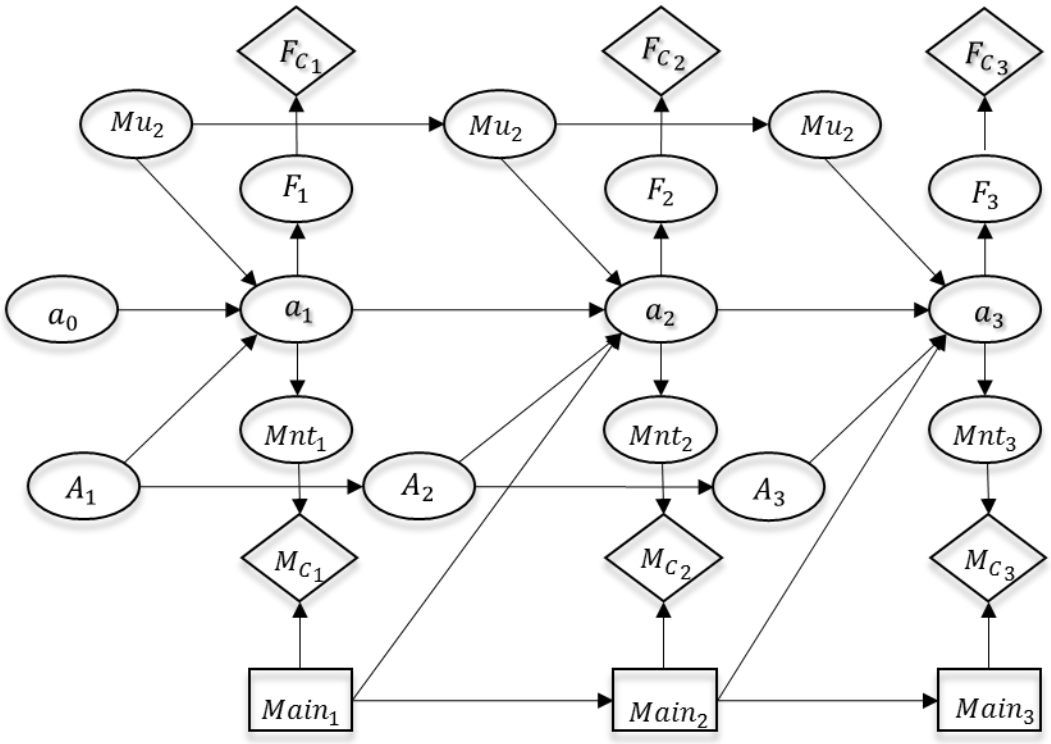

Figure 5-7. Developed limited memory influence diagram for maintenance planning of offshore pipelines. Network nodes are F_C: failure utility, *F:* failure of the structure, *a:* crack depth, *Mnt*: monitoring results, *Mu*: model uncertainty parameter, *A*: Weibull scale parameter (for stress range), M_C: maintenance utility and *Main*: decision on Maintenance.

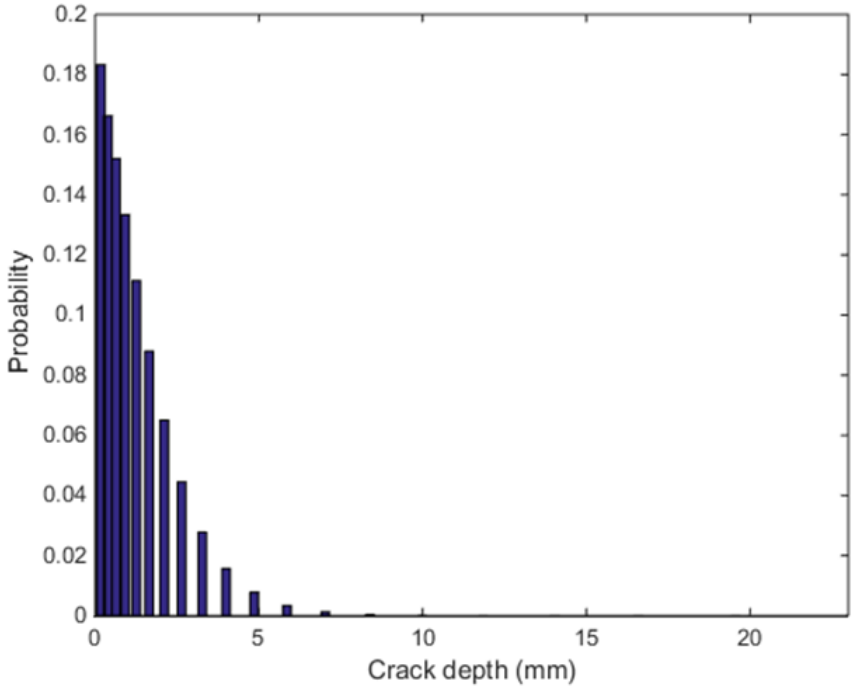

Figure 5-8. Discretised exponential distribution of initial crack size.

5.3.4 Utility functions

The maintenance scheduling process is continued by determination of decision alternatives. Considering the failure risk, the model aims at evaluating whether the fatigue crack should be maintained now or postponed, if required, and if which maintenance method minimizes the accident risk and the cost of repair. Therefore, three action alternatives including *welding*, *repair* or *continue* are added to the decision node. The welding option is assumed to be the solution for cracks with relatively small sizes [120] while the other alternative, repairing, is considered to be a more complicated task appropriate for major damage in the pipeline. This level of complexity is considered when defining the utility values of each action alternative. **Figure 5-9** illustrates a comparison between the costs associated with two maintenance tasks. As illustrated in the figure, if the damage size is within the first 15 intervals ($a_t \leq 10$mm), the cost required for welding the pipeline is lower than the cost of any major repair activities. However, due to the repair action's cost effectiveness and also significant increase in probability of failure in the last five intervals, welding cost exponentially increases. That is, for critical crack sizes ($a_t > 10$mm) it is essential to perform more extensive repair activities. Moreover, it is assumed that any repair recovers the state of the structure, regardless of its method. It should be noted that state 0 of the crack size

intervals in the figure represents the case in which no damage is detected in the pipe though operators are likely to incur a cost due to approaching the facility for performing repair. By adding the failure utility node, the cost associated with action alternative *continue* is considered to be -$80K as the cost for a corrective maintenance.

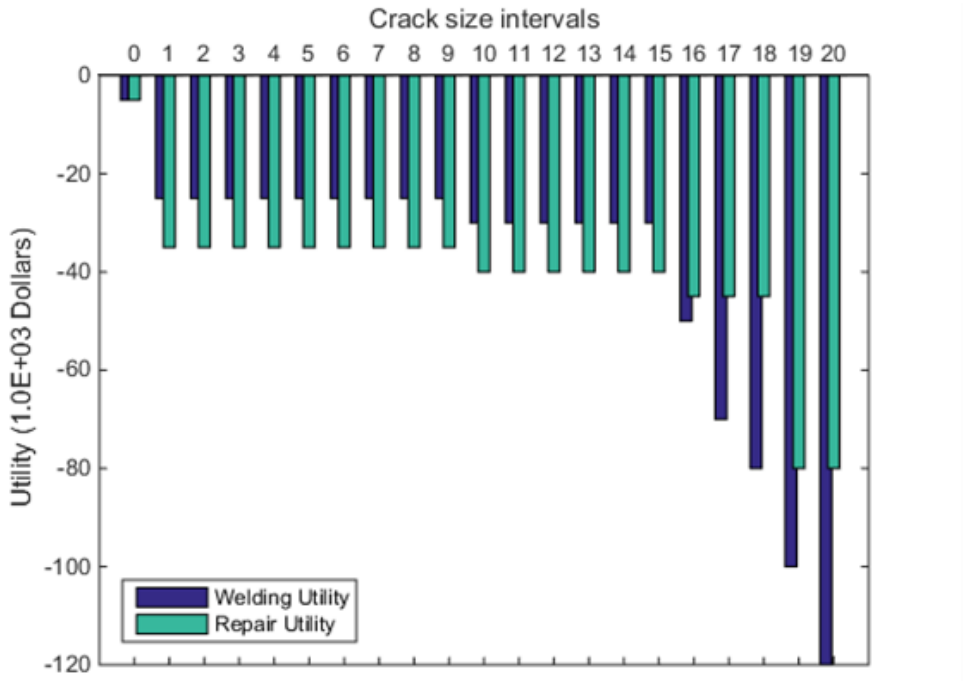

Figure 5-9. Utility values of maintenance alternatives, *Welding* and *Repair*, for each interval of crack size (State 0 of crack size intervals represents the case in which no crack is detected by the monitoring system).

5.3.5 Decision Making: Results

The capabilities of the developed decision model is assessed through three cases with different fatigue crack incidents in a five-year monitoring period. The results of the monitoring process is summarized in **Table 5-2.** Observations of fatigue crack in an offshore pipeline. Three cases were considered with different monitoring results. Note: the cells with dashes illustrate future times where monitoring is yet to be performed.. To clarify the presented information, in case B, the monitoring process resulted in no damage detection in the first and second year while in the third year an observation is made with a crack in state 11 of damage intervals. The state of the structure's health is not monitored for the following two years (years 4 and 5).

Table 5-2. Observations of fatigue crack in an offshore pipeline. Three cases were considered with different monitoring results. Note: the cells with dashes illustrate future times where monitoring is yet to be performed.

Year	1	2	3	4	5
Case A	No Det.	State 15	-	-	-
Case B	No Det.	No Det.	State 11	-	-
Case C	State 8	State 12	State 14	-	-

The results of monitoring is introduced as evidences into the influence diagram to estimate the expected utility (EU) of each decision alternative, as presented in **Figure 5-10** and **5-11**. For future times, no evidence is added to the network and the values are predicted based on relative damage growth probabilities.

During the monitoring process in case A, no damage is detected in year 1 (see **Figure 5-10**a). This results in reduction of failure probability to zero and consequently the maximum EU for continuing the operation of the pipeline. The low EU for welding and repair actions are due to the cost of the inspection for maintenance in the case no damage is found. Observation of a major crack in the structure (in state 15 and about 10mm deep) causes a dramatic drop in EU of continuing the operation (about -$120K) implying that the maintenance must be performed on the pipeline. Due to the significant probability of failure, the model suggests that an extensive repair activity, with EU of about -$55K, will have the optimum outcome between the two maintenance alternatives. Repairing the structure is predicted to increase all the expected utilities in the future (after year 2). However, as it can be seen in years 4 and 5, the continuous operation of the pipeline will reduce the EU as a result of the structural deterioration process.

In case B, the EU of continuing the operation remains negligible in the first and second year due to not being able to detect the damage. However, this results in reduction of failure probability between these two years and consequently increases the expected utility of both welding and major repair for about $2.5K. In the current time, the third year into the pipeline's operation, a damage within the crack depth interval of 4mm-5mm is detected suggesting that the structure must undergo a welding process to recover its healthy state. This action has the maximum EU of -$36k since the state of damage does not justify the cost required for performing an extensive repair (EU_{Repair} = -$41K). The capability of the model to suggest the optimum maintenance plan was not achieved in previous researches conducted by Friis-Hansen [55] and Nielsen and Sørensen [116]. In a similar way as case A, it is predicted that performing the appropriate maintenance task increases the EU in the future (years 4 and 5).

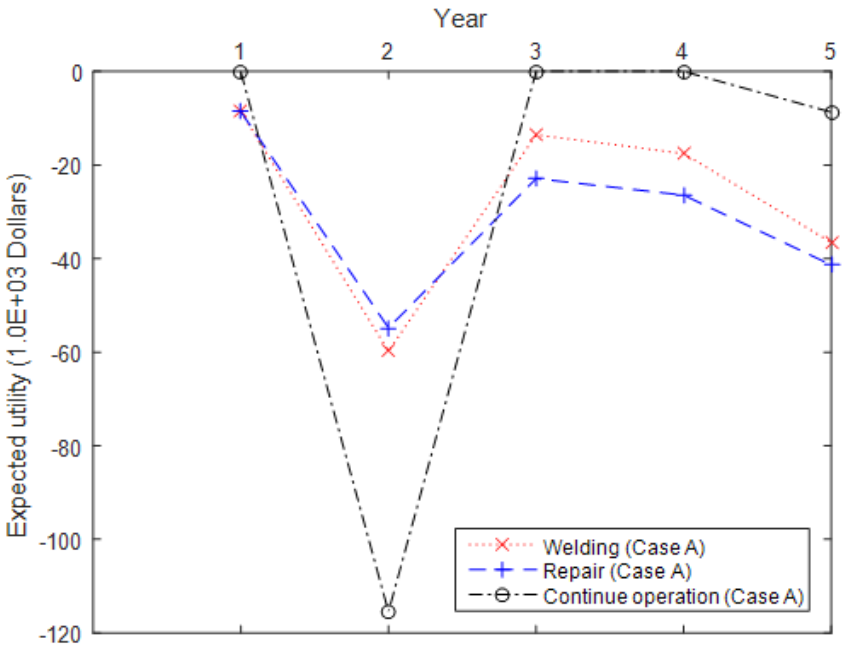

(a)

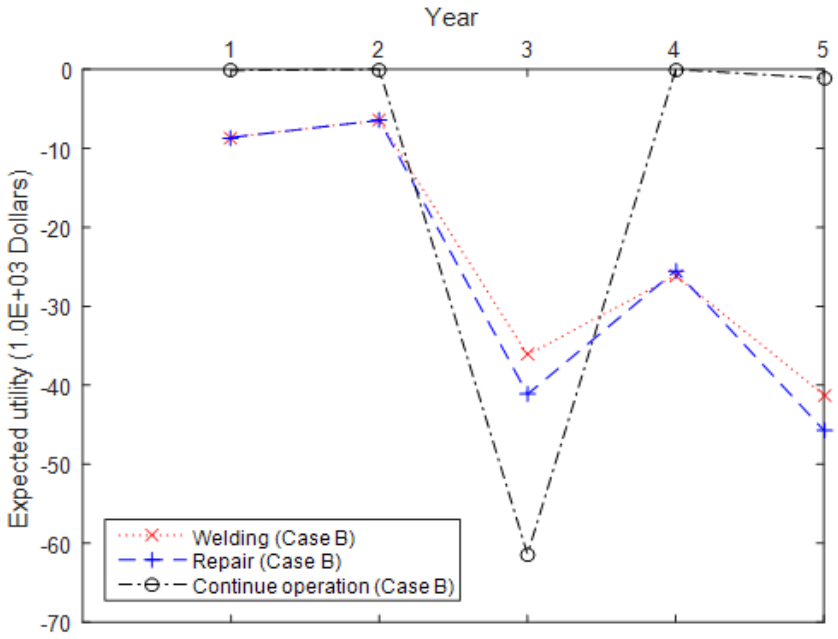

(b)

Figure 5-10. Expected utilities of three decision alternatives: *Welding*, *Repair* and *Continue operation* for case A (a) and B (b) with different fatigue crack incidents as detailed in **Table 5-2.** Observations of fatigue crack in an offshore pipeline. Three cases were considered with different monitoring results. Note: the cells with dashes illustrate future times where monitoring is yet to be performed.

Case C is a more realistic representation of a deterioration process where the fatigue crack in the pipeline grows gradually from state 8 in the first year, with about 2 mm depth, to state 14 in the third year of operation in which crack depth is between 7mm to 8.5mm, as illustrated in **Figure 5-11**. In spite of monitoring a growing crack in the first two years, the model suggests that continuing the operation has the maximum EU. In the third year, however, welding is to be performed on the pipeline due to the significant drop of the expected utility of continuing the operation. The entered evidences reduce the level of uncertainty between year 2 and 3 hence increasing the EU of both maintenance tasks, weld and repair, to -$37K and -$42K, respectively. Once performed, the repair activity leads to increasing all the expected utilities in the future (years 4 and 5).

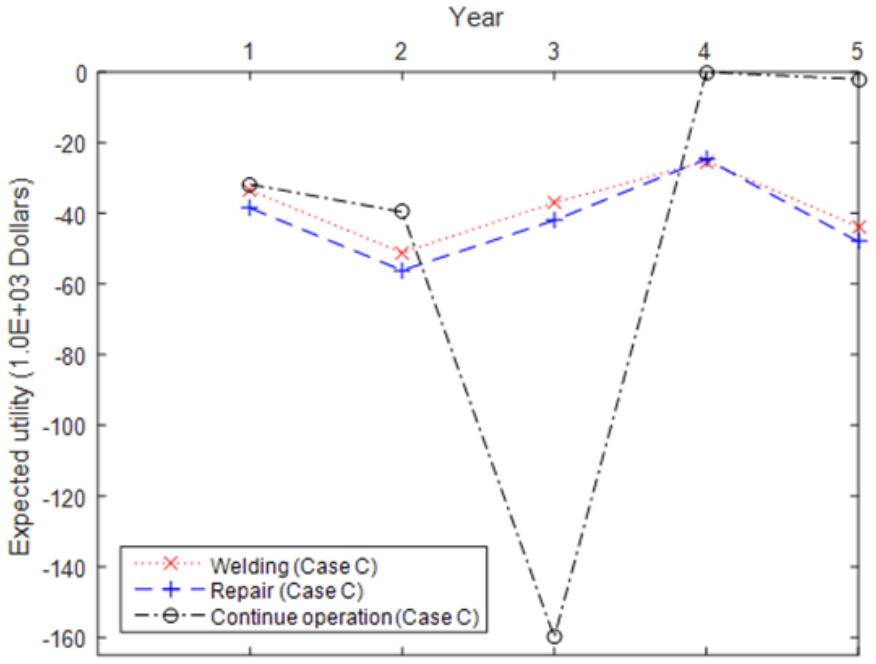

Figure 5-11. Expected utilities of three decision alternatives: Welding, Repair and Continue operation for case C with fatigue crack incidents as detailed in **Table 5-2.** Observations of fatigue crack in an offshore pipeline. Three cases were considered with different monitoring results. Note: the cells with dashes illustrate future times where monitoring is yet to be performed.

5.4 Conclusion

This paper presents a dynamic risk-based methodology for the maintenance scheduling of deteriorating structures. Planning maintenance activities for a subsea pipeline subjected to fatigue cracks is considered as the application of methodology. For this purpose, a BN-based on deterioration process is developed to model the state of damage and the failure probability in a finite number of time slices. A fracture mechanics-based method is adopted to model the fatigue crack growth using Paris' law. The BN is then extended to an influence diagram with the aim at estimating the expected utility for each decision alternatives whether to perform a maintenance task or not. The model is enabled to update the probabilities based on observation of the damage state. As a case study, repair activities in three cases with different crack incidents in an offshore pipeline are investigated. Three actions including welding, repairing and continuing the operation of the facility are considered as the decision alternatives. Based on the monitoring results and defined utility values, the maximum utility of each action is determined at each year of the operation. Such a cost-effective safety analysis enables the asset management to mitigate the risk of accident while minimizing the maintenance costs.

The priority of this study is to demonstrate the capabilities of the risk-based maintenance approach; however, the developed methodology can be adopted to integrate real-life utility functions enabling asset managers to apply the tool on industrial problems. For the sake of simplification, it is assumed that any repair action completely recovers the structure's state of health. However, the model can be readily used to incorporate the level of uncertainty of maintenance outcome. Further work can also be carried out to investigate the observation of various ranges and intensities of stress in the structure as a condition monitoring parameter.

Acknowledgement

The authors gratefully acknowledge the financial support provided by National Centre for Maritime Engineering and Hydrodynamic (NCMEH) at the Australian Maritime College (AMC) of the University of Tasmania. The first author also would like to express his sincere gratitude to Dr. Jonathan R. Binns for providing valuable comments to this research.

Chapter 6: Summary & Conclusion

6.1 Summary

Subsea pipelines are valuable assets of the oil and gas industry and are used for safe and cost-effective transmission of extracted hydrocarbons to different locations. These structures however, are subject to aging and deterioration processes which are progressive and may result in undesirable events. In particular, corrosion and fatigue damage play a key role in the failure of subsea pipelines. Such accidents may lead to substantial financial risk for the industry, in the form of excessive operational costs or loss of asset and production. At times, they may also pose catastrophic environmental risks to the marine ecosystem due to the loss of containment. Effective strategies are therefore required to ensure a safe and reliable operation be performed. However, most of the integrity management techniques in place currently rely on preventive maintenance approaches which neglect the actual condition of the structure or risk level of operation at the time of decision making. This Ph.D. research aims at improving the safety and availability of deteriorating subsea pipelines based on advanced risk-based approaches. Bayesian statistics are utilized in this study for deterioration modelling, probabilistic risk assessment and risk-based decision-making.

6.2 Conclusions

The major conclusions of this research are listed below according to the organization of the thesis:

- A probabilistic methodology was developed for predicting the corrosion and fatigue service life of subsea pipelines. The entire fatigue life, consisting of pit nucleation, pit growth, crack initiation, crack growth and failure is simulated using MCS and a DBN model. It was observed that this rate is significantly higher at later stages of the service life. For instance, in the 20^{th} year of operation, probability of failure is about 0.1 where due to faster growth of long cracks this value reaches to about 0.95 after 15 years, given that no maintenance is performed on the pipeline. The results highlight the capability of the method in prediction of corrosion fatigue life considering different growth rates of damage at each stage of the damage process.

- A novel methodology is proposed for predicting the stochastic fate and transport of spilled oil from fractured subsea pipelines. The conventional fugacity approach is integrated with HBA to incorporate the uncertainty of input variables and to improve the prediction of pollutant concentration in multimedia. In a case study, an oil release scenario in the Labrador Sea is simulated. The results suggest that the oil concentration in air and ice cover decreases significantly within the first few hours, however this requires approximately 10 hours for the concentration in water and sediment column to reduce to a same level. It is predicted, with 0.95 confidence, that oil concentration in air and ice cover phases reaches 10% of its maximum level within the first hour while this time is only enough to reduce the concentration in water column and sediment to 50% of the maximum level. By estimating the distribution of time to reach a concentration of stressor, this methodology can be used by operation and safety managers for developing effective risk contingency and remediation plans.
- The estimated distribution of pollutants concentrations is later used to evaluate the ecological risk posed to the aquatic species by the release of hydrocarbons in marine environment. For this purpose, a BN is established based on the RQ concept that compared the predicted exposure concentration of stressor with predicted no effect concentration of organisms. A case study scenario is adopted involving the release of 11,500 kg of oil during the operation of a subsea pipeline in the Kara Sea. The predictions suggest, with approximately 0.99 confidence, that the level of imposed risk to aquatic ecological habitants is less than 5×10^{-11}. From a comparison of the results of previous researches, it is concluded that those methods are likely to overestimate the risk profile, which may be due to not including the probabilistic dependency of input parameters in the analysis. The model was extended to a DBN for evaluating the effect of seasonal changes on the overall risk estimates. The results highlight that operations in more extreme environmental conditions require more attention from the operators and risk managers for development of risk mitigation strategies.
- In order to mitigate the consequences of subsea pipeline accidents due to degradation, a dynamic risk-based methodology is proposed for the maintenance scheduling of the structures, based on the predicted remaining useful life. A DBN-based deterioration model is extended to an ID for estimating the expected utility for each decision alternative. The alternatives are selected to identify whether or not maintenance is required, and more importantly which repair option will provide the optimum outcome. The results demonstrate that the developed method is able to improve the effectiveness of current maintenance planning techniques by improving

the availability of assets while minimizing the overall operational costs. The priority of this part of research is to demonstrate applicability of a risk-based approach to maintenance planning of deteriorating subsea pipelines. However, the developed methodology can be adopted to integrate real-life cost models and condition monitoring data to enable the extension of framework to an industrial support-decision tool.

6.3 Recommendations for Future Work

This research attempts to improve the asset integrity management strategies currently utilized in the oil and gas industries, however, further works can be carried out based on the following suggestions:

- The prognostic health assessment methodology proposed in this study can be extended to a subsea pipeline condition monitoring framework. This can be achieved by integrating fault detection algorithms that enable prediction of the useful life of the structures based on observations of faults in the operation.
- The risk associated with failure of subsea pipelines may also include the environmental risks imposed by the accident (i.e. the costs required for implementing remediation plans and even the financial penalties incurred by the asset owner/operators due to the causation of environmental damage). The model reported in Chapter 5 merely considers the cost of corrective repair as a failure consequence, however, future work can incorporate the environmental risk as an additional component failure costs. It is possible to account for the level of environmental damage if the spill accident is modelled using a multi-state failure event (i.e. various states representing different sizes of rupture).
- A decision-support tool can be developed based on the proposed risk assessment framework for optimizing the remediation of oil spill accidents. This can be helpful for operators and risk managers to allow them to take the optimum action while mitigating the consequences of an unwanted spill based on the actual extent of environmental damage.

References

1. Kaiser, M.J. and M. Liu, *Global offshore pipeline construction service market review 2017–Part II.* Ships and Offshore Structures, 2018. **13**(1): p. 96-118.

2. BP, *BP Statistical Review of World Energy* 2017.

3. UK, O.a.G., *Decommisioning of Pipelines in the North Sea Region*. 2013.

4. Davis, P. and J. Brokhurst, *Subsea Pipeline Infrastructure Monitoring: A Framework for Technology Review and Selection.* Ocean Engineering, 2015. **104**: p. 540-548.

5. PAROLC, *The Update of Loss of Containment Data for Offshore Pipelines*. 2001, Mott MacDonald.

6. Mansor, N.I.I., et al., *A review of the fatigue failure mechanism of metallic materials under a corroded environment.* Engineering Failure Analysis, 2014. **42**: p. 353-365.

7. Xue, H. and Y. Cheng, *Characterization of inclusions of X80 pipeline steel and its correlation with hydrogen-induced cracking.* Corrosion science, 2011. **53**(4): p. 1201-1208.

8. Wang, Y., G. Cheng, and Y. Li, *Observation of the pitting corrosion and uniform corrosion for X80 steel in 3.5 wt.% NaCl solutions using in-situ and 3-D measuring microscope.* Corrosion Science, 2016. **111**: p. 508-517.

9. The Victoria Advocate, in *The Victoria Advocate*. 2006: Texas.

10. Lee, R., *Louisiana oil spill is largest since 2010,* in *The Simmons Voice,*. 2017.

11. Dey, P.K., *A risk-based model for inspection and maintenance of cross-country petroleum pipeline.* Journal of Quality in Maintenance Engineering, 2001. **7**(1): p. 25-43.

12. Dey, P.K. and S.S. Gupta, *Risk-based Model Aids Selection of Pipeline Inspection, Maintenance Strategies.* Oil and Gas Journal, 2001. **99**: p. 54-60.

13. Sulaiman, N.S. and H. Tan, *Third Party Damages of Offshore Pipeline.* Journal of Energy Challenges and Mechanics, 2014. **1**(1).

14. Yuha, D. and Y. Datao, *Estimation of Failure Probability of Oil and Gas Transmission Pipelines by Fuzyy Fault Tree Analysis.* Journal of Loss Prevention in the Process Industry, 2005. **18**: p. 83-88.

15. Tolentino, D. and S.E. Ruiz, *Influence of structural deterioration over time on the optimal time interval for inspection and maintenance of structures.* Engineering Structures, 2014. **61**: p. 22-30.

16. Natarajan, S., et al. *Deepwater Spar Steel Catenary Riser Monitoring Strategy*. in *Offshore Mechanics and Arctic Engineering*. 2007. San Diego, California.

17. Bhandari, J., et al., *Modelling of pitting corrosion in marine and offshore steel structures – A technical review.* Journal of Loss Prevention in the Process Industries, 2015. **37**(Supplement C): p. 39-62.

18. Melchers, R.E. and R. Jeffrey, *Probabilistic models for steel corrosion loss and pitting of marine infrastructure.* Reliability Engineering & System Safety, 2008. **93**(3): p. 423-432.

19. Popoola, L.T., et al., *Corrosion problems during oil and gas production and its mitigation.* International Journal of Industrial Chemistry, 2013. **4**(1): p. 35.

20. Cheng, A. and N.-Z. Chen, *Corrosion fatigue crack growth modelling for subsea pipeline steels.* Ocean Engineering, 2017. **142**: p. 10-19.

21. Chen, G.S., et al., *Transition from pitting to fatigue crack growth—modeling of corrosion fatigue crack nucleation in a 2024-T3 aluminum alloy.* Materials Science and Engineering: A, 1996. **219**(1): p. 126-132.

22. Fang, B., et al., *Pit to crack transition in X-52 pipeline steel in near neutral pH environment Part 1–formation of blunt cracks from pits under cyclic loading.* Corrosion Engineering, Science and Technology, 2010. **45**(4): p. 302-312.

23. Harlow, D.G. and R.P. Wei, *Probability approach for prediction of corrosion and corrosion fatigue life.* AIAA journal, 1994. **32**(10): p. 2073-2079.

24. Shi, P. and S. Mahadevan, *Damage tolerance approach for probabilistic pitting corrosion fatigue life prediction.* Engineering fracture mechanics, 2001. **68**(13): p. 1493-1507.

25. Chookah, M., M. Nuhi, and M. Modarres, *A probabilistic physics-of-failure model for prognostic health management of structures subject to pitting and corrosion-fatigue.* Reliability Engineering & System Safety, 2011. **96**(12): p. 1601-1610.

26. Bai, Y. and Q. Bai, *Subsea pipelines and risers*. 2005: Elsevier.

27. Sadiq, R., et al., *Distribution of arsenic and copper in sediment pore water: an ecological risk assessment case study for offshore drilling waste discharges.* Risk analysis, 2003. **23**(6): p. 1309-1321.

28. Mackay, D., *Multimedia environmental models: the fugacity approach*. 2001: CRC press.

29. Mackay, D., M. Joy, and S. Paterson, *A quantitative water, air, sediment interaction (QWASI) fugacity model for describing the fate of chemicals in lakes.* Chemosphere, 1983. **12**(7-8): p. 981-997.

30. Nazir, M., et al., *Multimedia fate of oil spills in a marine environment—An integrated modelling approach.* Process Safety and Environmental Protection, 2008. **86**(2): p. 141-148.

31. Afenyo, M., et al., *Dynamic fugacity model for accidental oil release during Arctic shipping.* Marine pollution bulletin, 2016. **111**(1): p. 347-353.

32. Sadiq, R., *Drilling waste discharges in the marine environment: a risk based decision methodology*. 2001, Memorial University of Newfoundland.

33. Afenyo, M., et al., *A probabilistic ecological risk model for Arctic marine oil spills.* Journal of Environmental Chemical Engineering, 2017. **5**(2): p. 1494-1503.

34. Sadiq, R., et al., *Distribution of heavy metals in sediment pore water due to offshore discharges: an ecological risk assessment.* Environmental Modelling & Software, 2003. **18**(5): p. 451-461.

35. Scholten, M.C.T., C.C. Karman, and S. Huwer, *Ecotoxicological risk assessment related to chemicals and pollutants in off-shore oil production.* Toxicology Letters, 2000. **112-113**: p. 283-288.

36. Nazir, M., et al., *Subsea release of oil from a riser: An ecological risk assessment.* Risk analysis, 2008. **28**(5): p. 1173-1196.

37. Nevalainen, M., I. Helle, and J. Vanhatalo, *Preparing for the unprecedented—Towards quantitative oil risk assessment in the Arctic marine areas.* Marine pollution bulletin, 2017. **114**(1): p. 90-101.

38. Dey, P.K., S.O. Ogunlana, and S. Naksuksakul, *Risk-based maintenance model for offshore oil and gas pipelines: a case study.* Journal of Quality in Maintenance Engineering, 2004. **10**(3): p. 169-183.

39. Khan, F.I. and M.M. Haddara, *Risk-based maintenance (RBM): a quantitative approach for maintenance/inspection scheduling and planning.* Journal of loss prevention in the process industries, 2003. **16**(6): p. 561-573.

40. Arunraj, N. and J. Maiti, *Risk-based maintenance—Techniques and applications.* Journal of hazardous materials, 2007. **142**(3): p. 653-661.

41. Khan, F.I. and M. Haddara, *Risk-based maintenance (RBM): A new approach for process plant inspection and maintenance.* Process safety progress, 2004. **23**(4): p. 252-265.

42. Pui, G., et al., *Risk-based maintenance of offshore managed pressure drilling (MPD) operation.* Journal of Petroleum Science and Engineering, 2017. **159**: p. 513-521.

43. Khakzad Rostami, N., *Dynamic safety analysis using advanced approaches*. 2012, Memorial University of Newfoundland.

44. Weber, P., et al., *Overview on Bayesian networks applications for dependability, risk analysis and maintenance areas.* Engineering Applications of Artificial Intelligence, 2012. **25**(4): p. 671-682.

45. Yang, Y., et al., *Corrosion induced failure analysis of subsea pipelines.* Reliability Engineering & System Safety, 2017. **159**(Supplement C): p. 214-222.

46. Bhandari, J., et al. *Reliability assessment of offshore asset under pitting corrosion using Bayesian Network.* in *Corrosion 2016*. 2016.

47. Bhandari, J., et al., *Pitting Degradation Modeling of Ocean Steel Structures Using Bayesian Network.* Journal of Offshore Mechanics and Arctic Engineering, 2017. **139**(5): p. 051402.

48. Kondo, Y., *Prediction of fatigue crack initiation life based on pit growth.* Corrosion, 1989. **45**(1): p. 7-11.

49. Goswami, T. and D. Hoeppner, *Pitting corrosion fatigue of structural materials*, in *Structural integrity in aging aircrafts*, C. Chang and C. Sun, Editors. 1995, AMSE: New York. p. 39-129.

50. Kaynak, C. and T. Baker, *Effects of short cracks on fatigue life calculations.* International Journal of fatigue, 1996. **18**(1): p. 25-31.

51. Abaei, M.M., et al., *A robust risk assessment methodology for safety analysis of marine structures under storm conditions.* Ocean Engineering, 2018. **156**: p. 167-178.

52. Abbassi, R., et al., *Developing a Quantitative Risk-based Methodology for Maintenance Scheduling Using Bayesian Network.* Chemical Engineering Transactions, 2016. **48**: p. 235-240.

53. Yeo, C., et al., *Dynamic risk analysis of offloading process in floating liquefied natural gas (FLNG) platform using Bayesian Network.* Journal of Loss Prevention in the Process Industries, 2016. **41**: p. 259-269.

54. Bhandari, J., et al., *Risk analysis of deepwater drilling operations using Bayesian network.* Journal of Loss Prevention in the Process Industries, 2015. **38**: p. 11-23.

55. Friis-Hansen, A., *Bayesian Networks as Decision Tool in Marine Applications*, in *Department of Naval Architecture and Offshore Engineering*. 2000, Technical University of Denmark.

56. Straub, D., *Stochastic modeling of deterioration processes through dynamic Bayesian networks.* Journal of Engineering Mechanics, 2009. **135**(10): p. 1089-1099.

57. Arzaghi, E., et al., *Risk-based maintenance planning of subsea pipelines through fatigue crack growth monitoring.* Engineering Failure Analysis, 2017. **79**: p. 928-939.

58. Pearl, J., *Probabilistic reasoning in intelligent systems*. 1988, San Francisco, CA: Morgan Kaufmann.

59. Jensen, F.V. and T.D. Nielsen, *Bayesian Networks and Decision Graphs*. 2007, New York: Springer.

60. Murphy, K.P. and S. Russell, *Dynamic bayesian networks: representation, inference and learning.* 2002.

61. Madsen, H.O., S. Krenk, and N.C. Lind, *Methods of structural safety*. 2006: Courier Corporation.

62. Khon, V., et al., *Perspectives of Northern Sea Route and Northwest Passage in the twenty-first century.* Climatic Change, 2010. **100**(3-4): p. 757-768.

63. Giles, K.A., S.W. Laxon, and A.L. Ridout, *Circumpolar thinning of Arctic sea ice following the 2007 record ice extent minimum.* Geophysical Research Letters, 2008. **35**(22).

64. Gautier, D.L., et al., *Assessment of undiscovered oil and gas in the Arctic.* Science, 2009. **324**(5931): p. 1175-1179.

65. Bird, K.J., et al., *Circum-Arctic resource appraisal: Estimates of undiscovered oil and gas north of the Arctic Circle*. 2008, Geological Survey (US).

66. DNV, G., *The Arctic—the next risk frontier.* DNV GL, Høvik, Norway, 2014.

67. Afenyo, M., B. Veitch, and F. Khan, *A state-of-the-art review of fate and transport of oil spills in open and ice-covered water.* Ocean Engineering, 2016. **119**(Supplement C): p. 233-248.

68. Jonsson, H., et al., *The Arctic is no longer put on ice: evaluation of polar cod (Boreogadussaida) as a monitoring species of oil pollution in cold waters.* Marine pollution bulletin, 2010. **60**(3): p. 390-395.

69. AMAP, A., *Oil and Gas Activities in the Arctic–Effects and Potential Effects, vol. 1.* Arctic Monitoring and Assessment Programme (AMAP), Oslo, Norway, 2010.

70. Camus, L. and M.G. Smit, *Environmental effects of Arctic oil spills and spill response technologies, introduction to a 5 year joint industry effort.* Marine Environmental Research, 2018.

71. Dickins, D.F., *Arctic Oil Spill Response Technology Joint Industry Programme Synthesis Report. Arctic Response Technology JIP*. 2017.

72. Hasle, J.R., U. Kjellén, and O. Haugerud, *Decision on oil and gas exploration in an Arctic area: case study from the Norwegian Barents Sea.* Safety Science, 2009. **47**(6): p. 832-842.

73. Anon, *Prepared for Ecological Protection Agency (EPA). Guidelines for ecological risk assessment* 1998, Federal Register. p. 26846-26924.

74. Yang, M., et al., *Multimedia fate modeling of oil spills in ice-infested waters: An exploration of the feasibility of fugacity-based approach.* Process Safety and Environmental Protection, 2015. **93**: p. 206-217.

75. Siu, N.O. and D.L. Kelly, *Bayesian parameter estimation in probabilistic risk assessment.* Reliability Engineering & System Safety, 1998. **62**(1): p. 89-116.

76. Yang, M., F.I. Khan, and L. Lye, *Precursor-based hierarchical Bayesian approach for rare event frequency estimation: a case of oil spill accidents.* Process safety and environmental protection, 2013. **91**(5): p. 333-342.

77. Yu, H., F. Khan, and B. Veitch, *A flexible hierarchical Bayesian modeling technique for risk analysis of major accidents.* Risk analysis, 2017.

78. Bhandari, J., et al., *Dynamic risk-based maintenance for offshore processing facility.* Process Safety Progress, 2016. **35**(4): p. 399-406.

79. Kelly, D.L. and C.L. Smith, *Bayesian inference in probabilistic risk assessment—the current state of the art.* Reliability Engineering & System Safety, 2009. **94**(2): p. 628-643.

80. Yang, M., et al., *Risk assessment of rare events.* Process Safety and Environmental Protection, 2015. **98**: p. 102-108.

81. Commission, U.N.R., *EPRI/NRC-RES fire PRA methodology for nuclear power facilities (NUREG/CR-6850)*, in *Washington, DC*. 2005.

82. Ross, S., *A first course in probability*. 1976, Macmillan, New York, NY.

83. Rodionov, A., D. Kelly, and J. Uwe-Klügel, *Guidelines for analysis of data related to ageing of nuclear power plant components and systems. Joint Research Centre.* Institute for Energy, Luxembourg: European Commission, 2009.

84. Chang, S.E., et al., *Consequences of oil spills: a review and framework for informing planning.* Ecology and Society, 2014. **19**(2).

85. Orszulik, S.T., *Environmental technology in the oil industry*. 2008: Springer.

86. Pula, R., et al., *A Grid Based Approach for Fire and Explosion Consequence Analysis.* Process Safety and Environmental Protection, 2006. **84**(2): p. 79-91.

87. Karman, C.C. and H.G. Reerink, *Dynamic assessment of the ecological risk of the discharge of produced water from oil and gas producing platforms.* Journal of Hazardous Materials, 1998. **61**(1): p. 43-51.

88. French-McCay, D. *Oil spill modeling for ecological risk and natural resource damage assessment*. in *International Oil Spill Conference Proceedings (IOSC)*. 2011. American Petroleum Institute.

89. Khakzad, N., F. Khan, and P. Amyotte, *Quantitative risk analysis of offshore drilling operations: a Bayesian approach.* Safety science, 2013. **57**: p. 108-117.

90. Husain, T., et al., *Framework for ecological risk assessment: deterministic and uncertainty analyses.* The Gulf Ecosystem: Health and Sustainability, 2002: p. 199-218.

91. Barber, D., *Bayesian reasoning and machine learning*. 2012: Cambridge University Press.

92. Abimbola, M., et al., *Safety and risk analysis of managed pressure drilling operation using Bayesian network.* Safety Science, 2015. **76**: p. 133-144.

93. Eleye-Datubo, A.G., et al., *Enabling a powerful marine and offshore decision-support solution through bayesian network technique.* Risk Analysis, 2006. **26**(3): p. 695-721.

94. Khakzad, N., et al., *Domino effect analysis using Bayesian networks.* Risk Analysis, 2013. **33**(2): p. 292-306.

95. Anon., *Guidelines for Ecological Risk Assessment.* Federal Register, 1998. **63**(93): p. 26846–26924.

96. Afenyo, M., et al., *Modeling oil weathering and transport in sea ice.* Marine Pollution Bulletin, 2016. **107**(1): p. 206-215.

97. Logan, B.E., *Environmental transport processes*. 2012: John Wiley & Sons.

98. Arzaghi, E., et al., *A hierarchical Bayesian approach to modelling fate and transport of oil released from subsea pipelines.* Process Safety and Environmental Protection, 2018. **118**: p. 307-315.

99. Abbassi, R., F. Khan, and K. Hawboldt, *Ecological risk-based performance evaluation of a waste stabilization pond.* Environmental Engineering and Management Journal, 2010. **9**(6): p. 757-764.

100. Fahd, F., et al., *Developing a novel methodology for ecological risk assessment of thiosalts.* Stochastic environmental research and risk assessment, 2014. **28**(2): p. 383-391.

101. Olsen, G.H., et al., *Arctic versus temperate comparison of risk assessment metrics for 2-methyl-naphthalene.* Marine environmental research, 2011. **72**(4): p. 179-187.

102. CIN, *Chemical Hazard Assessment and Risk Management*

For. 2004.

103. Friis-Hansen, A., *Bayesian Networks as a Decision Support Tool in Marine Applications*, in *Department of Naval Architecture and Offshore Engineering*. 2000, Technical University of Denmark.

104. Miquel, J., *Environment and biology of the Kara Sea: a general view for contamination studies.* Marine pollution bulletin, 2001. **43**(1-6): p. 19-27.

105. Clark, K.E., F.A. Gobas, and D. Mackay, *Model of organic chemical uptake and clearance by fish from food and water.* Environmental science & technology, 1990. **24**(8): p. 1203-1213.

106. Brussaard, C.P., et al., *Immediate ecotoxicological effects of short-lived oil spills on marine biota.* Nature communications, 2016. **7**: p. 11206.

107. Mackay, D. and S. Paterson, *Evaluating the multimedia fate of organic chemicals: a level III fugacity model.* Environmental Science & Technology, 1991. **25**(3): p. 427-436.

108. Anon., *Prepared for Environmental Agency. Risk Assessment of Naphthalene*. 2007.

109. Khan, B., et al., *An operational risk analysis tool to analyze marine transportation in Arctic waters.* Reliability Engineering & System Safety, 2018. **169**: p. 485-502.

110. Mansor, N., et al., *A review of the fatigue failure mechanism of metallic materials under a corroded environment.* Engineering Failure Analysis, 2014. **42**: p. 353-365.

111. Singh, M. and T. Markeset, *A methodology for risk-based inspection planning of oil and gas pipes based on fuzzy logic framework.* Engineering Failure Analysis, 2009. **16**(7): p. 2098-2113.

112. Khakzad, N., F. Khan, and P. Amyotte, *Safety analysis in process facilities: comparison of fault tree and Bayesian network approaches.* Reliability Engineering & System Safety, 2011. **96**(8): p. 925-932.

113. Khakzad, N., F. Khan, and P. Amyotte, *Dynamic safety analysis of process systems by mapping bow-tie into Bayesian network.* Process Safety and Environmental Protection, 2013. **91**(1): p. 46-53.

114. Khakzad, N., F. Khan, and P. Amyotte, *Risk-based design of process systems using discrete-time Bayesian networks.* Reliability Engineering & System Safety, 2013. **109**: p. 5-17.

115. Holický, M., J. Marková, and M. Sýkora, *Forensic assessment of a bridge downfall using Bayesian networks.* Engineering Failure Analysis, 2013. **30**: p. 1-9.

116. Nielsen, J.J. and J.D. Sørensen. *Bayesian networks as a decision tool for O&M of offshore wind turbines*. in *Proceedings of the 5th international ASRANet conference*. 2010.

117. Khakzad, N., *Application of dynamic Bayesian network to risk analysis of domino effects in chemical infrastructures.* Reliability Engineering & System Safety, 2015. **138**: p. 263-272.

118. Khakzad, N. and G. Reniers, *Cost-effective allocation of safety measures in chemical plans with regard to land use planning* Safety Science, 2015.

119. Arzaghi, E., et al., *Developing a dynamic model for pitting and corrosion-fatigue damage of subsea pipelines.* Ocean Engineering, 2018. **150**: p. 391-396.

120. Palmer, A.C. and R. King, *Subsea Pipeline Engineering*. 2008, Tulsa, Oklahoma, USA: PennWell.